UNIVERSIDAD COMPLUTENSE DE MADRID
FACULTAD DE CIENCIAS ECONÓMICAS Y EMPRESARIALES

TESIS DOCTORAL

Climate Change Impacts on Renewable Energy Generation and Energy Generation Scenarios

Impactos del Cambio Climático en la Generación de Energía Renovable y Evaluación de Escenarios de Generación Energética

MEMORIA PARA OPTAR AL GRADO DE DOCTOR

PRESENTADA POR

Miguel Ángel Rodríguez López

Directores

Emilio Jaime Cerdá Tena
Pablo del Río González

Madrid

UNIVERSIDAD COMPLUTENSE DE MADRID

FACULTAD DE CIENCIAS ECONÓMICAS Y EMPRESARIALES

TESIS DOCTORAL

Climate Change Impacts on Renewable Energy Generation and Energy Generation Scenarios

Impactos del Cambio Climático en la Generación de Energía Renovable y Evaluación de Escenarios de Generación Energética

MEMORIA PARA OPTAR AL GRADO DE DOCTOR

PRESENTADA POR

Miguel Ángel Rodríguez López

DIRECTORES

Emilio Jaime Cerdá Tena
Pablo del Río González

UNIVERSIDAD COMPLUTENSE DE MADRID

Climate Change Impacts on Renewable Energy Generation and Energy Generation Scenarios

Impactos del Cambio Climático en la Generación de Energía Renovable y Evaluación de Escenarios de Generación Energética

Miguel Ángel Rodríguez López

01 Diciembre 2021

Directores: Emilio Jaime Cerdá Tena
Pablo del Río González

PROGRAMA DE DOCTORADO EN ECONOMÍA

FACULTAD DE CIENCIAS ECONÓMICAS Y EMPRESARIALES

"Los locos abren los caminos que más tarde recorren los sabios."

"Fools open the paths later traveled by wise men."

Carlo Dossi

"La mejor manera de predecir el futuro es creándolo."

"The best way to predict the future is creating it."

Peter Drucker

Acknowledgments

This Thesis has benefited greatly from the generous contribution of many people:

- Emilio Jaime Cerdá and Pablo del Río responded with understanding and affection to all the inconveniences and challenges encountered during the process. His mathematical expertise and meticulousness improved very significantly the manuscripts.
- Luis María López Gonzalez helped with his knowledge in future energy scenarios and transition technologies.
- Many participants in workshops and seminars where the papers were presented provided very valuable ideas and suggestions to improve the texts. Particularly the attendees to the seminars organized by the Universidad Complutense de Madrid.

But it would have been impossible without the support and understanding of my family andfriends.

Index

Index of figures

Modeling Wind-Turbine Power Curves: Effects of Environmental Temperature on Wind Energy Generation

Modeling and Evaluating the Effect of Environmental Temperature on Electricity Generation in a PV Power Plant

OPTIMIZING THE ENERGY GENERATION COST WITH RENEWABLE RESOURCES USING GENERIC ALGORITHMS AND EVALUATING THE IMPACT OF ELECTRICAL VEHICLES

Index of tables

Modeling Wind-Turbine Power Curves: Effects of Environmental Temperature on Wind Energy Generation

Modeling and Evaluating the Effect of Environmental Temperature on Electricity Generation in a PV Power Plant

Optimizing the Energy Generation cost with Renewable Resources Using Generic Algorithms and Evaluating the Impact of Electrical Vehicles

Acronyms and abbreviations

- ANN: Artificial Neural Networks.
- ANFIS: Adaptive Neuro-Fuzzy Inference System.
- ARIMA: Autoregressive Integrated Moving Average.
- BEV: Battery Electric Vehicle.
- BENEF: Bloomberg Energy Finance.
- CMIP-3: Coupled Model Interpolation Project.
- CNN: Convolutional Neural Network.
- DE: Differential Evolution.
- DNN: Deep Neural Network.
- ELM: Extreme Learning Machine.
- EV: Electric Vehicle.
- FEVCS-WPE: Electrical Vehicle Fast Charge System.
- GA: Genetic Algorithm.
- GB: Gradient boosted.
- GDP: Gross Domestic Product.
- GHG: Greenhouse Gas.
- GHI: Global Horizontal Irradiance.
- GW: Gigawatt.
- GWh: Gigawatt hour.
- IDAE: Institute for the Diversification and Saving of Energy under the Ministry for the Ecological Transitionin Spain.
- IEA: International Energy Agency.
- IEC: International Electrotechnical Commission.
- IGSM: Integrated Global System Model.
- INE: Spanish Statistical Office.
- IPCC: Intergovernmental Panel on Climate Change.
- IRENA: International Renewable Energy Agency.
- kWh: Kilowatt.
- kWhp: Kilowatt peak.
- kWh: Kilowatt hour.
- LCOE: Levelised Cost of Energy.
- MLP: Multi Layer Perceptron.
- MPPT: Max Power Point Tracking.
- MT: Medium Tension.
- MW: Megawatt.
- MWh: Megawatt hour.
- NLARX: Exogenous Variables.
- NREL: National Renewable Energy Laboratory.
- OMIE: Operador del Mercado Ibérico(Iberian Market Operator).
- OPC: Operating Conditions.
- P-V: Power-Voltage.
- PC: Power Curve.
- PHEV: Plug-in Electrical Vehicle.
- PV: Photovoltaic.
- RCA4: Rossby Centre.
- REH: Residential Energy Hub.
- RET: Renewable Energy Technologies.
- RF: Random Forest.
- SCADA: Supervisory Control and Data Acquisition System.

- STC: Standard Test Conditions.
- SVM: Support Vector Machine.
- SVR: Support Vector Regression.
- TDNN: Time Delay Neural Network.
- TOPSIS: Technique for Order Preference by Similarity to Ideal Solution.
- USD: US Dollar.
- V2G: Vehicle to Grid.
- W: Watt.
- XGBF: Extreme Gradient Boosted.

Motivation and structure of the Thesis

1. Motivation

Climate change represents a serious global challenge. Global surface temperatures have reached unprecedented levels [1]. As it is well-known, the accumulation of greenhouse gas emissions (GHG) is directly related to the combustion of fossil fuels in all sectors of the economy, notably electricity generation, transport and industry [2]. But at the same time, it will be severely affected by the impacts of climate change [3, 4]. This will impact electricity supply and demand, as it can alter consumption patterns in various sectors [5].

Climate change mitigation will require the adoption of decarbonisation strategies everywhere, e.g., in all sectors and countries. Concern about climate change has led to the Paris Agreement, whereby governments committed to reduce those emissions in order to keep a global temperature rise this century well below 2 degrees Celsius (ºC) above pre-industrial levels and to pursue efforts to limit the temperature increase even further to 1.5ºC. This entails a considerable reduction in emissions, around 50% in 2050 compared to 1990 levels [6].

For that reason, Climate change has become an increasingly important area of research and as a result an exponential increase of scholarly publications on this topic has been registered in the last few years [7, 8]. Within climate related areas, risks and adaptation played a smaller role in literature and in the reports by the Intergovernmental Panel on Climate Change (IPCC) until its Fourth Assessment Report [7, 9]. This gap is still relevant in practical issues like climate finance [10].

Measures will have to be put in place to improve the energy efficiency of production and consumption patterns and to increase the uptake of low carbon technologies, in order to balance the different economic and environmental trade-offs in place. In this context, it is a widely shared view that the deployment of renewable energy technologies (RETs) is a critical alternative to abate GHG emissions, whose accumulation leads to global warming. Several simulation models have shown that RETs will play a crucial role in achieving temperature increases below 2ºC or 1.5ºC [11, 12]. However, in its World Energy Investment report [13], the International Energy Agency (IEA) has indicated that the trend of decarbonisation investments is not enough in order to ensure climate sustainability. Furthermore, those simulation models implicitly assume that the renewable energy resources and the performance of renewable energy generation facilities will remain constant in the next decades. The fact is that climate change may affect those resources and, thus, renewable energy generation and additional investment would be required.

One of the main changes from the demand side will come from the decarbonisation and electrification of the automobile fleet [14]. The progressive penetration of the electric vehicle will increase electricity demand, requiring more renewable electricity generation, which cannot be obtained when necessary, if not when there is a renewable resource available. For this, it will be necessary to correctly dimension the renewable generation systems, including storage systems such as batteries, as well as taking other demand management measures.

For all these scenarios, renewable energies are usually mentioned as one of the most promising solutions the sector can offer reduce of GHGs [15, 16]. But they rely on resources that depend on climate variables and therefore can also be affected by climate change [17], and it has to be considered when the energy generation systems is set up.

2. Objectives of the Thesis

In this thesis, there were two objectives on one hand, the impact of global warming due to climate change on wind and photovoltaic renewable generation has been assessed, and on the other hand, the impact of the penetration of the electric vehicle (EV) on the need of additional renewable generation and the cost of energy generation has been evaluated.

To cover these objectives, we had to get several goals, starting with the development of modeling methodologies for renewable generation and energy demand, to later carry out simulations of different global warming scenarios. Modeling the performance of renewable generation plants based on ambient temperature is not easy, and it was necessary to use complex machine learning algorithms and Fuzzy logic, among others.

In the studies of global warming impact on renewable generation, several scenarios of average thermal increase were simulated in the production sites with the 2050 horizon. Given these scenarios, the loss of performance in a wind and a photovoltaic installation was quantified. This loss of performance will affect the investment needs in renewables to meet the objectives set at COP 21, as well as affect the profitability of this type of facility and the reduction of CO_2 emissions.

Given the complexity to simulate and quantify the impact of climate change on renewable generation, a "*ceter paribus*" approach was carried out, considering only an increase in the average temperature at the sites, keeping constant the rest of the variables that would affect renewable production.

Regarding the evaluation of the impact of EV on renewable generation and the cost of energy in the system, it was necessary to model and simulate the consumption behavior of a population group, which was supplied with 100% renewable generation sources. The objective was to design an algorithm that would result in the best configuration of wind and photovoltaic assets, as well as battery storage systems, in such a way that the cost of power generation was minimized, in the face of various EV penetration scenarios.

With all these studies, our objective has been to draw attention to the effect of global warming on renewable generation and the impact of EV penetration in a system with renewable generation that will be affected by warming itself. The tools presented have a high adaptability, in such a way that an infinity of very useful simulations for decision makers can be carried out.

3. Structure of the Thesis

The thesis as a whole is made up of tree chapters. For the time being, one of them has been published as papers a scientific journal and other in a scientific congress. A reference will be made at the beginning of each chapter.

The first and second chapters are dedicated to analyzing the loss of performance of wind energy and photovoltaic power plants, respectively. This loss of performance due to global warming are caused by the increase of the average temperature in the sites. In both studies, the evolution of global warming was simulated based on the different energy mix scenarios considered by the IEA and in accordance with the agreements signed at COP21. After carrying out the simulation of the scenarios, the loss of production in the facilities during their life was calculated, as well as the impact on CO_2 emissions considering that this lack of production will be covered with conventional energy sources.

The first chapter analyzes the production of a wind farm in southern Spain, combining climatological, operational and economic data with other simulated ones of environmental conditions typical of global warming. The density of the air, which has a direct relationship with temperature, affects the performance of wind turbines. Given that no information was available on the possible evolution of the air density at a site, but there was information on the evolution of the mean temperature, a model composed of two neural networks was carried out that characterized in a first stage the air density of the location as a function of ambient temperature and, in a second stage, a neuro-fuzzy model to calculate the wind turbine's production as a function of temperature and wind speed.

The second chapter evaluated the photovoltaic solar generation in a plant in southern Spain. In the study, a high correlation was observed between the performance of the plant and the ambient

temperature. This temperature is increased throughout the day around the panels due to the thermal losses of the PV production process. This local thermal increase, together with the average thermal increase due to global warming, have a great impact on the performance of the installation.

In the chapter, the production of photovoltaic panels was modeled by using historical data and neural network models, also using a dummy variable created for the study, which represented the thermal evolution of the site throughout the day and year. A model was obtained that was capable of reproducing the plant's production as a function of environmental variables, including temperature, wind speed and irradiation, and subsequently the aforementioned global warming scenarios were simulated.

In the third chapter, the electricity consumption of a group of homes in southern Spain was analyzed, characterizing the intra-daily, weekly and annual consumption of the site using statistical models. Via Monte Carlo simulations, the expected consumption was reproduced for population groups of different sizes. Subsequently, the EV consumption curve was characterized and scenarios with different EV penetration levels were simulated. This population group was feed with the real production of a wind farm and a photovoltaic plant in southern Spain, thus simulating the renewable energy supply curves. The genetic optimization algorithm calculated the number of wind turbines, PV panels and batteries needed to supply energy to the population group, minimizing the cost of generating it.

The results showed, among other conclusions, that the penetration of the EV would help reduce the system's power generation costs on small size cities, although in general terms the LCOE will be progressively increased by the need for a greater number of batteries in the system.

References

1. Edenhofer O, Sokona Y, Seyboth K, Eickemeier P, Matschoss P, Hansen G, Kadner S, Schlömer S, Zwickel T, von Stechow C (eds). Special Report on Renewable Energy Sources and Climate Change Mitigation 2016. Intergovernment Pannel on Climate Change (IPCC), Geneve ISBN 978-92-9169-131-9 https://www.ipcc.ch/pdf/special-reports/srren/SRREN_FD_SPM_final.pdf.
2. Intergovernmental Panel on Climate Change (IPCC), Climate Change 2014 Mitigation of Climate Change, 2014. https://doi:10.1017/CBO9781107415416.
3. J. Ebinger, W. Vergara, Climate Impacts on Energy Systems: key issues for energy sector adaptation, The World Bank, Washington, DC, USA, 2011.
4. [8] P.C. Johnston, Climate Risk and Adaptation in the Electric Power Sector, Asian Development Bank - Publications, Manila, Phillippines, 2012. https://www.adb.org/sites/default/files/publication/29889/climate-risks-adaptation-power-sector.pdf.
5. L. Wenz, A. Levermann, M. Auffhammer, North – south polarization of European electricity consumption under future warming, (2017) 1–9. https://doi:10.1073/pnas.1704339114.
6. Schreurs M. Breaking the impasse in the international climate negotiations: The potential of green technologies, Energy Policy 2012; 48: 5-12. http://dx.doi.org/10.1016/j.enpol.2012.04.044.
7. R. Haunschild, L. Bornmann, W. Marx, Climate Change Research in View of Bibliometrics, PLoS One. 11 (2016) e0160393. https://doi:10.1371/journal.pone.0160393.
8. A. Hillier, R.P. Kelly, T. Klinger, Narrative style influences citation frequency in climate change science, PLoS One. 11 (2016) 1–13. https://doi:10.1371/journal.pone.0167983 .
9. T.J. Bassett, C. Fogelman, Déjà vu or something new? The adaptation concept in the climate change literature, Geoforum. 48 (2013) 42–53. https://doi.org/10.1016/j.geoforum.2013.04.010
10. I. Larrea, I. Galarraga, K. Solaun, Las finanzas del clima. Una revisión, Ekonomiaz. (2018) 246–266. https://dialnet.unirioja.es/servlet/articulo?codigo=6490666
11. International Energy Agency (IEA). World Energy Outlook 2015. 2015, Paris. ISBN: 978-92-64-24366-8.
12. Bloomberg New Energy Finance. New Energy Outlook 2016. Long-term projections of the global energy sector. Wind. 2016.
13. International Energy Agency (IEA). World Energy Investment 2016. 2016, Paris.
14. Boqiang Lin, Wei Wu, The impact of electric vehicle penetration: A recursive dynamic CGE analysis of China, Energy Economics, Volume 94, 2021, 105086, ISSN 0140-9883, https://doi.org/10.1016/j.eneco.2020.105086.
15. OECD/ IEA, Energy and Climate Change. World Energy Outlook Special Report, International Energy Agency, Paris, France, 2015. https://doi.org/10.1038/479267b .
16. IRENA, Global Energy Transformation. A roadmap to 2050, International Renewable Energy Agency, Abu Dhabi, United Arab Emirates, 2018.
17. R. Contreras-Lisperguer, K. de Cuba, The Potential Impact of Climate Change on the Energy Sector in the Caribbean Region, OAS Pap. (2008). http://www.oas.org/dsd/documents/effects_of_climate_on_energy_dsd_energy_division.pdf

Modeling Wind-Turbine Power Curves: Effects of Environmental Temperature on Wind Energy Generation.

Abstract: Global warming represents a serious challenge, which requires the adoption of renewable energy technologies worldwide. However, it can negatively affect the availability of renewable energy resources, such as wind, which are needed for electricity generation. In this context, there is an increasing need for more accurate evaluations of wind turbine power curves. A novel methodology to model the power curves of wind turbines, which combines the use of artificial neural networks (ANN) and Fuzzy logic rules, is proposed in this paper. This methodology assesses the role of environmental temperature in the power curve and the impact of temperature increases on wind energy production. The application of this methodology is illustrated with the simulation of the impact of global warming on the electricity generation of a wind farm. Due to the non-linear relationship between the power output of a turbine and its primary and derived parameters, it is shown that ANN combined with an expert system formed by a Fuzzy logic module fit power curve modeling processes well. The application of the methodology shows that an increase in temperatures would trigger a small reduction in the performance of wind turbines.

Keywords: wind turbine; power curve; global warming; electricity generation; artificial neural networks

1. Introduction

Climate change represents a serious global challenge. Global surface temperatures have reached unprecedented levels [1]. As it is well-known, the accumulation of greenhouse gas emissions (GHG) is directly related to the combustion of fossil fuels in all sectors of the economy, notably electricity generation, transport and industry.

Climate change mitigation will require the adoption of decarbonisation strategies everywhere, e.g., in all sectors and countries. Concern about climate change has led to the Paris Agreement, in which governments committed to reduce those emissions in order to keep a global temperature rise well below 2 degrees Celsius (ºC) above pre-industrial levels and to pursue efforts to limit the temperature increase to 1.5ºC [1]. This entails a considerable reduction in emissions, around 50% in 2050 compared to 1990 levels [2].

Actions will need to be taken in order to improve the energy efficiency of production and consumption patterns and to increase the uptake of low carbon technologies. In this context, it is a widely shared view that the deployment of renewable energy technologies (RETs) is a critical alternative to abate GHG emissions, whose accumulation leads to global warming.

According to the IEA 2DS scenario, the installed wind capacity will need to increase from the 433 GW in 2015) [3, 4] to 2.7[1] -3.5TW [5, 6] in 2050. The total investment in wind power required in the 2DS scenario would be $3.45 trillion (2018 USD) [6].

However, global warming can negatively affect the availability of renewable energy resources, such as wind, which are needed in order to generate electricity with those technologies. Focusing on the case of wind energy, a reduction of the performance of a wind turbine due to thermal losses, operational behavior changes and a change in air density in the location caused by global warming will

[1] Calculated from the TWh estimated in [8] (see Figure 1.7) and the performance of the installed capacity and energy to be generated in [5] (Figures 1.10 and 1.11)

reduce the number of full-load hours of the wind farm. This will decrease the amount of electricity generation in the existing and new installations.

The purpose of this article is to develop a methodology to evaluate the impact of environmental temperature on wind energy generation and to simulate the losses in a real wind farm.

The power curve (PC) of a wind turbine is a relationship that describes the power output for a given wind speed [7]. The PC is currently used in the energy sector to estimate the annual production in a given location. It is a part of the control system which tries to capture most of the energy from the wind [8,9], and a tool to monitor the quality or condition of the wind turbines [10, 11].

The industry standard for PC estimation based on a field test is the IEC PC, which was developed by the International Electrotechnical Commission (IEC) and described in IEC 61400-12-1 (2005). Here, wind speed and generated power used for curve representation are 10-minute average values, with the purpose of reducing the effect of outliers, noise and serial correlation [12].

However, it has been criticized that the IEC estimate ignores the non-linearity of the ideal PC [13]. This paper analyses the effect of external temperature on the non-linearity of the PC through artificial neural network (ANN) models. A novel methodology which combines the use of ANN and Fuzzy logic rules in order to model the power curves of a set of wind turbines is proposed. The application of this methodology is then illustrated with a simulation of the impact of global warming on the electricity generation of a wind farm.

ANN models are generally parametric or non-parametric [14]. The parametric models are built from a set of mathematical equations that include parameters that must be adapted through a set of continuous data [15]. Parametric methods generally use linear, non-linear, polynomial and differential equations.

With the recent arrival of powerful databases and data science techniques, new modeling methods have emerged. Instead of assuming a physical or analytical relationship between the input and the output data, the non-parametric methods set up correlations based only on the data provided [15]. The main advantage of these non-parametric models with respect to previous methodologies lies in the fact that it is not necessary to know the nature of the dataset to be represented. Rather, the ANN itself gathers the essential characteristics of such dataset through the training process [16]. Other advantages include:

- Non linearity: the nonlinear behavior of the functions of activation of the neurons will enable the neural networks to act as universal proxies of nonlinear functions.
- They can be adapted to the development of any type of data representation by just retraining them. In contrast to physical models [17], they are less dependent on the knowledge of the "experts" for model development.

Recent efforts were mainly oriented toward the improvement of the evaluation of the actual power performance. Helbing and Ritter [7] provided a methodology for improving the wind turbine power curve with standardization. The authors developed a parametric model taking into account the role of wind turbulence in the power curve. Fan and Zhu [18] developed an optimization method of the power curve based on a parametric approach to solve the problems of large wind speed variation and low wind turbine efficiency in low wind-speed regions. Lydia et al. [19] proposed a methodology for wind resource estimation using predictive models based on ANN. It was built using exogenous variables (NLARX) combined with power curves modeled with a five parametric logistic expression. The values of the parameters were assessed with differential evolution (DE). Marčiukaitis et al. [20] proposed a non-lineal regression to model the ramp of the power curve. The model had several advantages, such as the fitting of the physical properties of the wind turbine (i.e., the power curve does not exceed the highest value generated power as it is the physically possible maximum) and the dependency with other variables such as wind direction. Pelletier et al. [15] used multilayer perceptron

ANN to model the wind turbine power curve, reducing the error of the model compared to IEC methods. In their study, power curves at wind farm level were modeled using six operational parameters, like air density, turbulence intensity or wind shear. These authors also designed a complex system with several ANN. Ouyang et al. [21] used support vector machine (SVM) algorithms to build a power curve model. In their study, authors identified three representative points of the power curve that divide it into four regions with a completely different behavior.

Regarding energy losses in the wind farm due to environmental changes, previous contributions have analysed the impact of climate change on electricity generation with RETs in general and wind energy in particular. Pryor and Barthelmie [22] provided a review proposing possible mechanisms through which global climate variability and change could influence wind energy resources. They concluded that evidences for small magnitude changes could only appear by the end of twenty-first century. In more recent studies, Fant et al. [23] presented a methodology based on the combination of the risk-based climate projection from the Integrated Global System Model (IGSM) and data from the Coupled Model Interpolation Project (CMIP-3). Their results show that significant changes in wind speed resources cannot be expected by 2050. Similar conclusions were reached by Davy et al. [24] in their assessment based on the use of a single-model-ensemble from the Rossby Centre (RCA4). Notwithstanding , using models from the HAPPI project and taking into account the distributions of sub-daily viability, the height of the wind turbine and power losses due to the grids, Scott Hosking et al. [25] concluded that the potential for wind energy in some regions may be greater than previously thought, considering a scenario of a 1.5ºC warmer world.

Compared to those contributions, this paper advances knowledge on several fronts. It provides a methodology to model the wind turbines power curve for the assessment of production losses, using a combination of ANNs and Fuzzy logic rules. This combined system takes into account the effect of the control system on the power curve model, whereas this effect is disregarded in the previous literature [7, 18-20]. If this effect is not included, then a poor adjustment in the transition parts of the power curve results. Second, although previous studies consider air density as a parameter in their model, the environmental temperature is used in this paper as a parameter with an indirect relation with air density. Our methodology reduces the number of input variables which are needed in order to take into account the effect of air density from five [19] or six [15] to just one. This is useful since the air density measurement during the resource evaluation process may be available for wind farms, but not during the whole life cycle of the asset. Third, a two-stage model (formed by two ANN in cascade) was used to simulate the production in the ramp of the power curve. In contrast, only one ANN or SVM [15, 21] model was used to characterize this part of the power curve in the previous literature. Fourth, an analysis of the impact of global warming on wind energy production is carried out, using a model of wind energy generation based on ANN. The energy and economic losses in the wind farm used for this study have been assessed. Whereas simulations are mostly carried at macroscopic level in the literature and special attention to environmental temperature is not given, different scenarios with several increases in environmental temperature due to global warming at wind farm level are simulated in this paper.

Accordingly, the paper is structured as follows. Section 2.1 briefly describes ANN and Fuzzy logic techniques. The methodology developed in this article to assess the relationship between energy production and temperature is elaborated in section 2.2. Section 2.3 describes the analytical model. The methodology is illustrated with an application in section 3, where simulations of performance losses under different environmental conditions, as well as the economic losses in the wind farm, are provided. The paper closes with some conclusions and suggestions for future research.

2. Materials and Methods

2.1. A description of modeling methods.

2.1.1. Artificial neural networks (ANN)

Artificial neural networks (ANN) are systems inspired by biological neural systems (animal brain). They are made up of a set of simple processing elements, called neurons or nodes, which are connected among each other through links which have a modifiable value called "weight".

Each neuron can receive information from other neurons (which are inputs to them) and from an external input and it can generate output information which, in turn, can be input information for other neurons. With the information which each neuron receives, the neuron creates an output value which is a function of the linear combination of the values of its inputs, as included in expression (1). In such expression, y_i refers to the output value of the neuron i, x_j is the input value of j (output value of the neuron, also named with the index j), w_{ij} is the weight of the connection between neurons i and j, θ_i is the threshold or *bias* of the neuron and f_i is the activation function. This activation function can be linear, but it is usually non-linear (sigmoidal, gaussian, etc.). This non-linearity of the activation function allows the neural network to be the universal proxy of non-linear functions. The structure of one neuron is shown in Figure 1.

$$y_i = f_i\left[\sum_{j=1}^{n} w_{ij} \cdot x_j - \theta_i\right] \quad (1)$$

Neural networks can be split into feed-forward networks and recursive networks, depending on how the neurons are connected. In feed-forward (or unidirectional) networks, the neurons are connected following the direction of the input to the output. The recursive networks have connections between neurons in the opposite direction.

The structure of a neural network is determined by the arrangement of the neurons, their interconnections and their activation functions. Neurons are organized in layers. Those which are not input layers (i.e., those which provide an external output) are considered as "hidden". The set of values which are presented to the neurons of the input layer (a value per neuron), which correspond to the inputs of the neural network itself, are called "value of the input vector".

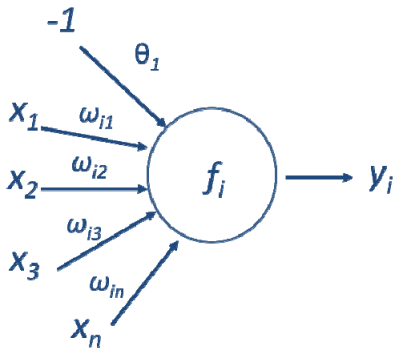

Figure 1. Processing of the information in a feed-forward neuron.

The main characteristic of neural networks is their learning capacity. This learning is the adjustment of the weights of the connections between the neurons which takes place in an interactive manner in order to achieve a desired effect. It refers to "learning" the existing relationships between

pairs of values of vectors of inputs-outputs, or finding a common pattern in the input data in order to classify them according to the different patterns.

The multilayer perceptron (MLP) or neural network MLP is a type of feed-forward neural network in which the neurons are organized in layers and, thus, the inputs for a neuron located in an intermediate layer can only be the outputs of the preceding layer and its output serves as the input for the neurons of the following layer. Its graphical representation is provided in Figure 6, which shows two consecutive networks. In the first one, the blue neurons make up the input layer (each neuron of the input layer has an external value), the red neurons make up the intermediate layers (or "hidden" layers) and the gray neurons make up the output layer (the output value of each neuron is one of the outputs of the neural network).

A MLP neural network can have several hidden layers, although a single hidden layer could be able to approximate any continuous delimited function (whether linear or not) with a small error and two hidden layers are able to approximate any continuous function (without any error).

The design of a MLP neural network implies the selection of the number of hidden layers and the number of neurons in each layer. The greater the number of layers and neurons, the greater the capacity of the MLP neural network to adjust any function.

However the time needed to train it (in order for the network to learn) will increase and there is a risk that the network is overtrained. Supervised learning techniques of the neural network have been used. Previous data, which allow comparing the fitness of the model and reality, are used in those techniques. The model is adjusted depending on the estimation errors. However, a drawback of these techniques is that there is a risk that the model is over-trained. The result of over-training is that the neural network perfectly fits values that have been given to it in the input vector, giving the required value of the output vector or a very relatively close value which, however, has been "adapted" too much to those data. This leads to a loss of capacity to generalize the prediction. Any value of the input vector other than that used in the training of the neural network can provide poor results.

There are different learning and training techniques for MLP neural networks. In this study, the error back-propagation technique has been used. This technique basically consists of updating the weights of the connections between neurons in proportion to their contribution to the error. In our case, the weights of the neural network are updated after presentation of the entire set of values of the input vector of the training data (which constitutes an "epoch").

The updating of the weights of the neural network is carried out after each value of the input vector is presented. The variation in the weight of the value of the input vector n, $\Delta w_{ij}(n)$, the connection between the neurons i and j (neuron i located in a layer posterior to the neuron j), is given by expression (2) where η refers to the so-called learning factor (a constant number, also called "step"), δ_j is the gradient of the local error of the neuron j, $o_i(n)$ is the output value of the neuron i for the value of the input vector n, α is a coefficient called "moment" and $\Delta w_{ij}(n-1)$ represents the variation of the weight of the connection between neurons i and j for the value of the input vector $n-1$.

$$\Delta w_{ij}(n) = \eta \delta_j o_i(n) + \alpha \Delta w_{ij}(n-1) \qquad (2)$$

The gradient of local error for a neuron of the output layer is the product of the derivative of the chosen error function and the activation function of the neuron. The gradient of the local error for a neuron of a hidden layer equals the weighted sum of the gradients of local errors of the neurons to which the connections from such neurons are linked (the weight of each connection acts as the weighting factor). The weighting of the connection between neurons i and j for the following value of the input vector $(n+1)$ is given by expression (3).

$$w_{ij}(n+1) = w_{ij}(n) + \Delta w_{ij}(n) \quad (3)$$

In expression (2), the coefficients η and α are two constants. A high value of the learning factor η implies that the neural network reacts quickly to changes in the inputs, but it also leads to an unstable neural network if it is very high. On the contrary, a low learning factor leads to an increase in the time needed for training the neural network.

The coefficient α, (or "moment") describes the part of the change in the weight which is added to the next updating of the weights. A low value of the moment leads to an unstable training, it causes fluctuations in the values of the weights of the connections and hinders the learning of the neural network. The maximum value for the moment is 1 and the most usual values are between 0.5 and 0.9.

Various techniques prevent over-fitting or over-training of the neural network, including limitation of the number of epochs in the training process (these were limited to 5,000), the addition of white noise to the values of the input variables and the use of cross-checking. In the latter technique, which is the most widely used, the available data are divided into two groups: training and cross-checking (15% in the case presented here).

The data from the training group are used in order to fit the parameters of the neural network according to the training method which has been chosen. The data from the cross-checking group are not used in determining the error which has to be minimized with the training of the neural network, but instead are presented to the neural network after each training epoch. The training process is interrupted when a given number of epochs have gone through without a reduction in the error from the cross-checking data.

2.1.2. Fuzzy logic

The Fuzzy logic is a technique which aims to include the structured human knowledge in efficient algorithms. Many human intellectual processes are based on inductive reasoning. A clear example is the reasoning which leads to logical structures such as "IF…THEN". We can thus argue that human knowledge is structured in rules such as "IF…THEN", and that this combination of rules leads to actions and decisions. A rule of this type is a function of multiple variables which relates the variables associated to "IF" and named "antecedents" or "causes" to the variables associated to "THEN", which are named consequences or effects.

One of the features of human knowledge is that it characterizes situations, elements, properties, etc. in a fuzzy or vague manner. However, there is an inherent uncertainty in this idea: which is the frontier between a high and a normal ambient temperature? This uncertainty can be delimited in mathematical terms through a so-called membership function. This is the mathematical expression of degree between 0 and 1 which values the membership of an element to a given set defined by an specific fuzzy term (in this case "very high").

A fuzzy universe can be one which applies to different zones of the power curve of the wind turbines defined in section 2.2. Fuzzy sets can be applied, for example, to zones of start-up, rise and nominal capacity of the equipment, as a function of the control strategy of the manufacturer, as shown in Figure 2.

A fuzzy set is represented by a label (for instance, Z), which takes values within the universe X. This is characterised through a membership function μ_Z, which takes values between 0 and 1. The mathematical expression for a fuzzy set is reflected in expressions 4.1 and 4.2

$$A = \{(x, \mu_Z(x)) \mid x \epsilon X\} \quad (4.1)$$

$$\mu_Z : X \rightarrow [0,1] \quad (4.2)$$

The membership function is a function which links each element of the fuzzy set to a value within the interval (0,1) and within the universe. The most usual membership functions are: triangular, trapezoidal, Gaussian, sigmoidal and normal. Figure 4 shows four membership functions for four fuzzy sets defined for the universe in the interval (0,30). The four membership functions are trapezoidal and represent the different strategies for the operation of a wind turbine.

2.2. Wind turbine power curve and performance dependency with environmental temperature

Horizontal axis wind turbines generate energy based on the power curve of Figure 2. As is shown, the power depends on the wind speed (for a reference air density). The energy generated by a wind turbine will therefore be the integral of the instant power ($P(t)$) in a given period ($[t_0,t_1]$), according to expression (5). Currently, the dominant method to calculate the energy produced by wind farms is based on the use of this static curve.

$$E_{t0}^{t1} = \int_{t0}^{t1} P(t) \cdot dt \quad (5)$$

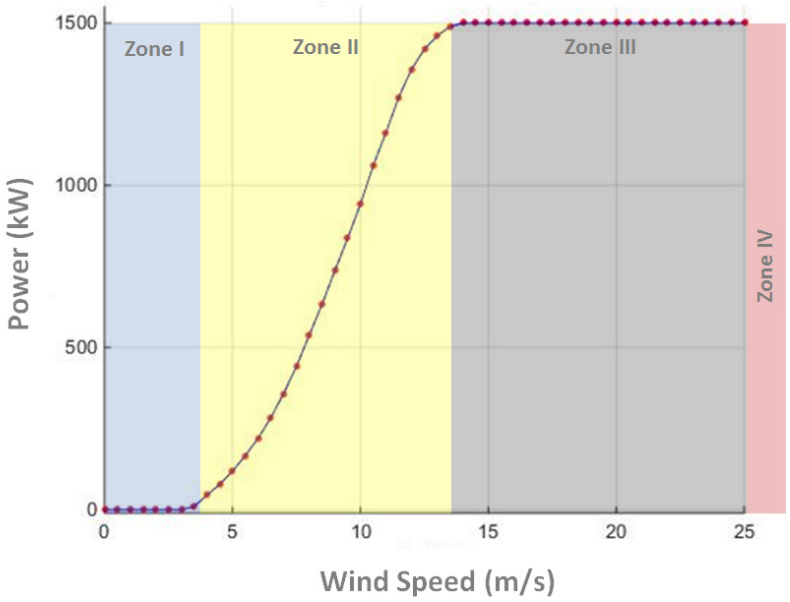

Figure 2. Wind turbine power curve (*Pow-ws*) for reference air conditions (with T_{ref}=25ºC and P_{ref}=1,001 bar).

The power curve can be divided into four different zones according to the control strategy [21], which will affect the behavior of the pitch control and, thus, the exposure of the surface of the blades to airflow changes. In Zone I, the wind turbine stops due to the fact that there is not enough wind to move the hub. Zone II represents the acceleration slope, in which the blades expose their entire surface to capture as much energy as possible from the air. When the wind turbine reaches its nominal power, represented in Zone III, the control system changes the pitch in order to keep the energy captured from

the air constant. Finally, in zone IV, the wind speed is too high to operate the wind turbine in safety conditions and it is stopped.

This power curve depends on the air density at each moment. For that reason, the wind turbine manufacturer provides power curves for different air density scenarios. According to Betz's Theory, the ideal relationship between the wind speed and the power generated by the wind turbines can be defined by expression (6) [7,19,21]:

$$Pow = Cp \cdot \frac{1}{2} \cdot \rho \cdot A \cdot ws^3 \quad (6)$$

Where Cp is the power coefficient, ρ is the air density, A represents the whipped area of the blades and ws is the wind speed.

There is a relation between air density and external temperature and, consequently, the production model should automatically change according to this effect. In this article, a production model that characterizes this power curve for a specific wind turbine technology [15] has been developed, but the wind speed as well as the external temperature have been included as inputs to the model. We illustrate this methodology with different production scenarios, considering different levels of increase in the environmental mean temperature. The power curve is provided by equipment manufacturers for a given air density since, depending on such density at a given moment, wind will transport more or less energy (for a given wind speed) [18]. Since density is equal to the mass divided by the volume, air density affects mass per unit of volume. Thus, the greater the mass (per unit of volume) is, the greater its energy for a given wind speed will be. This effect is shown in Figure 3.

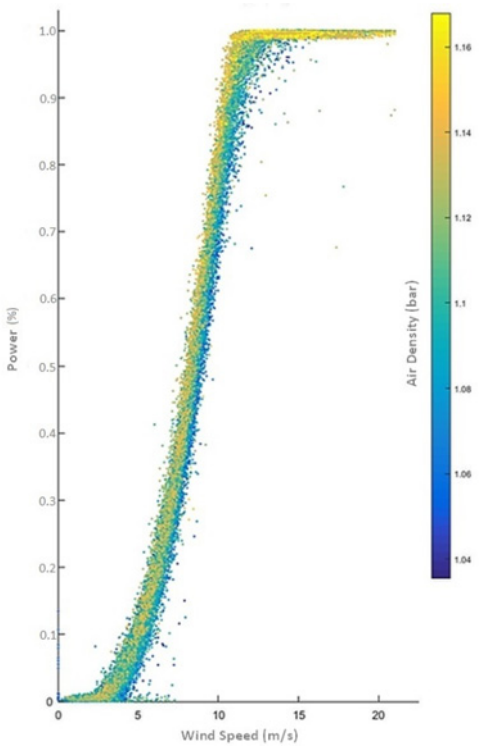

Figure 3. Wind turbine power curves (*Pow-ws*) for different air densities (in the color scale).

Figure 3 represents the normalized power (*Pow*) generated as a function of wind speed measured at the rotor hub (*ws*). The figure shows the power curves of a wind turbine of the wind farm analysed in this article at different moments during the year. The colour indicates air density in each moment. In the inner part of the figure, a greater concentration of blue points (low air density) can be observed, whereas there is a concentration of yellow points (greater air density) in the outer layer of the figure. When air density is higher, the power curve shifts to the left. With a lower wind speed (but higher air density), more energy is produced. Therefore, with a lower air density, the turbine needs a higher wind speed in order to generate the same amount of electricity. A Higher density air entails more particles (mass) in the same volume of air. All these particles have kinetic energy that can be captured by the blades. Temperature increases reduce the number of particles in the same volume of air. For that reason, the energy of a volume of wind in movement is lower. Using expression (6) and the Ideal Gas Law expressions (7), the wind speed measured (ws_{real}) can be adjusted to the effective or reference wind speed (ws_{ref}) through two physical variables: atmospheric pressure (*P*) and temperature (*T*) measured at the site. As suggested by expression (8), a higher T_{real} (measured at the site) leads to a lower effective speed.

$$P \cdot V = n \cdot R \cdot T \tag{7.1}$$

$$P \cdot V = \frac{m}{M} \cdot R \cdot T \tag{7.2}$$

$$P \cdot M = \frac{m}{V} \cdot R \cdot T \tag{7.3}$$

$$\frac{P \cdot M}{R \cdot T} = \frac{m}{V} \tag{7.4}$$

$$\rho = \frac{P \cdot M}{R \cdot T} \tag{7.5}$$

It can also be observed that, according to expression (6), the theoretical power depends on the air density (ρ) which, in turn, depends on other factors such as temperature. The parameter (*R*) is the constant of ideal gases. We can use the ideal gas law (expression (7.1)) and perform some stoichiometric calculations of the density of a gas (expression 7.5). This expression shows how the density of the gas depends on temperature. The number of moles is equal to *m*/*M*, where *m* is the present mass, *M* refers to the molecular mass of the gas and the density is *m*/*V*. From expression (6) it is possible to obtain expression (8) by considering two different environmental scenarios and matching the energy produced.

$$ws_{ref} = ws_{real} \cdot \sqrt[3]{\frac{P_{real} \cdot T_{ref}}{P_{ref} \cdot T_{real}}} \tag{8}$$

The reference values (ws_{ref}, T_{ref} y P_{ref}) are the parameters that feature the conditions of operation of the equipment (determined by the manufacturer). The power curves used by the SCADA (Supervisory Control And Data Acquisition system) of operation are fixed for predefined (or reference) conditions (based on the fact that the operation of the equipment is regulated).

The methodology developed in this paper is based on the fact that the neural network itself is able to transform the values measured in the wind turbine (ws_{real}) at an effective wind speed (ws_{ref}), only considering the variable ambient temperature (T_{real}). Therefore, the neuronal network will be able to

reproduce the hidden nonlinearity in the relationship (P_{real}/P_{ref}). It is necessary to follow this approach since, although the average thermal increase is known, it is unknown how climate change will affect the barometric pressure of the sites (P).

2.3. Wind turbine power curve model

This section describes the methodology developed to assess the performance losses based on the wind turbine power curve [21].

2.3.1. Data pre-processing

The data used for the development of the models come from 20 wind turbines located in Spain, with 1.5MW of unit power for a period of 4 years (approximately 4,204,800 ten-minute time records). The first years of operation of the 20 wind turbines were considered for building up the model (2008 and 2009) and the data of the following two years (2010 and 2011) were used to calculate the errors of the model. The production history of the wind farm which is used to perform simulations of the loss of performance corresponds to the entire period of 4 years (2008-2011).

Based on the expert assessment and preliminary studies, the variables of the wind turbines considered for building the energy production model of the wind turbines were:

- Air Temperature [ºC].
- Barometric Pressure [bar].
- Wind speed [m/s].
- Power [kW].

Once the variables are selected, outliers in the samples need to be identified. These outliers can be physically impossible temperatures (due to failures in measurement equipment) or non-typical data due to abnormal operation condition of the turbine [15]. The data processing consists of two stages: filtering (manual/statistical filter) and data normalization. For each of the variables under consideration, this filter only eliminates values that do not make any sense taking into account the logical perspective of operation [26,27]. These values are possibly due to faults in the sensorics or a result of a clearly anomalous operation. Given that no limits of the operating variables were known, a statistical study was undertaken through an assessment of distribution parameters (mean and standard deviation). Based on the values obtained, the operating limits (lowest and highest) were obtained for each variable based on an expert judgment.

The applied manual/statistical filter has been:

- $-10 < T$ (ºC) < 50
- $4 \leq ws$ (m/s) ≤ 13 (when modeling zone 2)
- $900 < P$ (bar) $< 1{,}050$
- $0 <$ *Pow* (% of rated power) $< 96\%$ (1,450kW) (when modeling zone 2)
- *ws* (m/s) ≥ 5 & *Pow* (% of rated power) < 2.5[2]
- *ws* (m/s) < 4 & *Pow* (% of rated power) > 7.5[3]

[2] If the wind speed is higher than 5 m/s but the *Pow* is lower than 2.5, the turbine is damaged or stopped and, thus, the corresponding data should be removed.

[3] Likewise, if the wind speed is lower than 4 m/s but the *Pow* is higher than 7.5, the anemometer is either damaged or broken. Therefore, the corresponding data should be removed.

- The equipment has been available 100% of the 10-minute period of the data.

Because the models are built with input variables from different units and scales, the data have to be normalized in order to be able to compare the fluctuation scale of different variables and to ensure that more weight is not given to a variable with higher figures. The variables were normalized according the expression (9):

$$i_{t\ Normalized} = \frac{i_t - i_{min}}{i_{max} - i_{min}} \quad (9)$$

Where i_t is the value recorded by one of the variables at time *t*, i_{min} is the minimum value of each variable in the entire population set and i_{max} refers to the maximum value of each variable in the entire population set. The entire data set, including simulation data, is considered.

However, the i_{max} value must be corrected taking into account the ambient temperature variable. This variable is increased manually in simulations with values up to 6ºC higher than those registered. Therefore, the neural network model must be prepared for this if the aim is to correctly simulate those temperatures. This is achieved by changing $i_{maxS} = i_{max} + 6$ºC.

During the process of the standardization of variables, the statistical parameters of each variable should be saved, due to the fact that the data which is subsequently used as input in the model for global warming simulations should be normalized based on these parameters. Therefore, the global warming simulation temperature data set must be normalized with i_{min} and i_{maxS} of the training data set in order for the model to be applicable.

The model of electricity production based on neural networks applies only to the zone of the ramp of the power curve because, for wind speeds higher than 13m/s and lower than 25m/s, the power delivered by the equipment will be the nominal one. This is because the adjustment of the pitch will allow capturing more energy from wind in order to maintain the torque (or the revolutions of the generator).

2.3.2. Power curve modeling methodology

Currently, the dominant method to calculate the energy that can be produced by wind farms is the curve Power-Speed of wind at a given site (Figure 2). The drawback is that this curve is fixed for a given air density and the power which can potentially be produced is estimated only as a function of the wind at a given moment. However, as shown above, the actual power being produced is not only dependent on the wind but also on air density.

Therefore, there should be a different power curve for each air density or a non-linear model which considers the electricity which can be produced as a function of wind and density (or alternatively, as a function of other representative variables such as temperature and humidity). There is a wide array of mathematical and statistical techniques which can be used to calculate the power curve of a wind turbine [28,29]. However, the difficulty to build an analytical model based on equations which simultaneously include the impact of the aforementioned factors led us to use "black box" modeling methods and, particularly, ANN [15,30,31].

The model is an expert system made up of a module of Fuzzy logic rules and three submodels. The module of Fuzzy logic rules is responsible for the selection of the submodel which applies at each moment. It identifies the operation zone of the power curve (Figure 2) where the wind turbine is at each moment (t).

The power curve can be divided into four (4) different regions:

1. Zone (1), where the wind energy is insufficient to start-up the wind turbine movement. In that case the expert system would apply the model $Pow = 0$.
2. Zone (2) is called the ascending ramp, where the wind turbine is accelerated until its nominal rotation speed rises. In that case, the expert system will apply the neural network model later described .
3. Zone (3), where the wind turbine rises to nominal power. In that case, the expert system will apply the model $Pow = Pow_{nominal}$.
4. Zone (4), where the wind energy is excessive to operate under safe structural conditions. In that case, the expert system will apply the model $Pow = 0$.

For each operational zone, a model was built. The Fuzzy logic rules system identifies which model should be used at each moment. According to these rules (Figure 4), data will be marked every ten minutes with the number of the zone it belongs to. The transition between zone 1 and 2 is effective when $ws_{real}(t) \geq 3$m/s. The transition between zones 2 and 3 is effective when $ws_{real}(t) \geq 13$m/s. Finally, the transition between zones 3 and 4 is effective when $ws_{real}(t) > 25$m/s.

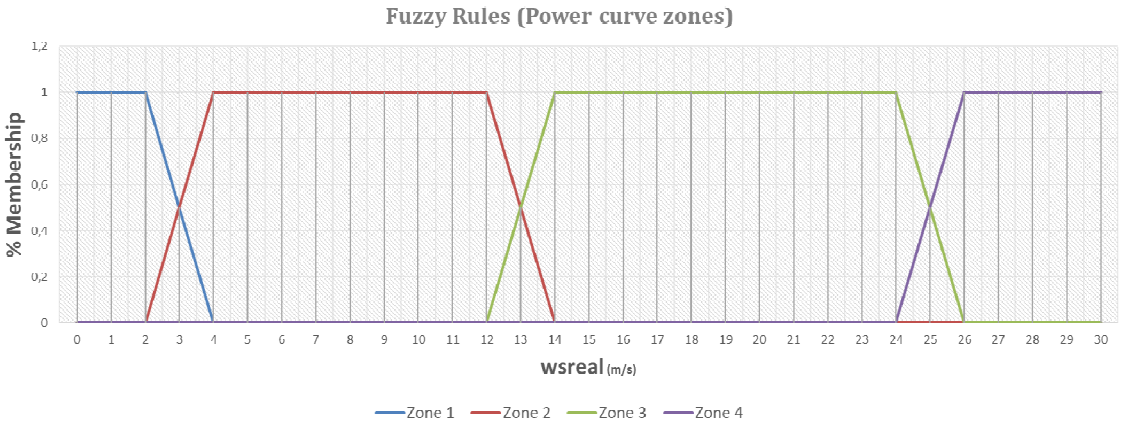

Figure 4. Fuzzy logic rules to classify the operational state.

As it was shown in Figure 3, the air density mainly affects the zone 2, which corresponds to the acceleration ramp. For that reason, it has been assumed that global warming will not affect the performance of the wind turbine when it works in zones 1, 3 or 4.

Figure 5 represents the expert system that activates the model which applies in each moment according to ws_{real}. The model for zone 2 (red line in Figure 4) is made up of two neural networks (Figure 6). One of them adjusts the wind speed ws_{real} to ws_{ref} (with T_{ref}=25ºC and P_{ref}=1,001 bar), whereas the other network estimates the power that can be produced from ws_{ref}. This second neural network could be replaced by the power curve of the manufacturer for the given reference conditions. However, we have decided to calculate the real curve for the wind turbines of the wind farm since, as mentioned in the literature [15,28,29], each wind turbine has a specific curve as a function of many determining factors, including its location, presence of nearby wind turbines and configuration parameters.

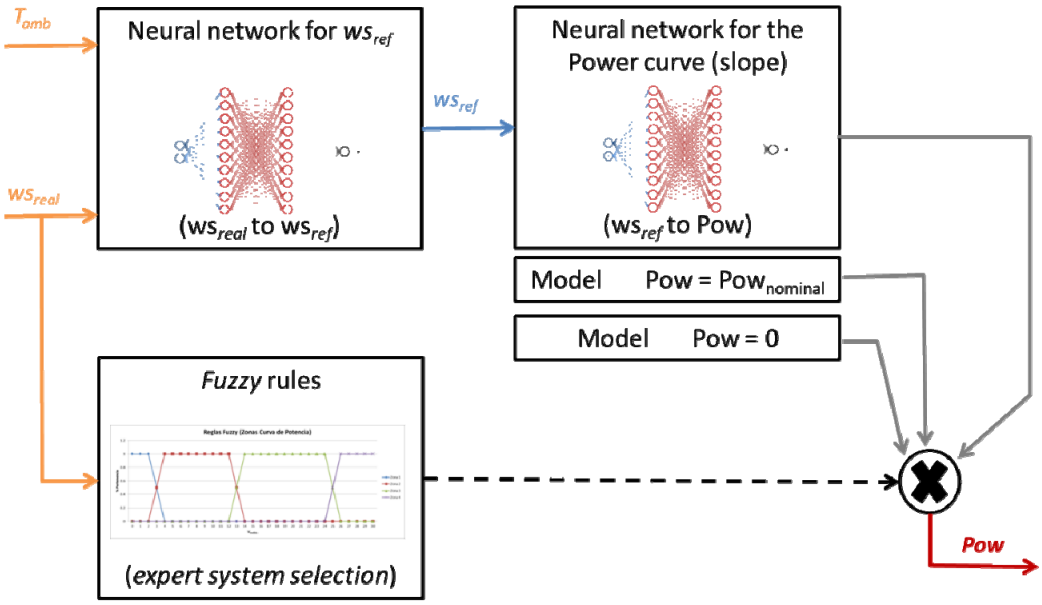

Figure 5. Conceptual scheme of the expert system with the Fuzzy logic rules and two neural networks models used for the characterization of the energy that can potentially be produced in the zone corresponding to the ramp.

Therefore, two neural networks of the MLP type were used in order to build the production model which includes global warming variables. This is a type of neural network in which the neurons are organized in layers, so that the input of a neuron located in an intermediary layer can only be the output of the preceding layer, while its output serves as the input for neurons in the next layer. This is shown in the graph in Figure 6, where the input layer is formed by the aforementioned operating variables, two inputs for the first net in blue (ws_{real} and $T_{real\text{-}simulated}$) and the corrected wind speed (ws_{ref}) for the second net in green. After the input layer come the neurons named intermediary or hidden layer. A structure of two hidden layers [15] with ten neurons (n) per layer was used in the development of both neural nets ($n_{1.x}$ for the first layer and $n_{2.x}$ for the second one, where $x \in \{1,\ldots,10\}$). Finally, the nets present the neurons forming the output layer in grey, the output values are the ws_{ref} in the first net (out_1 in Figure 6) and the energy production (Pow) for the second one (out_2 in Figure 6) during the interval of time.

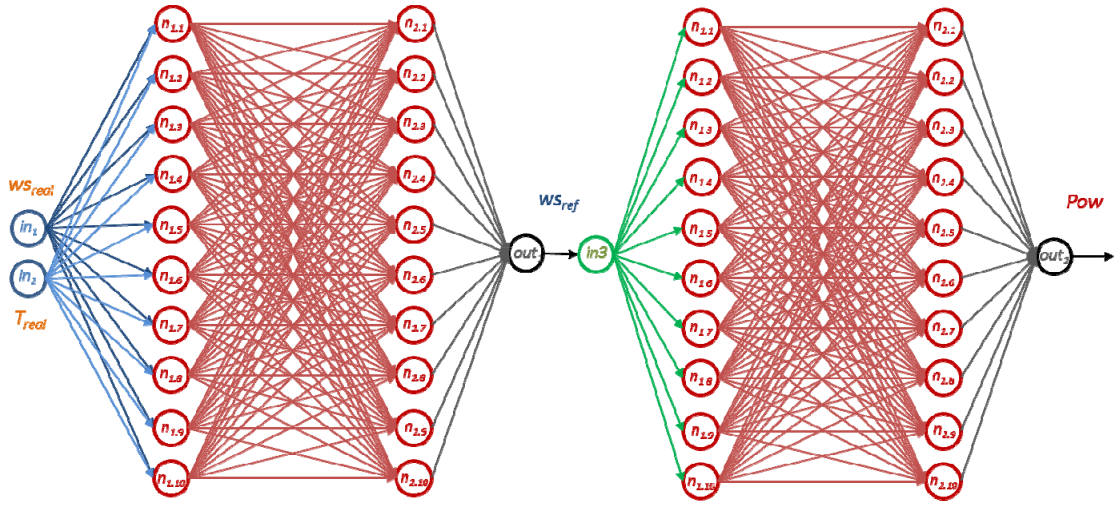

Figure 6. Illustration of both MLP ("MultiLayer Perceptron") neural networks, with the wind adjustment on the left and the power curve on the right.

As mentioned above, the first neural network replaces expression (8) that relates ws_{real} with ws_{ref} based on barometric pressure and ambient temperature. Therefore, it is necessary to have the operating data of the first two years for several variables in order to train this neuronal network: wind speed (ws_{real}), measured barometric pressure (P_{real}) and measured temperature (T_{real}). Expression (8) is applied and the reference wind speed (ws_{ref}) has been calculated for this data set. Using this procedure, the neural network can be trained, considering ws_{real} and T_{real} as inputs and the objective variable ws_{ref}. Thanks to this training, the ws_{ref} can later be estimated considering only ws_{real} and T_{real} as inputs. This will allow us to carry out simulations in which T_{real} is changed according to the temperature increases due to the effects of global warming (T_{realGW}).

3. Results

3.1. Estimating wind production with the model

The model of wind energy generation, which takes into account wind speeds and the temperatures at the site, has been estimated and increases in temperatures have been simulated.

In order to visually verify the goodness of fit of the model, Figure 7 shows the real production of the wind turbine (in blue) and the production estimated by the model (in green) for a short period of time as an example.

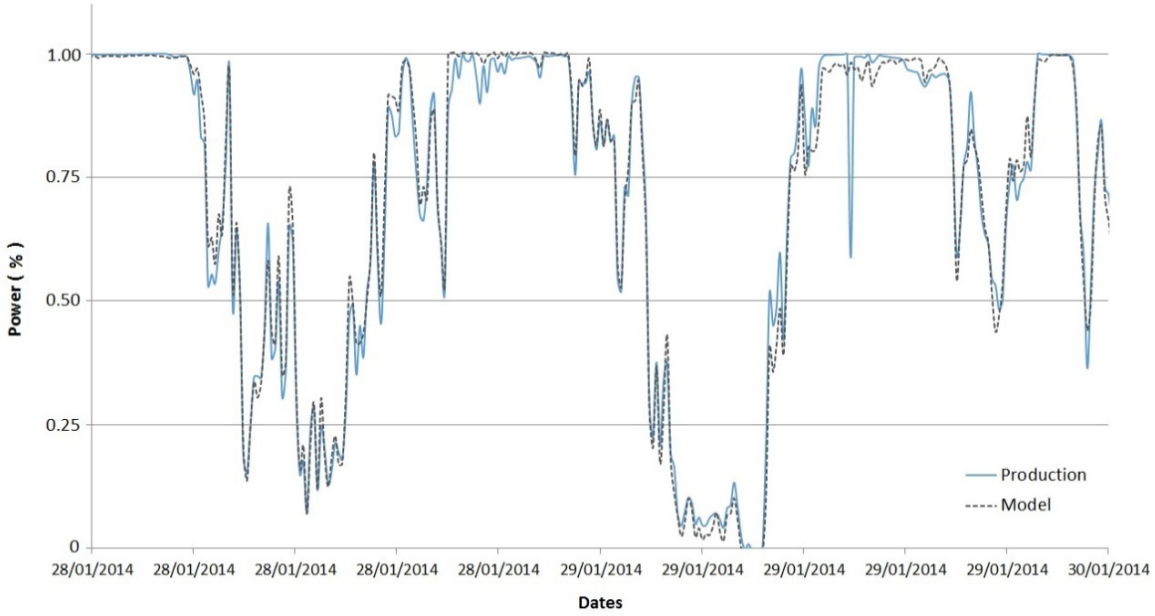

Figure 7. Illustrating the difference between real and estimated production.

Note: the continuous line refers to the real normalized production of a wind turbine and the dotted line represents the estimated production.

The goodness of fit of the model (zone 2) is very good (R2 = 0.9935 in Figure 8), since it is a wind farm or a technology-level model. A single model of producible energy at the wind farm level was built. 283,681 10-minute records of zone 2 were available for the 20 wind turbines in the farm. Since the first 2 years of operation of the 20 wind turbines were used for model training, a total of 2,102,400 records were used for training and another 2,102,400 different records were used for the validation. It should be taken into account that a large number of these records had "null" data due to the filtering criteria. The average percentage error obtained with the validation data set was -0.39% and the average error was -8.69kW. The average percentage error of the whole expert system, considering zones 1 to 4, was -0.23% (see the joint response of the models in Figure 9).

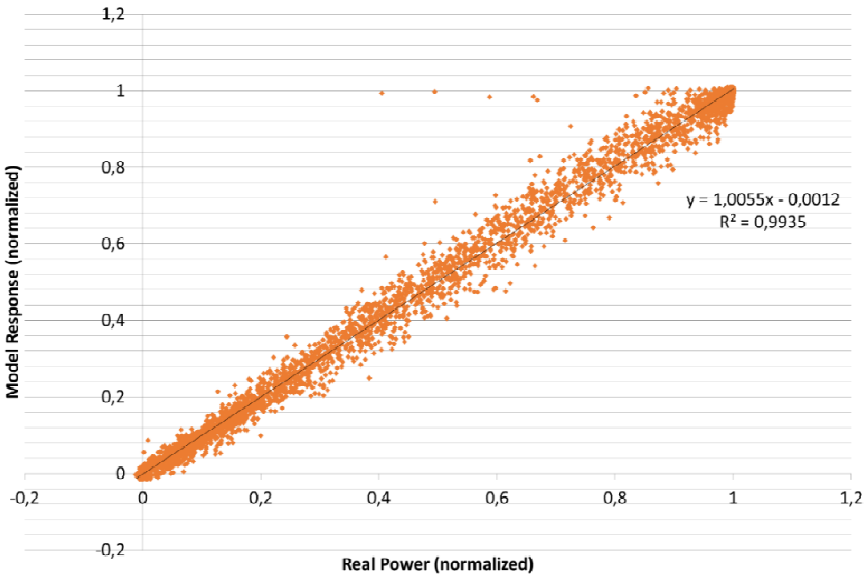

Figure 8. Regression line between the normalized real power (x-axis) and power estimated by the wind energy model (y-axis).

Figure 9 shows the power curve for different environmental conditions. The x-axis refers to wind speed (ws_{real} in m/s), whereas the y-axis represents wind energy generation (Pow) for different temperature values (shown in color). The degradation due to climate change will only affect the ramp-up part of the curve ($ws_{real} \geq$ 4m/s and $ws_{real} \leq$ 13m/s). In the upper part (ws_{real} >13m/s), the wind turbine reaches the nominal revolutions and these are maintained by adjusting the angle of the blades. As a result, the wind turbine is able to capture more energy. This will mitigate the losses due to climate change, i.e. they will not be as high as expected. The plotted model shows the relevant impact of external temperature, mainly in the zone close to nominal power, where the control system starts the adjustment of the blades' pitch. It can be observed that days with higher temperatures move the curve to the right.

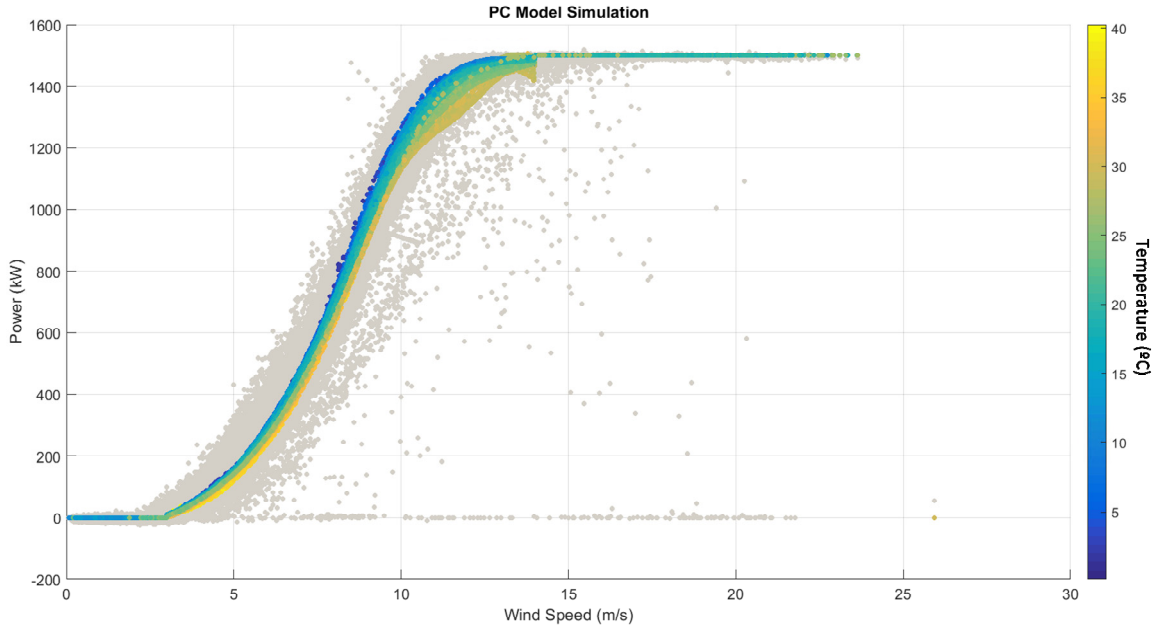

Figure 9. Power curve of a wind turbine. Real sample data vs fitted model for reference parameters.

3.2. An application of the methodology

This section illustrates the methodology with a calculation of the loss of performance of the wind turbines under different warming conditions (e.g., for each additional degree of global warming). It has been shown that the thermal increase would affect the ramp-up part of the curve. As it can be observed in Figure 10, neural networks estimate a power curve for the turbines depending on the temperature (ws_{real} – *Pow*). Using this model, different global warming scenarios were simulated by gradually increasing the temperature at the site. In other words, if the temperature registered was 30ºC, one additional degree of global warming would have increased the temperature to 31.5ºC in the 2DS scenario (since, currently, warming is around 0.5ºC [32]).

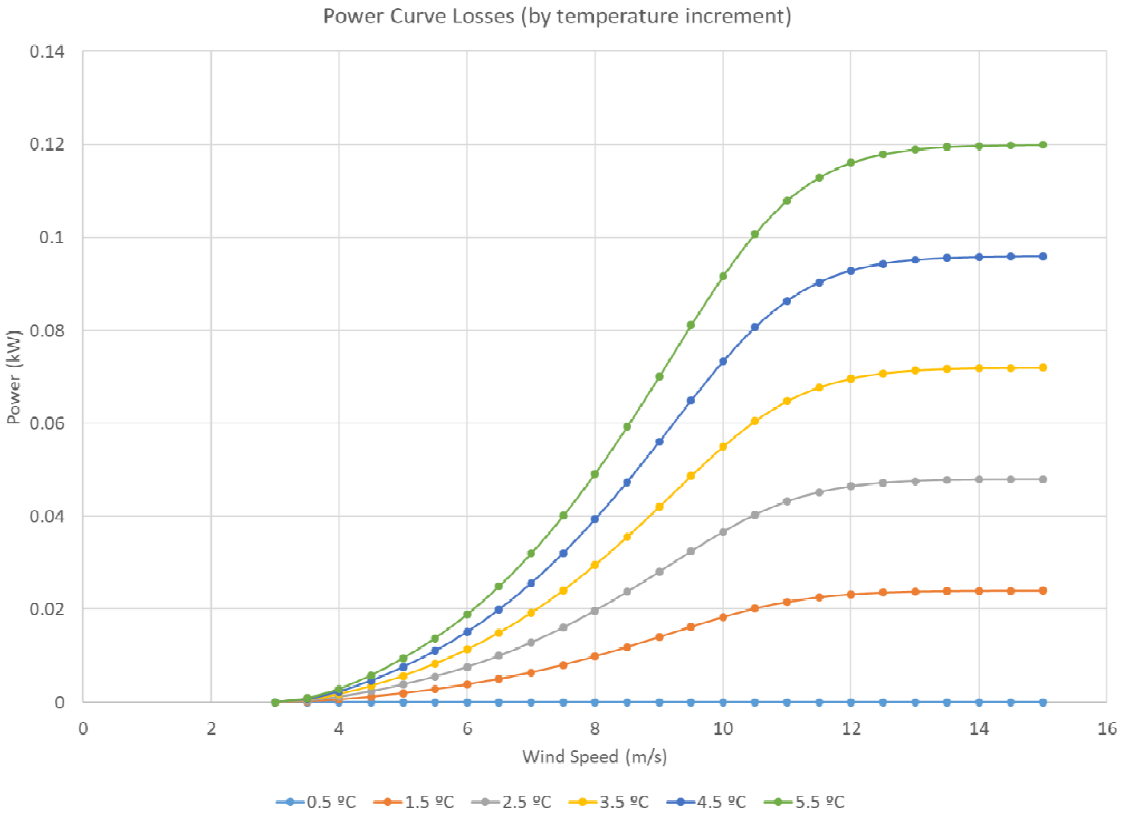

Figure 10. Losses in the power curves for the different global warming scenarios. Temperature increases from the current reference situation are considered. Power represents the losses from the reference scenario (0.5ºC).

The historical data of the wind farm used in this article refer to the period 2008-2011. According to [31], the global warming experienced in this period was above 0.5ºC. Departing from this starting point we have analysed scenarios with higher global warming (at 0.5ºC intervals, from 0.5ºC to 6ºC).

In order to simulate the possible impact of global warming on the wind farm's electricity production, it has been assumed that wind conditions (direction, frequency and intensity) are constant and that only average temperatures (and, thus, density) change [22-24]. Under these premises, the production of the wind farm has been simulated (as a sum of the individual production of each turbine) using the available historical data and increasing the average temperature.

Since there is an intrinsic error between the model and the real production of the turbine, the performance loss will be calculated with respect to the production estimated by the model under current temperature conditions (0.5ºC) and not with respect to the current production. A performance indicator was created, from which the percentage loss of installed power based on temperature was

obtained (Figure 11). By way of example, the wind farm performance in a scenario of a global warming of around 6ºC is calculated as $Performance(\%)_{6ºC} = 100 \cdot (Production_{6ºC} / Production_{0.5ºC})$.

Since global warming will gradually increase over time, the loss of performance will not immediately start now, but will also be gradual from 2015 to 2050. Therefore, a continuous function which relates the loss of performance and the thermal increase due to global warming has been used ($\eta = f(\Delta T_{GW})$). The adjustment shown in Figure 11 and its adjustment function are represented by expresion (10). This expresion of the thermal increase (and, thus, the progressive degradation of the performance) is used in order to calculate the energy which has been lost during the period. It was obtained through an assessment of the trend curve that best fitted the discrete values of the performance losses of the different simulations.

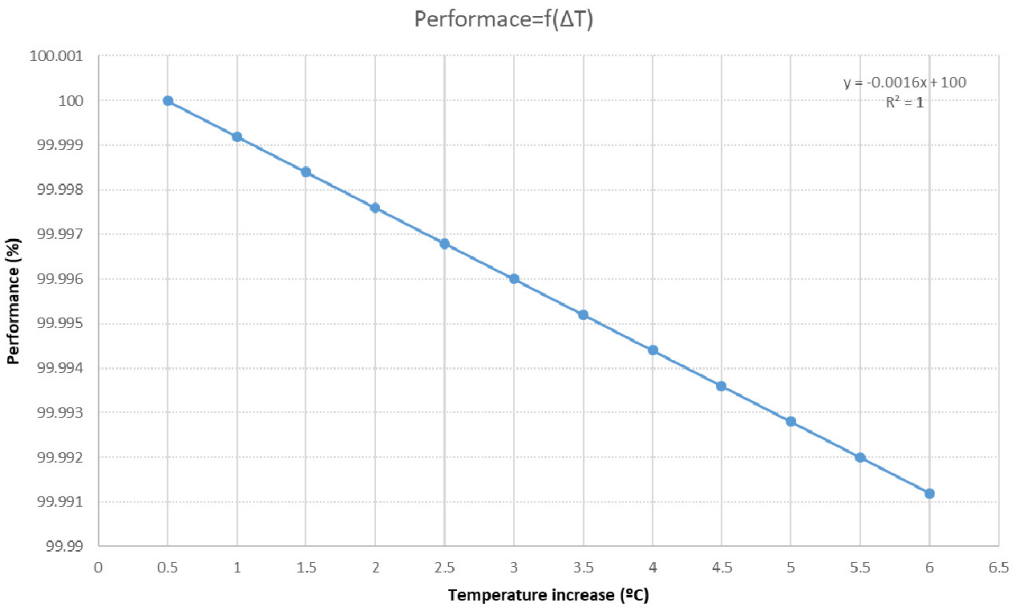

Figure 11. Continuous performance losses as a function of external temperature increases for the considered scenarios.

$$Performace = 100 - 0.0016 \cdot (\Delta T - t_0) \qquad (10)$$

where ΔT represents the increase in temperature due to global warming. The offset t_0 corresponds to the current warming of 0.5ºC.

The environmental thermal increase has been simulated according to expressions (11) and (12). Figure 12 shows the thermal increase in the 2015-2050 period in the different scenarios: Current scenario (0.5ºC), 2DS scenario (2ºC) and Current Policies scenario (6ºC). This last scenario would be the one projected until 2050 by the IEA if current energy policies continue to be implemented [5] and the generation mix is similar to the one that we have today.

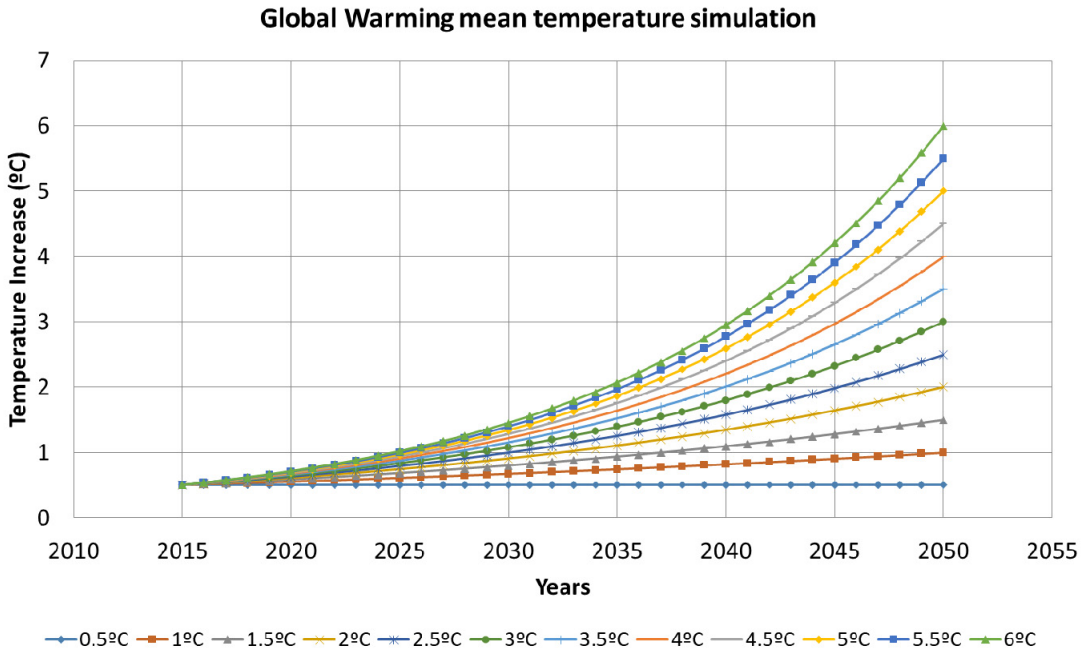

Figure 12. Mean temperature for the different scenarios.

The curves for the thermal increase have been built according to expressions (11) and (12):

$$\Delta T_x = t_0 . a^x \tag{11}$$

$$a = \sqrt[35]{\frac{t_f}{t_0}} \tag{12}$$

where ΔT_x represents the thermal increase (y-axis), t_0 is the initial temperature (0.5ºC for 2015), t_f is the maximum admissible temperature for 2050 (in the 2DS), 35 is the number of intervals from 2015 to 2050 and x is the number of intervals for which we would like to know the warming (for 2030, x=15).

The joint expression obtained after merging expressions (10), (11) and (12) allows us to directly calculate the performance loss over time according to the expected evolution (expression 13). These expressions have been jointly represented in Figure 13.

$$Performace_i = 100 - 0.0016 \cdot t_0 \cdot \left(\left(\sqrt[35]{\frac{t_f}{t_0}} \right)^{year_i - year_0} - 1 \right) \tag{13}$$

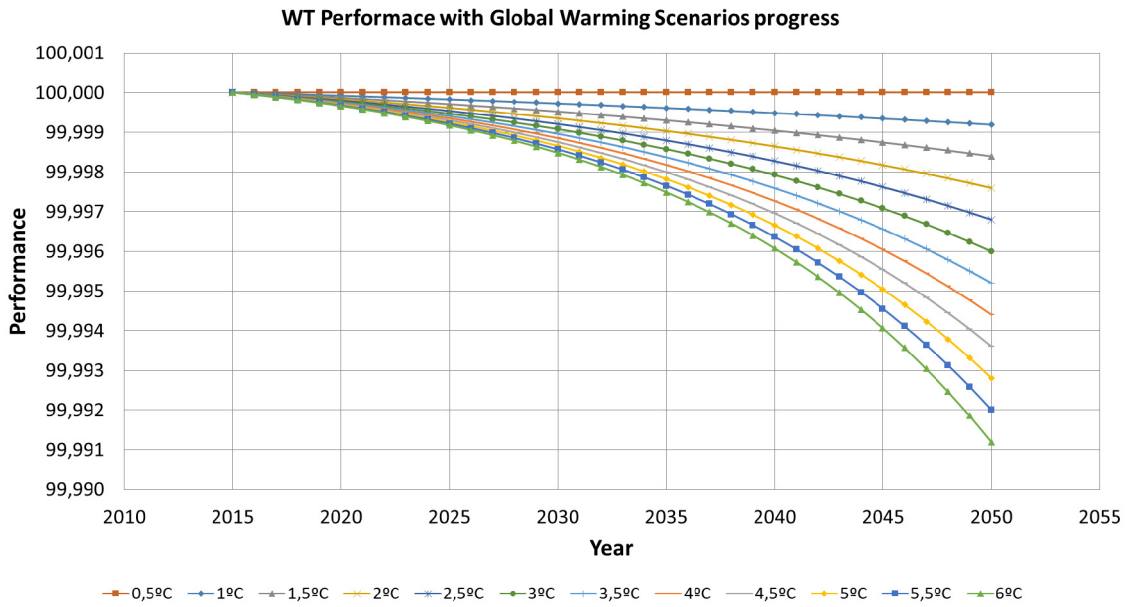

Figure 13. Performance curve over time vs global warming temperature.

In Figure 13, it is observed how the loss of performance in the worst case scenario will not be representative, with $\%_{6ºC}$ being equal to 99.99%.

It is possible to estimate the economic loss of the installation used for this paper from expression (13), which jointly considers the performance loss and the thermal evolution presented in Figure 12,. The performance loss will affect the balance sheets of the companies that operate the wind farms, since their revenues will be reduced for a period of 30 years. This is the amortization period which is typically required for new renewable energy plants with life-cycle extension systems. A performance loss of 0.0024% per year, for similar turbines deployed after 2050, results in a 0.072% accumulated loss over the life cycle. This represents $655 (2018 USD) for a standard 1.5MW wind turbine in a site with 2700 full-load hours[4] [33,34]. However, it is necessary to analyze the gradual loss of performance of the installation under study during the global warming process. The energy lost during the period 2015-2050 has been calculated in monetary terms taking into account the loss of performance in each year (which depends on the global warming of each scenario) and multiplying it by the installed capacity of the wind farm (30MW) and the production ratio (2067 equivalent hours for this wind farm). The results are shown in Table 1. The loss (in terms of the electricity which would not be generated) would be $12,000 in the case of 2 degrees of global warming and $43,000 (2018 USD) in the case of 6 degrees.

[4] We have assumed an expected average electricity selling price in the EU of 158€ (2013)/MWh for the period 2030-2050, according to [22]. OECD exchange rates have been used [23].

Table 1.- Performance and economical losses summary

ΔT(ºC) (from 1990)	Performance (%)	Lost Energy MWh	Lost Incomes (k$)´18*	Additional $ktCO_2$**
0.5	100	0	0	0
1.0	99.9992	17.4	3.9	5.7
1.5	99.9984	34.7	7.8	11.5
2.0	99.9976	52.1	11.7	17.2
2.5	99.9968	69.4	15.59	22.9
3.0	99.9960	86.8	19.49	28.6
3.5	99.9952	104.2	23.39	34.4
4.0	99.9944	121.5	27.29	40.1
4.5	99.9936	138.9	31.18	45.8
5.0	99.9928	156.3	35.08	51.6
5.5	99.9920	173.6	39.98	57.3
6.0	99,9912	191	42.9	63.0

***1€´13 = 1.328$´13 ; 1$´13=1.075$´18[32]; **$tCO_2$/kWh from electricity generation mix (2011)**

[1] Summary of the global warming effects for the wind farm.

Furthermore, the wind electricity which is not generated will need to be produced by other sources in order to avoid supply cuts. This will lead to an increase in GHG emissions if these other generation sources are fossil-fuel fired. Assuming the electricity mix in Spain (with a large share of renewables), the average emissions from electricity generation would be 0.33 tCO_2/kWh. Therefore, 17,000 tCO_2 will have been emitted in 2050 in the case of 2 degrees of global warming (63,000 tCO_2 in the case of 6 degrees).

4. Discussion

The impact of environmental temperature on the production of a wind farm has been analysed in this paper. A model of the electricity which can potentially be generated by wind turbines, taking into account both the wind speed and the temperature at the site, has been developed. The method allows simulating the impact of the average thermal increases due to global warming. Using a complex model of wind energy generation based on ANN and Fuzzy logic rules, the reduction in the performance of the wind farm and, thus, the reduction in electricity generation from wind can be calculated.

Our results show that an increase in temperatures will trigger a reduction in the performance of wind turbines. However, the impact of temperature increases on wind energy performance will probably be modest, since the wind turbine control system is able to correct the wind energy loss through adjustments in the angle of the wind blades.

Climate change and energy models, and particularly integrated assessment models, should take into account the bidirectional impact of temperature increases and (wind) electricity generation. The changes (increase or reduction) of potential electricity generation from wind that can be expected as a result of higher temperatures should be included in these models. The methodology developed in this paper provides a useful contribution in this regard since it could be added to existing integrated assessment models.

Further research could be devoted to the analysis of other possible effects, including changes in the features of winds, lower availability of equipment and extensions to other RETs. First, the impact of changes in the features of winds (frequency, direction and intensity) should be analyzed. Global warming can be expected to extend the summer season, which is when the winds are softer.

Second, the increase in average temperatures will reduce the availability of wind energy equipment. Such increase will lead to more frequent overheating of the equipment which, in turn, will lead to more frequent shutdowns of the wind turbines in order to cool some components. The availability of the equipment will be reduced. In addition, electricity consumption due to cooling as well as the electricity losses in wires, transformers and generators will increase. A thermal increase could also accelerate the degradation of some components, including oils, bearings, windings, etc., which would increase the operational costs.

Finally, the methodology used in this article should be applied to different wind turbine technologies and to installations located in different places around the world. However, this will be the focus of future research, since the operation data which would be required for such analysis are not currently available. The analysis can also be extended to other renewable energy technologies and, in particular, to solar PV. It is likely that the performance losses will be higher for this technology than for wind (given the absence of control devices, as it is the case with wind turbines).

References

1. Edenhofer, O.; Sokona, Y.; Seyboth, K.; Eickemeier, P.; Matschoss, P.; Hansen, G.; Kadner, S.; Schlömer, S.; Zwickel, T.; von Stechow, C. (eds). *Special Report on Renewable Energy Sources and Climate Change Mitigation* ***2016***. Intergovernmental Pannel on Climate Change (IPCC), Geneve ISBN 978-92-9169-131-9 https://www.ipcc.ch/pdf/special-reports/srren/SRREN_FD_SPM_final.pdf
2. Schreurs, M. Breaking the impasse in the international climate negotiations: The potential of green technologies, *Energy Policy* **2012**; 48: 5-12. http://dx.doi.org/10.1016/j.enpol.2012.04.044.
3. Global Wind Energy Council (GWEC). *Global Installed Wind Power Capacity*. **2012** http://www.gwec.net/wp-content/uploads/2012/06/Global-Installed-Wind-Power-Capacity-MW-%E2%80%93-Regional-Distribution.jpg (accessed on 16/01/2020).
4. Global Wind Energy Council. *Global Wind Report Annual Market Update 2015*, **2016** http://www.gwec.net/wp-content/uploads/vip/GWEC-Global-Wind-2015-Report_April-2016_22_04.pdf
5. International Energy Agency (IEA). *World Energy Investment 2016*. Paris, **2016**.
6. International Energy Agency (IEA). *Energy Technology Perspectives 2016*. Towards sustainable Urban Energy Systems. Paris, **2015**. ISBN: 978-92-64-25233-2.
7. Helbing, G.; Ritter, M. Improving wind turbine power curve monitoring with standardization. *Renewable Energy*, Volume 145, **2020**, Pages 1040-1048, ISSN 0960-1481, https://doi.org/10.1016/j.renene.2019.06.112.
8. Kusiak, A.; Zheng, H.; Song, Z. On-line monitoring of power curves. *Renewable Energy*, Volume 34, Issue 6, **2009**, Pages 1487-1493, ISSN 0960-1481, https://doi.org/10.1016/j.renene.2008.10.022.
9. Wang, L.; Zhang, Z.; Xu, J.; Liu, R. Wind Turbine Blade Breakage Monitoring with Deep Autoencoders. *IEEE Transactions on Smart Grid*, **2016**. Doi: 10.1109/TSG.2016.2621135.
10. Lu, L.; Yang, H.; Burnett, J. Investigation on wind power potential on Hong Kong islands—an analysis of wind power and wind turbine characteristics. *Renewable Energy*, Volume 27, Issue 1, **2002**, Pages 1-12, ISSN 0960-1481, https://doi.org/10.1016/S0960-1481(01)00164-1.
11. Ritter, M.; Deckert, L. Site assessment, turbine selection, and local feed-in tariffs through the wind energy index. *Applied Energy*, Volume 185, Part 2, **2017**, Pages 1087-1099, ISSN 0306-2619, https://doi.org/10.1016/j.apenergy.2015.11.081.
12. Cambron, P.; Lepvrier, R.; Masson, C.; Tahan, A.; Pelletier, F. Power curve monitoring using weighted moving average control charts. *Renewable Energy*, Volume 94, **2016**, Pages 126-135, ISSN 0960-1481, https://doi.org/10.1016/j.renene.2016.03.031.
13. Trivellato, F.; Battisti, L.; Miori, G. The ideal power curve of small wind turbines from field data. *Journal of Wind Engineering and Industrial Aerodynamics*, Volumes 107–108, **2012**, Pages 263-273, ISSN 0167-6105, https://doi.org/10.1016/j.jweia.2012.04.026.
14. Verbraucherschutz, B.f.J.u.f. (ed.). Gesetz für den Ausbau erneuerbarer Energien. *Erneuerbare-Energien-Gesetz - EEG 2017*, **2017**.
15. Pelletier, F.; Masson, C.; Tahan, A. Wind turbine power curve modelling using artificial neural network. *Renewable Energy*, Volume 89, **2016**, Pages 207-214, ISSN 0960-1481,

https://doi.org/10.1016/j.renene.2015.11.065.

16. Ata, R. Artificial neural networks applications in wind energy systems: a review. *Renewable and Sustainable Energy Reviews* **2015**; 49: 534-562. http://dx.doi.org/10.1016/j.rser.2015.04.166 .

17. Nayeripour, M.; Mansouri, M.M. An advanced analytical calculation and modeling of the electrical and mechanical harmonics behavior of Doubly Fed Induction Generator in wind turbine. *Renewable Energy* **2015**; 81: 275-285. http://dx.doi.org/10.1016/j.renene.2015.03.018.

18. Fan, Z.; Zhu, C. The optimization and the application for the wind turbine power-wind speed curve. *Renewable Energy*, Volume 140, **2019**, Pages 52-61, ISSN 0960-1481, https://doi.org/10.1016/j.renene.2019.03.051.

19. Lydia, M.; Suresh Kumar, S.; Immanuel Selvakumar, A.; Edwin Prem Kumar, G. Wind resource estimation using wind speed and power curve models. *Renewable Energy*, Volume 83, **2015**, Pages 425-434, ISSN 0960-1481, https://doi.org/10.1016/j.renene.2015.04.045.

20. Marčiukaitis, M.; Žutautaitė, I.; Martišauskas, L.; Jokšas, B.; Gecevičius, G.; Sfetsos, A. Non-linear regression model for wind turbine power curve. *Renewable Energy*, Volume 113, **2017**, Pages 732-741, ISSN 0960-1481, https://doi.org/10.1016/j.renene.2017.06.039.

21. Ouyang, T.; Kusiak, A.; He, Y. Modeling wind-turbine power curve: A data partitioning and mining approach. *Renewable Energy*, Volume 102, Part A, **2017**, Pages 1-8, ISSN 0960-1481, https://doi.org/10.1016/j.renene.2016.10.032.

22. Pryor, S.; Barthelmie, R. Climate change impacts on wind energy: A review. *Renewable and Sustainable Energy Reviews* **2010**; 14(1):430-437. https://doi.org/10.1016/j.rser.2009.07.028.

23. Fant, C.; Schlosser, C.; Strzepek, K. The impact of climate change on wind and solar resources in Southern Africa. *Applied Energy* **2016**; 161:556-564 https://doi.org/10.1016/j.apenergy.2015.03.042.

24. Davy, R.; Gnatiuk, N.; Pettersson, L.; Bobylev, L. Climate change impacts on wind energy potential in the European domain with a focus on the Black Sea. *Renewable and Sustainable Energy Reviews* **2018**; 81(2):1652-1659 https://doi.org/10.1016/j.rser.2017.05.253.

25. Scott Hosking, J.; MacLeod, D.; Phillips, T.; Holmes, C.R.; Watson, P.; Shuckburgh, E.F.; Mitchell, D. Changes in European wind Energy generation potential within a 1.5ºC warmer world. *Environmental Research Letters* **2018**: Volume 13, Number 5. doi:10.1088/1748-9326/aabf78.

26. Schlechtingen, M.; Ferreira-Santos, I.; Achiche, S. Wind turbine condition monitoring based on SCADA data using normal behavior models. Part 1: System description. *Applied Soft Computing* **2013**; 13 (1): 259-270. http://dx.doi.org/10.1016/j.asoc.2012.08.033.

27. Kusiak, A.; Verma, A. Analyzing bearing faults in wind turbines: A data-mining approach. *Renewable Energy* **2012**; 48: 110-116. http://dx.doi.org/10.1016/j.renene.2012.04.020.

28. Lydia, M.; Suresh Kumar, S.; Immanuel Selvakumar, I.; Edwin Prem Kumar, G. A comprehensive review on wind turbine power curve modeling techniques. *Renewable and Sustainable Energy Reviews* **2014**; 30: 452-460 https://doi.org/10.1016/j.rser.2013.10.030.

29. Taslimi-Renani, E.; Modiri-Delshad, M.; Fathi Mohamad Elias, M.; Abd. Rahim, N. Development of an enhanced parametric model for wind turbine power curve.

Applied Energy **2016**; 177; 544-552, http://dx.doi.org/10.1016/j.apenergy.2016.05.124.

30. Gil, A.; Sanz-Bobi, M.A.; Rodríguez-López, M.A. Behavior Anomaly Indicators Based on Reference Patterns – Application to the Gearbox and Electrical Generator of a Wind Turbine. *Energies* **2018**; 11(1), https://doi.org/10.3390/en11010087.
31. Lapira, E.; Brisset, D.; Davari Ardakani, H.; Siegel, D.; Lee, J. Wind turbine performance assessment using multi-regime modeling approach. *Renewable Energy* **2012**; 45: 86-95 http://dx.doi.org/10.1016/j.renene.2012.02.018.
32. National Aeronautics and Space Administration (NASA). http://climate.nasa.gov/system/internal_resources/details/original/647_Global_Temperature_Data_File.txt (accessed on 16/01/2020).
33. European Union. EU Reference Scenario 2016, Energy, transport and GHG emissions Trend to 2050. doi:10.2833/001137. https://ec.europa.eu/energy/sites/ener/files/documents/ref2016_report_final-web.pdf
34. OECD. Exchange Rates. https://data.oecd.org/conversion/exchange-rates.htm (accessed on 01/05/2019).

Modeling and evaluating the effect of environmental temperature on electricity generation in a PV power plant.

Abstract: Climate change, and the need to adopt clean technologies, together with a drastic reduction of the costs of photovoltaic (PV) panels has led to the deployment of this technology, the one with the highest growth rates in the last years. This growth suggests the need to have estimation models of the electricity generated in order to ensure its appropriate integration into the grid and its stability. Power curve models of PV panels allow calculating the energy generated by the panels for given environmental conditions and, thus, assessing its real performance with respect to the reference curve. In this context, the environmental temperature is one of the factors with the greatest influence on the performance of PV panels. The aim of this paper is to provide a methodology to calculate the real power curve of a set of PV panels in a given location as a function of environmental temperature, among other variables, including wind speed and solar irradiation. As a result, models with a high precision have been created. This methodology has been applied to a real-world case in order to calculate the loss in the performance of a PV installation as a function of environmental temperature and the impact on solar PV electricity generation has been simulated in several global warming scenarios. Our results show that an increase in the average ambient temperature would severely reduce the performance of PV plants leading to a lower level of electricity generation for the same level of installed capacity.

Keywords: Global Warming, ANN, performance losses, solar PV, electricity generation.

---

1. Introduction

Renewable energy technologies (RETs), such as wind and solar (both PV and thermoelectric) are the main alternatives to reduce greenhouse gas emissions and energy dependency [1, 2]. Solar energy is a clean, cheap, abundant and eternal source of energy [3, 4]. Several simulation models show that RETs play a crucial role in climate change mitigation in order to keep global warming under 1.5-2º C [5, 6].

However, the same global warming that RETs are aimed to mitigate may affect the performance of renewable energy installations and, particularly, PV plants. A reduction of the performance of PV panels due to the increase of average temperatures in the location [3, 7, 8] will reduce electricity generation throughout the whole lifecycle of the asset and, thus, the profitability of investments.

Electricity generation with PV panels are contingent upon some random factors which makes it difficult to estimate the energy produced. The main variables which affect the electricity generation of a PV panel are solar irradiation and other meteorological factors, such as atmospheric temperature (and the temperature of the panel), humidity, wind speed in the location and its direction, among others. All these environmental factors do not only affect the performance of PV panels, but the installation as a whole (transformers, converters, wires etc.) [9].

The aim of this paper is two-fold. On the one hand, an optimized methodology to estimate the real expected production in a real world PV power plant as a function of the environmental variables beyond the theoretical curves is provided. On the other hand, an evaluation of the impact of several scenarios of mean environmental temperature increases over time is carried out.

All sources of solar energy are sensitive to climate change, but existing literature focuses mainly on photovoltaic generation (PV) and on changes in solar irradiation, as the most relevant source. A global reduction in direct normal irradiation of 5% is suggested, with increases in Western Europe and

the Easter Mediterranean (up to 10%) and reductions in other regions of the world such us Eastern Europe and Africa (up to 10%) [10].

This paper develops a methodology based on the use of artificial neural networks (ANN) in order to assess the performance loss of the PV installations due to the impact of environmental conditions such as temperature or wind, taking into account all the electrical elements which make up such installation in addition to PV panels [3, 7]. Fictitious variables were also designed, taking into account the date and the hour in the day, which considerably improved the response of the model. This methodology has been applied to a real-world plant to analyze the performance loss of the plant and the associated economic losses, simulating different scenarios for the increase in the environmental temperature due to global warming [8, 11, 12].

The panel manufacturers provide power curves of their equipment so that the expected production can be estimated under given irradiation and temperature conditions. However, the total production of a plant depends on more factors, such as the electricity losses of the wires, the cooling of the panels depending on the local terrain and the specific distribution of the plant, the losses in transformers etc.

There is a wide variety of mathematical and statistical techniques which can be used to calculate the power curve of a renewable energy installation [13, 14]. However, the difficulty to build an analytical model based on equations ("*white-box*" models) [7] which simultaneously takes into account the impact of the aforementioned factors led us to use "*black-box*" modeling methods and, particularly, ANN [15, 16].

The modeling of PV panels has historically been carried out with white-box type models. According to Chen et al. (2019), these modeling processes are based on equivalent circuits and usually consist of four steps: (1) select an appropriate model structure, i.e., equivalent circuits; (2) determine the translation relationships of the model parameters with respect to the input irradiance and operating condition temperature; (3) extract the model parameters under operating conditions (OPC) from measured I-V (Intensity-Voltage) curves; (4) identify the model parameters under the standard test conditions (STC, i.e., the irradiance in 1.000W/m^2 and temperature of 25ºC).

These white-box models are based on physical equations, as done by Lindsay et al. [18], which analysed the effect of the solar spectrum on PV production models. They reached the conclusion that the models that consider global solar irradiation but do not include the different spectra may have errors which can be as high as 15 %. Seapan et al. [19] presented an analytical formula to correct the performance of the crystalline silicon panels as a function of the temperature based on physical models and experiments. Kermadi et al. [20] presented an analytical approach for PV array modeling under partial shading conditions. In their method, it was only needed the STC parameters of the PV modules and the irradiance level imposed on each module and obtained the P-V (Power-Voltage) and I-V curves, being usable for simulating. Chao et al. [21] did a review on dynamic equivalent modeling of large PV power plans. Their parametric model was used to simulate PV plans under large disturbances.

Black-box models use data-driven approaches, which need no predetermined equivalent circuits and only rely on the measured data to directly build the black-box model. There are several techniques based on machine learning and deep learning such as ANN, supported vector regression (SVR), random forest (RF), gradient-boosted (GB), convolutional neural networks (CNN) or recurrent neural networks (RNN), among others. The next section describes the ANN that were used in this paper, although most of the aforementioned methodologies could be used. The GB technique is used to solve non-lineal problems and Wang and Mamo [22] used this method to build a regression model to analyse the degradation of prismatic cells. Kumari and Toshniwal [23] used the extreme gradient-boosted (XGBF) combined with deep neural networks (DNN) to predict global horizontal irradiance (GHI) in different locations, obtaining better results than using other simple models.

These black-box models are used to model and simulate the production in PV panels or to forecast the future environmental and production values. There are several publications which use all these techniques for different purposes, as image processing, being the CNN the technique selected by Akram et al. [24] to do detect PV cells degradation analyzing thermography's.

Yap and Karri [25] used one ANN model to predict solar irradiation based on more commonly available weather data, and another ANN to predict the power output from a PV array. The authors use, in the same study, ANN for forecasting and modeling. Similar contributions include Yona et al. [26] which used three ANN, two of them to predict irradiation and temperature and the third one to simulate the PV power. Mellit and Massi [27], who improved the contribution of Yona et al. [26], obtained better results by including the day of the month as relevant input data in the model. Han et al. [9] also took into account this seasonal effect and built a model of energy production based on a system made up of an ELM (extreme learning machine) and a Kernel density function. RNN were also used by Jung et al. [28] in order to learn the periodic trends from data, with the final objective of estimating the performance of the PV panel over time.

As a variation of ANN, Almonacid et al. [29] built a model to predict the energy that can be produced with a PV plant with one hour in advance, including also environmental variables. In this study, time series made up of time delay neural networks (TDNN) were used. These TDNN allowed the estimation of future irradiation levels and temperature in the location. However, the power is estimated through the inclusion of these environmental variables in a parametric model. Chen et al. [17] pointed out that ANN has a limited performance and used a one-dimensional Deep residual network (1-D ResNet) to find the relation between I-V and other environmental factors.

Raza et al. [30] provided a classification of the different methodologies to model the power curve of PV panels, mentioning, among others, persistent forecast, physical model, statistical techniques, new techniques as Fuzzy and hybrid systems (ANFIS, adaptive neuro-fuzzy inference system). In such study, the main factors which are considered in the models are reviewed, including the main environmental variables which affect the performance of PV plants and show the correlation of those variables with electricity production. Ahmed et al. [31] indicate in their review that the temperature of the panel has a great impact on its performance and, thus, this is also the case with ambient temperature. In that study, the authors also mention how production changes across different seasons and they developed their own model for each season (spring, summer, autumn and winter). Hamou el al. [32] analysed the efficiency of PV modules under real working conditions using mathematical models. They found outperformance losses close to 10 % at working temperatures of 50 ºC.

As it was mentioned, these regressive and machine learning techniques can be used for forecasting and modeling. When forecasting, the aim is to identify the future values of a variable in advance, whereas in modeling and simulation the aim is to estimate the current value of a variable depending on others. Although forecasting is not within the scope of the present study, we found a large number of papers where machine learning techniques were used. El Mentaly et al. [33] proposed a methodology based on a linear regression model correlated with ambient temperature and solar irradiation in order to optimize the solar tracking algorithms (MPPT- max power point tracking). Mellit et al. [34] built a model which combined two ANN into a single model, one of them for sunny days (or standard conditions) and another one for rainy days. A similar approach was followed by Das et al. [35], who used a support vector regression model (SVR). The authors previously identified the data as belonging to a rainy day or a standard day. Similarly, Wu et al. [36] compared the response of several models based on ARIMA (autoregressive integrated moving average), SVM (support vector machine), ANN and ANFIS and combined them with GA (generic algorithms) techniques. They found out that the combined models substantially improved the estimations of energy production. Patel et al. [37] used a fist stage SVR model combined with a second stage ANN, RF or SVR models to create tree fusion models (SVR-ANN, SVR-RF and SVR-SVR) for stock market index prediction. Most of these techniques are commonly used for forecasting [38].

Although deep learning algorithms could have a better accuracy, a variation of the common ANN is used in this study because of the good result we obtained in previous studies [39, 40] and due to the fact that it is the most commonly used in the literature. The ANN technology is described in the next section.

Compared to previous contributions, this study advances knowledge on several fronts. First, this paper refines previous ANN methodologies to better characterize the power curve for PV generation in a real location using neural networks with TDNN and combining techniques provided in other publications in order to directly estimate the expected power. Second, for such model, two fictitious entry variables have been created (date/season and hour), which improve the predictive capability of the models. Third, a parametric model to assess the performance loss of a PV plant as a function of environmental temperature (and not only for the temperature of the PV panels) has been developed. Finally, the production losses in the analysed plant are simulated under different scenarios corresponding to different increases in ambient temperature.

This paper is structured as follows. Section 2 provides a review of the methodology, the analytical model of energy production and the data of the plant used for the analysis. Section 3 applies the methodology and calculates the performance loss of the analysed plant in different scenarios of temperature increase due to global warming. Section 4 discusses the results and provides some avenues for future research.

2. Materials and Methods

2.1. PV power curve modeling methodology

The behavioural model is made up of a single ANN. However, in order to identify the best model, many network configurations were checked, combining different entry variables and two types of ANN (MPL and TDNN).

The main characteristic of ANN is their learning capacity and through the training process, extracts the essential characteristics of the used dataset [41]. This learning is the adjustment of the weights of the connections between the neurons which takes place in an interactive manner with the aim to achieve a desired effect. It refers to "*learning*" the existing relationships between pairs of values of vectors of inputs-outputs, or finding a common pattern in the input data in order to classify them according to the different patterns. ANN are less dependent on the knowledge of the experts, in contrast to the case of physical models [42].

The multilayer perceptron (MLP) is a type of feed-forward ANN in which the neurons are organized in layers and, thus, the inputs for a neuron located in an intermediate layer can only be the outputs of the preceding layer and its output serves as the input for the neurons of the following layer.

In Figure 1 a TDNN with two input variables and one time delays formed by four neurons in the input layer (blue color) in represented. There are two hidden layers (red color) and one output layer (grey color). What is specific about the TDNN is that the input layer has several more neurons than the inputs of the ANN: the number of neurons in the input layer is a multiple of the inputs of the network and the time delays. The first group of n neurons receives the value of the network inputs. The second group of n neurons of the input layer stores the previous value of the input vector of the neural network. This structure allows the TDNN to maintain a memory of the activity of the neurons in the network with previous values of the input vector. The input groups of neurons are united by delay units *(t-1)* and receive the values of the input variables. A TDNN with k time delay units and two inputs $x_1(t)$ and $x_2(t)$ is equivalent to a MLP neural network with inputs $x_1(t)$, $x_2(t)$, $x_1(t-1)$, $x_2(t-1)$, $x_1(t-2)$, $x_2(t-2)$, … , $x_1(t-k)$ and $x_2(t-k)$.

Various techniques prevent over-fitting or over-training of the neural network, including limitation of the number of epochs in the training process (these were limited to 5000), the addition of

white noise to the values of the input variables and the use of cross-checking. In the latter technique, which is the most widely used, the available data are divided in two groups: training and cross-checking (15% in the case presented here).

The data from the training group are used in order to fit the parameters of the neural network according to the training method which has been chosen. The data from the cross-checking group are not used in determining the error which has to be minimized with the training of the neural network, but instead are presented to the neural network after each training epoch. The training process is interrupted when a given number of epochs has gone through without a reduction in the error from the cross-checking data.

Given that PV panels accumulate heat during the day, their temperatures at a given moment *t* depend on the working conditions at such moment but also, given the thermal inertia, on the previous operative conditions at times *t-1*, *t-2*, etc. For that reason, we decided to use TDNN whose complete structure is shown in Figure 1 [43, 44, 45, 46].

Some authors have shown that, in order to have an efficient computational design, the number of neurons in each hidden layer of the network should be two-thirds of the variables in the entrance layer (in blue, Figure 1) plus the number of exit neurons (in gray) [47]. However, in this study, a structure with 10 neurons per layer (in red) was chosen due to the good results that this structure has shown in previous studies [39, 40] and the fact that an efficient computational design was not required.

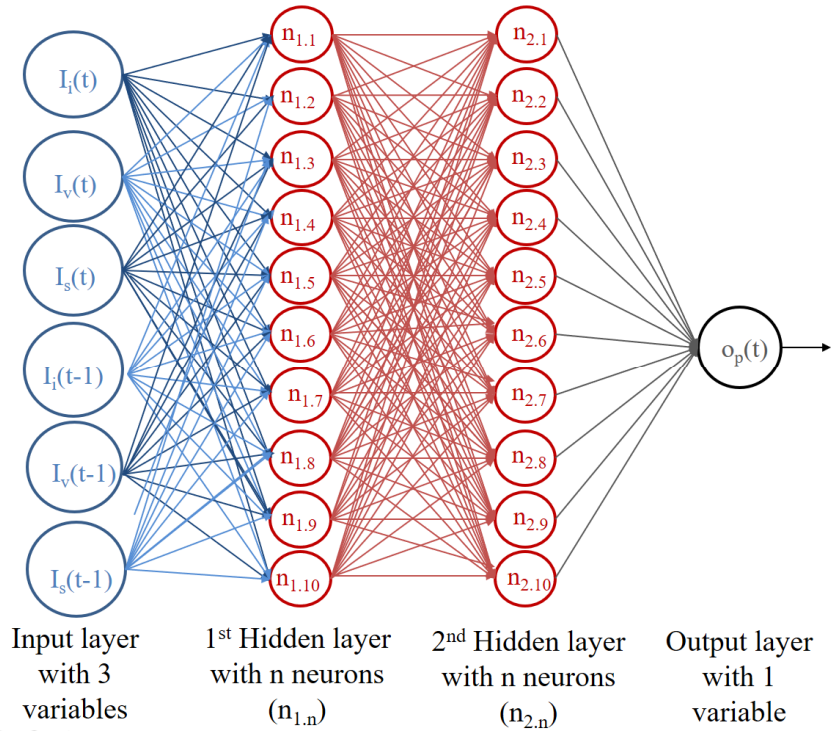

Figure 1.- Illustrating the used Time Delay Neural Network (TDNN).

Once the model on energy production, which takes into account the temperature of the location as well as other factors such as the wind speed, is available, then the effect of an average increase of the ambient temperatures on the potential energy production can be simulated. Therefore, the energy that the installation can generate under the current conditions and the energy that could be generated under future global warming conditions can then be compared.

2.2. Relationship between the performance of the panels and the ambient temperature

Some authors point out that the PV installations are very inefficient compared to other technologies such as nuclear technologies [3]. On the other hand, panels absorb around 85 % of the sunlight and only 12-15 % is transformed into electricity (up to 20 % for some improved systems) [2], whereas the rest is residual heat. This thermal increase around the panels can increase the local temperature by 0.4 ºC [1] and up to 4 ºC in the nearest locations [48, 9]. The performance of these systems is researched through energy and exergy studies, and depend on the laws of thermodynamics [2].

The electricity production of a PV panel depends mainly on the level of irradiation which it receives and the working temperature, which is closely related to wind since this influences the cooling capacity of the panels. In addition to its low intrinsic performance, such performance goes down as the temperature increases [3, 7]. Several studies parametrise the performance of panels taking into account the physical characteristics of its materials [7]. However, in this paper, the analysis of the change in the performance of the analysed plant was based on the use of an ANN-based model. This type of models allow the identification of the hidden relationship between temperature and production using historical data.

Once the relationship between temperature, irradiation and production has been obtained, different global warming scenarios can be simulated (see section 3). Then, the production of the installation with higher and higher environmental temperatures can be calculated.

The studies on performance losses have been carried out on the basis of a curve of maximum production in a given location, without considering performance losses due to unavailability or the presence of clouds. The installation used in this study is connected to the grid and made up of 50 PV plants with a nominal nameplate capacity of 100 kW and two-axis tracking. Therefore, the total nameplate capacity of the installation is 5,000 kW (5,800 kWp).

The PV plant transforms the energy from the sun into alternate electricity, which directly feeds the medium-tension (MT) grid of the company through an underground line which ends in the transformer substation which is close to the installation and where the meters of the energy produced are located.

Therefore, in addition to the own losses of the PV panels, the increase in the losses in the MT transformation systems (and the evacuation circuits to the substation where the meters are located) are taken into account for the estimation of the loss of performance of the plant due to the effect of ambient temperature

Generally, the available power curve of the panels is the one provided by manufacturers according to the IEC 61215-2 norm (under given temperature and humidity conditions). However, both the efficiency of the PV cells as well as the electricity losses in the installation depend on the ambient temperature (among other factors, including wind speed). Figure 2 shows several operational registers for different environmental conditions. For the same intensity of irradiation, the installation will generate less electricity and will have more losses with higher local temperatures. In Figure 2 the x-axis represents the global irradiation, whereas the y-axis represents the average power in each hourly interval, whereas the color refers to the local temperature in a central point of the installation. A high correlation between the performance of the plant and the ambient temperature was found. The performance of the plant is drastically reduced in the hours with the highest local temperature.

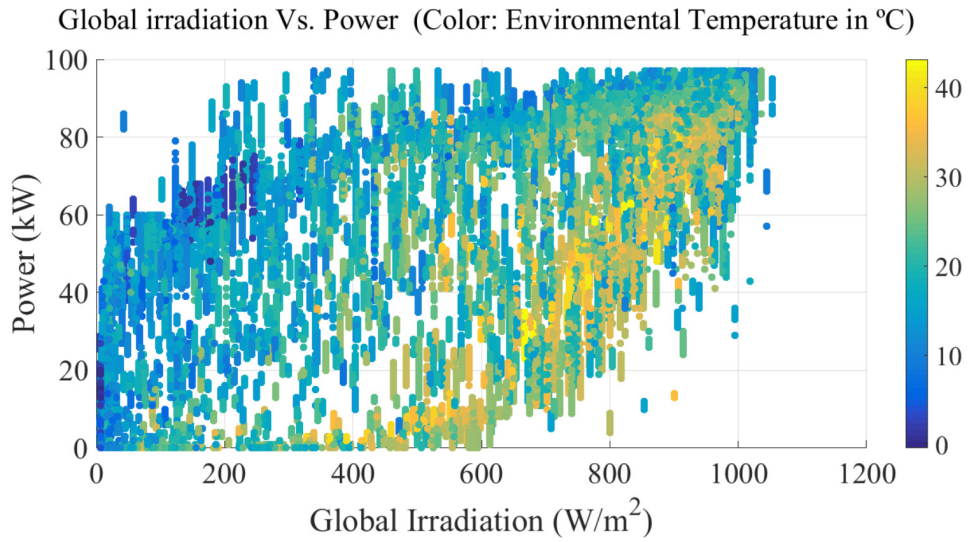

Figure 2.- Power curve (y-axis) of the installation as a function of irradiation (x-axis) and the ambient temperature (color).

Some manufacturers of crystalline silicon PV indicate that PV panels suffer losses of 4 % for each 10 ºC of increase of the operation temperature, although the losses at the level of the installation due to the thermal effect are greater. The ideal situation would be to have a measure of temperature for each of the panels since their temperature in the summer can be between 40-70 ºC [49]. However, a measure of the ambient temperature in a central point of the plant is only available. Figure 3 represents the maximum power of the installation (y-axis) and the local temperature (x-axis), with the color referring to the level of irradiation. Each point in the figure represents a time record. It can be observed that the maximum power of the plant is reduced by 10 % for those records with the highest irradiation and the highest temperature. The power of the PV panels is higher with the same or even lower irradiation but lower environmental temperature.

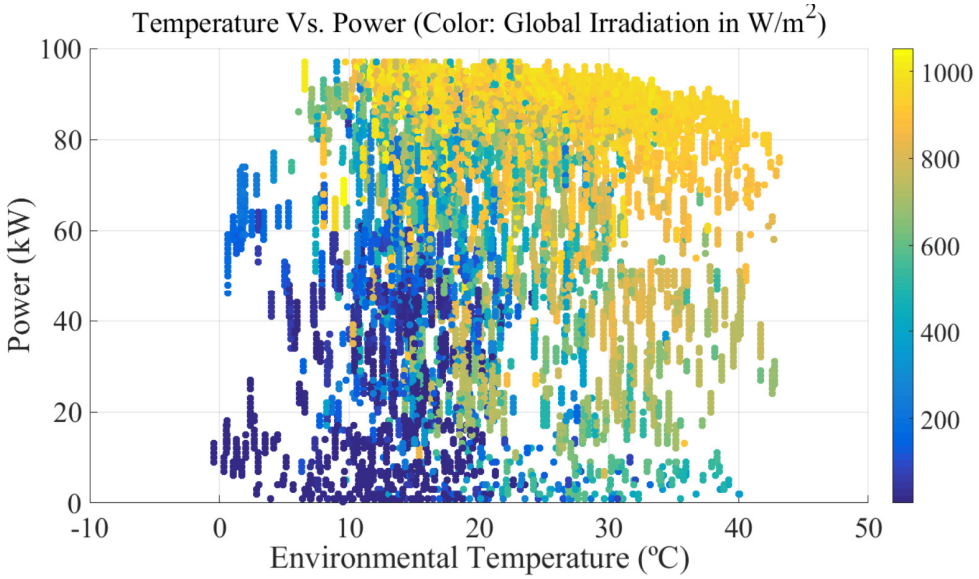

Figure 3.- Power (y-axis) as a function of the ambient temperature (x-axis) and irradiation (color).

These results show a relationship between the performance of the PV plant and temperature. Therefore, an increase of the average ambient temperature will affect the performance of the plant as a

whole. The following section describes how the model of energy production as a function of the measured irradiation and other environmental factors was built.

2.3. Variable selection, cleaning and treatment of the samples

According to the available data in the database, the following variables were considered to build the energy production model of the PV plant:

- Ambient temperature close to the panels [ºC].
- Global irradiation in a tilted panel [W/m²].
- Wind speed [m/s].
- Power [kW].

Models were developed using a large quantity of production data from 50 individual plants during a period of 2 years (2008 and 2009). Only the first years of operation were considered for the building of the model, although data for the years 2010 and 2011 were used in order to calculate the errors of the model. The historical production data for the PV plant between 2008 and 2011 were used to carry out the simulations. The PV power plant was located in the south of Spain and was built with panels in solar tracking posts.

A unique model for a generalist panel of 100 kW, combining all the production registers, was built. In Table 1 an example of the production in each one of the fifty panels is shown. An extra variable called "*percentgood*" for each operational variable is included for each SCADA (supervisory control and data acquisition system) data record (Table 2). This "*percentgood*" variable is used to remove invalid data due to failures in the sensors or in the communication system. We removed all the time records with a "*percentgood*" value below 0.8 (80 %). Outliers in the input samples, including physically unfeasible temperatures or non-typical data due to abnormal operation conditions, needed to be identified. Data processing consisted on a filter with two stages (manual and statistical) and data standardisation. For each of the variables considered, this filter removes those values which make no sense from a logical operation point of view [50, 51]. This is probably due to failures in the measurement as a result of sensor calibration or abnormal cases from an operational point of view. Given that the limits of the operation variables were unknown, a statistical assessment of the parameters of the distribution, such as the average (μ) and the standard deviation (σ), was carried out. Taking into account the values obtained, the operation limits were set for each variable on the basis of an expert judgement.

Table 1. PV panels production, statistical filtering and mean assessment.

Date	Pow Panel 1 (kW)	Pow Panel 2 (kW)	…	Pow Panel 50 (kW)	Statistical filter and aggregation	Mean Pow per Panel (kW)***
…	…	…	…	…	→	…
01/01/2015 01:00 pm	94.2	93.4	…	91.9	→	93.9
01/01/2015 02:00 pm	94.8	93.7	…	12.8*	→	94.2**
01/01/2015 03:00 pm	95.1	94.1	…	93.7	→	95.2
…	…	…	…	…	→	…
	*Removed data in the statistical filter; **Calculated based on 49 panel measurements; ***Per active panel					

In Table 1 a time record removed applying a statistical filter is shown. Panel 50th presented a production too low compared to the other 49 PV panels. That could be due to O&M activities, like the execution of a work order where the PV panel had to be disconnected. This low value could also be due to degradations of the PV panel. We have replaced the production of the 50th PV panel with a NaN ("Not a Number"), which is used in Mathlab® to ignore values. In that case, the Mean Pow per panel was assessed as the mean value of the other 49 panels, meanwhile in the other rows it was calculated with the 50 panels data of the corresponding time interval.

Since the models were built with entry variables with different units, scales etc., the data had to be normalized so that the scale of fluctuation of the different variables could be compared. This also guarantees that a higher weight is not given to a variable with higher numbers. The standardisation has been carried out by subtracting the average of the variable and dividing it by the standard deviation.

During the standardisation process, the statistical filter can be applied, removing any data whose standardized value is greater than three. Aberrant data in statistical terms are, in a given sample, those which are outside the limits $\mu \pm 3\sigma$ for each variable. If data are removed in the process of removal of aberrant data, they have to be standardized with the remaining sample. This process is carried out only once.

During the process of standardisation of variables, the statistical parameters of each variable have to be kept, since the data which are latter used as an entry to the model in the global warming simulations have to be standardized on the basis of these parameters. Therefore, the global warming simulation data have to be normalized with μ and σ of the set of training data in order for the model to be applicable. The fictitious variables do not require the application of any additional cleaning or standardisation process.

Apart from the statistical filter, the applied manual filter has been:

- $0 \leq$ ambient temperature (ºC) ≤ 50
- $0 \leq$ Global irradiation of the tilted cell (W/m^2) ≤ 1.500
- $0 \leq$ Wind speed (m/s) ≤ 40
- $0 \leq$ Power (kW) ≤ 120
- $0.8 <$ Percentgood
- Other aberrant data were removed when the condition that global irradiation >3 W/m^2 was met and, simultaneously, Power = 0 kW (in data showed in Table 1).

All the considered variables have been measured as hourly average values. New data are recorded in the database when there are changes in each sensor measurement, adding the time stamp when that happened. The raw database, storage each variable with different timestamps depending on the precision of each sensor. After that, the system automatically generate the average value of each variable for the required interval (10 minutes, 1 hour, etc.).

When invalid data are found in Table 2, as it is the case with a low "*percentgood*", or those out of the manually fixed boundary limits, the whole time record (the row) is replaced with NaN values. These records are not used in the TDNN model training.

Table 2. Completed Database with all used variables.

Date	Global Irradiation (W/m²)	Global Irradiance % good	External Temp. (ºC)	Ext. Temp. % good	Wind Speed (m/s)	Wind Speed % good	Fictitious Variable season	Fictitious Variable hour	Mean Pow per Panel (kW)
…	…	**…**	…	…	…	…	…	…	…
01/01/2015 01:00 pm	210	**1**	34.4	1	8.1	1	0	0.866	93.9
01/01/2015 02:00 pm	214	**1**	34.8	1	8.1	1	0	0.899	94.2
01/01/2015 03:00 pm	220	**0.53***	35.1	1	7.9	0.98	0	0.933	95.2
…	…	**…**	…	…	…		…	…	…
								*Removed data in the manual filter	

Among the variables registered by the SCADA, several fictitious variables were generated which represented the hour of the day and the season (or day) of the year. As mentioned in a previous section, the current local temperature depends on previous operative conditions. Figures 4 and 5 show that the highest temperatures are registered in the afternoon/evening and they start to go down when the panels do not generate electricity anymore (the temperature increase can reach 3-4 ºC compared to places which are close to the installation [48]). The panels are heated during the day and they become thermal batteries which increases the temperature of the location, which leads to a lower performance in the afternoon/evening.

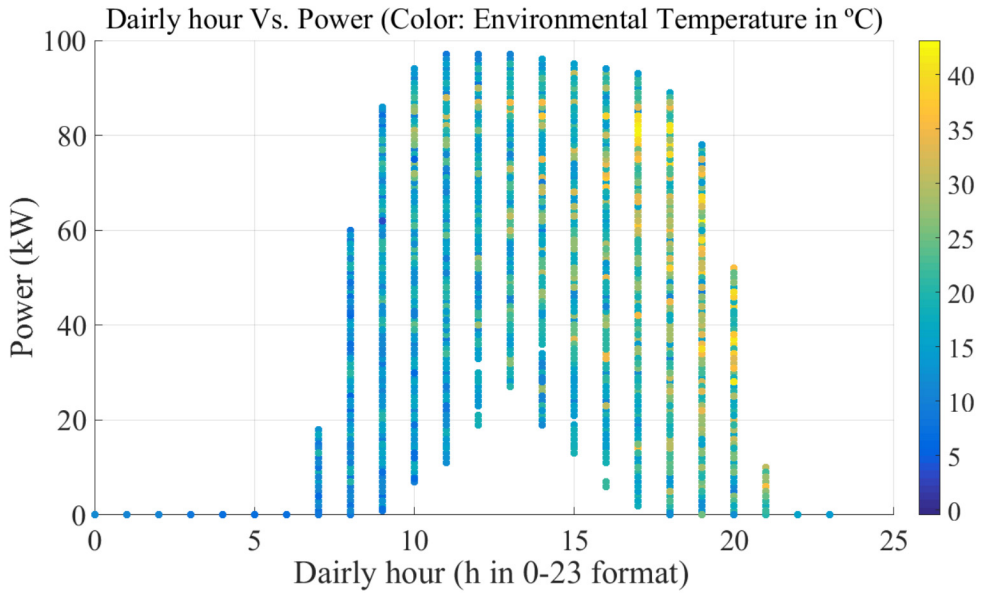

Figure 4.- Power curve in different hourly intervals (color refers to the local temperature registered in the location).

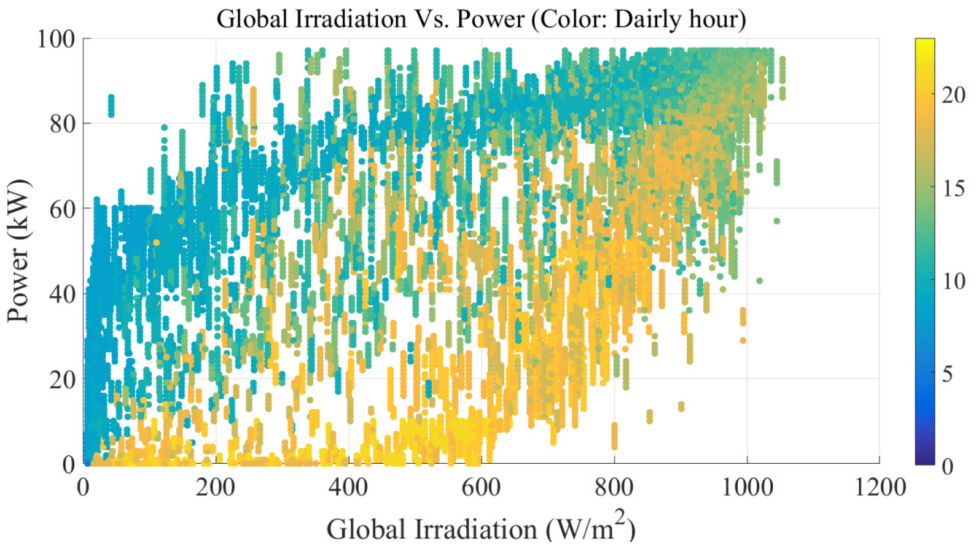

Figure 5.- Power (y-axis) as a function of irradiation (x-axis) and the hours of the day (color).

Given that, for the same level of the global irradiation, the PV plant does not generate the same amount of electricity as a function of temperature and the hour of the day (ramp-up and ramp-down the power curve), two special variables were used, called "hour" and "season" of the year.

The curves appearing in Figure 6 have been manually created according to the local climate. The seasonal variable in Figure 6.a allocates the value of 1 (standardized values) to the warmest month (July). The value decreases for the mild months and it reaches -1 for the coldest month (January). In Figure 6.b the hourly variable represents the evolution between the warmest (around 4:00 pm) and coldest hours (around 4:00 am) within a standard day. The transition between the different hours of the day is non-linear, due to the fact that during the first hours in the morning the thermal increase is lower than at mid-day. These variables help the neural network to identify the time of the day and the year, since the cooling of the component will depend on this (thermal evolution of the environment). This configuration is valid only for the studied site and other areas in Spain and it should be adjusted for other locations.

As an illustrative example in order to have a better understanding of the variables: for a SCADA data set registered at 2015/01/05 7:00 am, the fictitious variables would be 0.3333 for the season and -0.6667 for the hourly variable (included in Table 2).

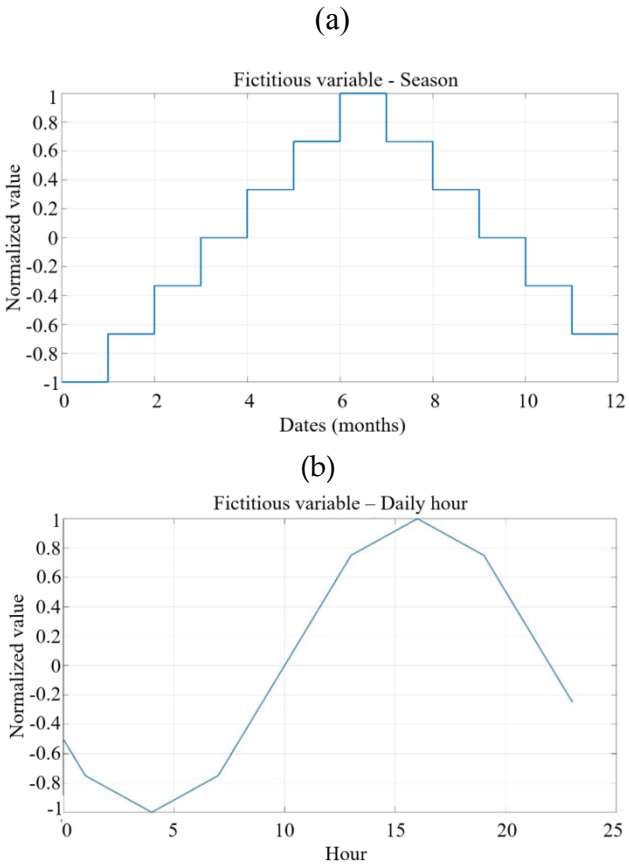

Figure 6.- (a) Standardised values of the fictitious variable "season". (b) Standardised values of the fictitious variable "hour".

If the power curve of the special variable "hour" is represented in the color scale, then it can be observed that the greatest loss of performance occurs in the hours of maximum temperature (Figure 7). The result is comparable with Figure 5.

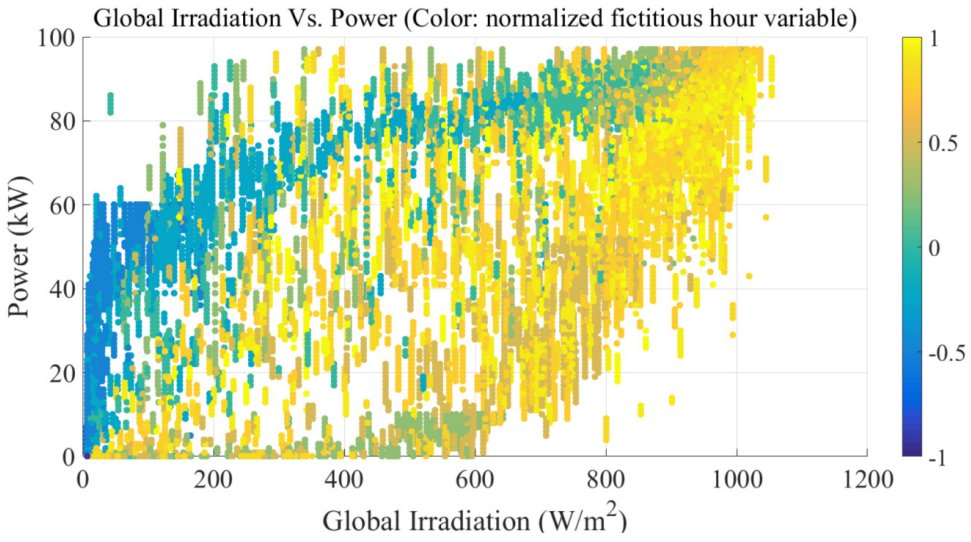

Figure 7.- Power curve (y-axis) of the installation as a function of irradiation (x-axis) and the special variable "hour" (color).

In order to develop the behavior models, several combinations of entry variables and neural network configuration were carried out, and the goodness of fit was checked for each of the models. Finally, the model which showed the best results was chosen.

3. Results

3.1. Comparison of the PV production models

Six experiments with different configurations were undertaken. In the first four experiments, the wind variable was not considered as an entry variable and the entry variables were irradiation and ambient temperature (models 1 to 4). In the last two models, the variable wind speed was introduced (models 5 and 6). Models 1 and 3 did not use the fictitious variables as entry variables. In order to assess and compare the goodness of fit of the different models which were developed, both the average error and the standard deviation were used. On the basis of the results shown in Table 3, we decided to choose model 6 since, although its average error was slightly above model 1, the deviation was much lower.

Table 3.- Models errors for different ANN configuration.

Model	Delays	Special Variables	Wind speed	μ (kW)	σ(kW)
1	0	No	No	0.041	4.91
2	0	Yes	No	0.116	6.38
3	1	Yes	No	0.79	9.86
4	2	Yes	No	0.105	7.26
5	0	Yes	Yes	0.86	7.76
6	2	Yes	Yes	0.097	1.58

The use of the wind speed variable has a large effect on the improvement of the model fit. The dispersion was reduced, as shown in Figure 8.

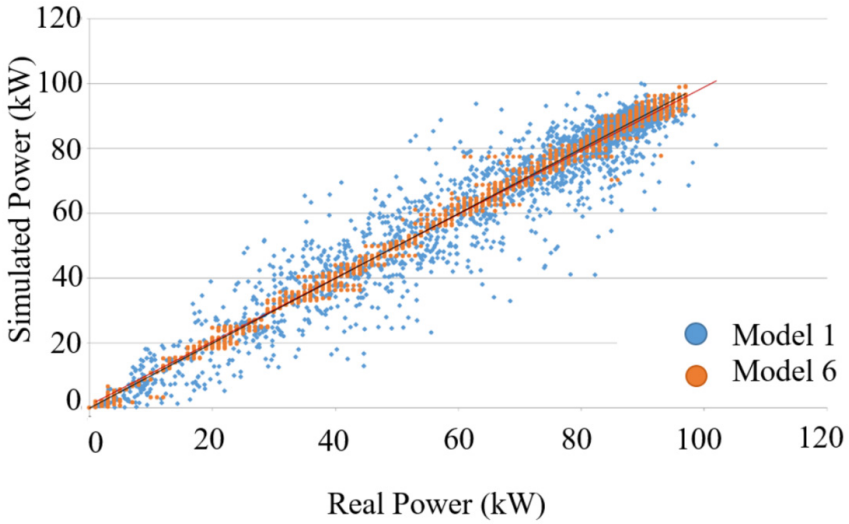

Figure 8.- Regression on the real power of the PV panel and the estimated power for production model 1 (without the wind speed variable, in blue) and for model 6 (wind speed variable, in red).

In order to verify the impact of external temperature on production, Figure 9 shows the real production of the PV plant (blue discontinuous line) and the estimated production with the reference model (red discontinuous line) and other possible global warming scenarios. For each scenario, according the hypothesis "*ceteris paribus*", the average temperature of the site was increased. In Figure 9, it can be observed how the model estimates greater power losses with higher temperatures.

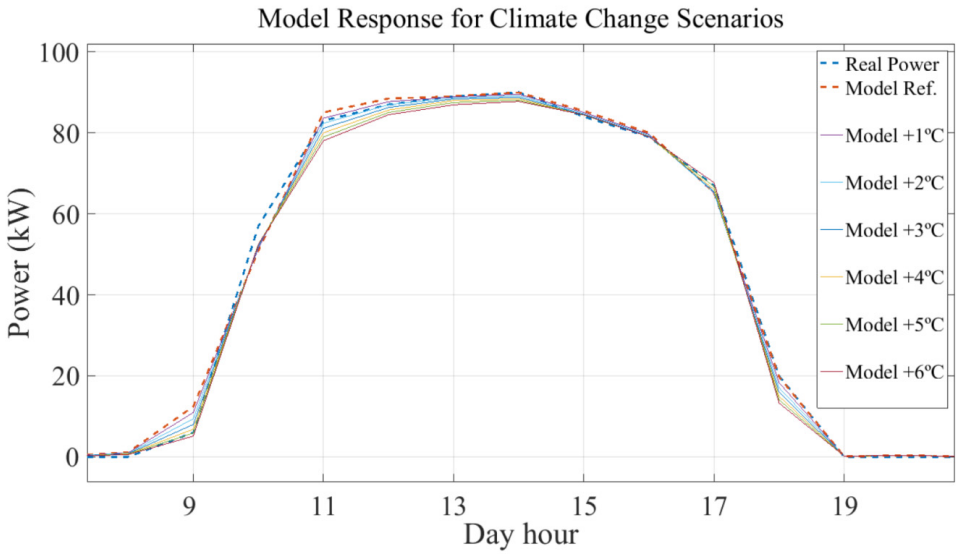

Figure 9.- Response of the model under different global warming scenarios.

It can be observed that, in the upper part of the power curve, the performance loss is more obvious. This corresponds to the first hours in the day, when the thermal accumulation is lower. The reference model corresponds to the current situation (increase of average temperature of 0.5 ºC). The other models correspond to a simulation of increase of temperature of 1 to 6 ºC, with successive increases of 1 ºC.

3.2. Calculation of the performance losses: production simulation in different scenarios with increases in average temperature

The historical data for the PV installation used in this article correspond to the period 2008-2011. Thus, the experienced global warming would have already been higher than 0.5 ºC [52]. Starting from this point, scenarios with a higher degree of global warming have been analysed, considering intervals of 0.5 ºC (from 0.5 ºC to 6 ºC).

In order to simulate the effect of an increase in the ambient temperature on the production of the PV installation, the wind registries have been maintained, assuming that, at a macroscopic level, the wind conditions (direction, frequency and intensity) are kept constant and only the average temperature of the site changes ("*cetris paribus*"). Under these premises, the production of the plant has been simulated with the available historical data, but increasing the average temperature of the site, as with the calculation of the curves in Figure 11.

Given that there is an intrinsic error between the production estimated with the model and the real production, the performance loss will be calculated with respect to the production estimated by the model under the current temperature conditions (+0.5 ºC) and not against the real production. Starting from the discrete data, obtained in each simulation, the performance loss indicator has been created. From this indicator, we can calculate the percentage loss of installed capacity, which has been represented in Figure 10. It can be observed that the loss of performance of the installation is

substantial, even under small temperature increases (x-axis). The losses can reach 9 % if the average increase in temperature is 6 ºC (worse projected scenario for 2050).

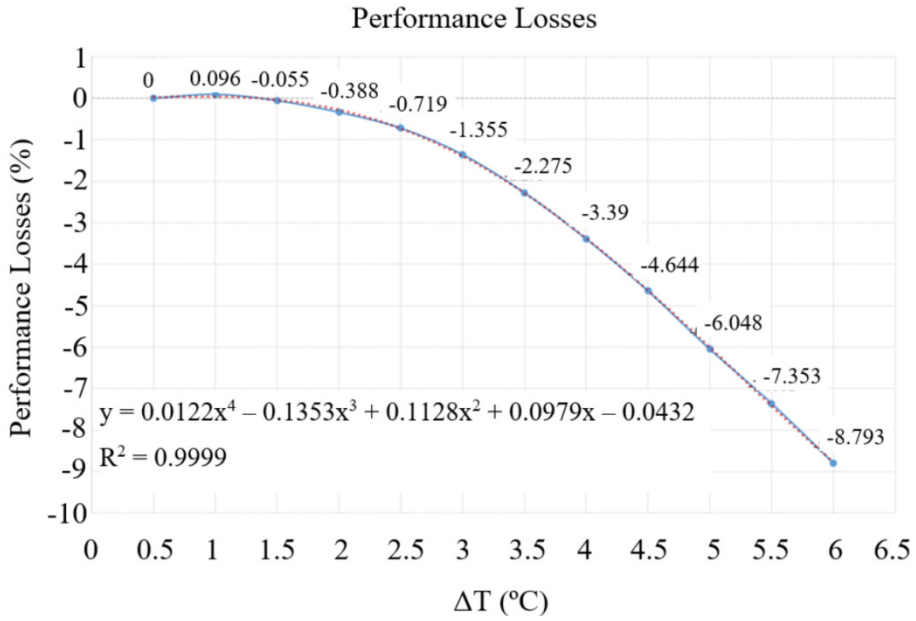

Figure 10.- Continuous function of performance losses due to the increase in temperature (as a result of global warming).

Given that the thermal increase will be gradual, Eq. (1) was obtained in order to know the performance loss over time. This was a polynomial curve of degree 4, which better adjusted to the points in Figure 10.

$$\text{Performace Losses} = 0.0122\,\Delta T^4 - 0.1353\,\Delta T^3 + 0.1128\,\Delta T^2 + 0.0979\,\Delta T - 0.0432 \quad (1)$$

$$\text{Performace} = 100 + \text{Performance Losses} \quad (2)$$

In order to better estimate the losses of our plant over time, it is necessary to know how global warming evolves in each scenario and to relate it to the loss of performance in Eq. (1). It was estimated that global warming will be gradual and exponential [39]. Therefore, the thermal increase has been simulated according to Eq. (3) and Eq. (4). In Figure 11, the thermal increase in the 2015-2050 period in different scenarios has been represented, starting with the current scenario (0.5 ºC) and then the 2DS (2 ºC) and ending up with the Current Policies (6 ºC). This last scenario would be the one projected by the IEA up to 2050 in case the current energy policies are maintained and the electricity mix in 2050 would be similar to the current one.

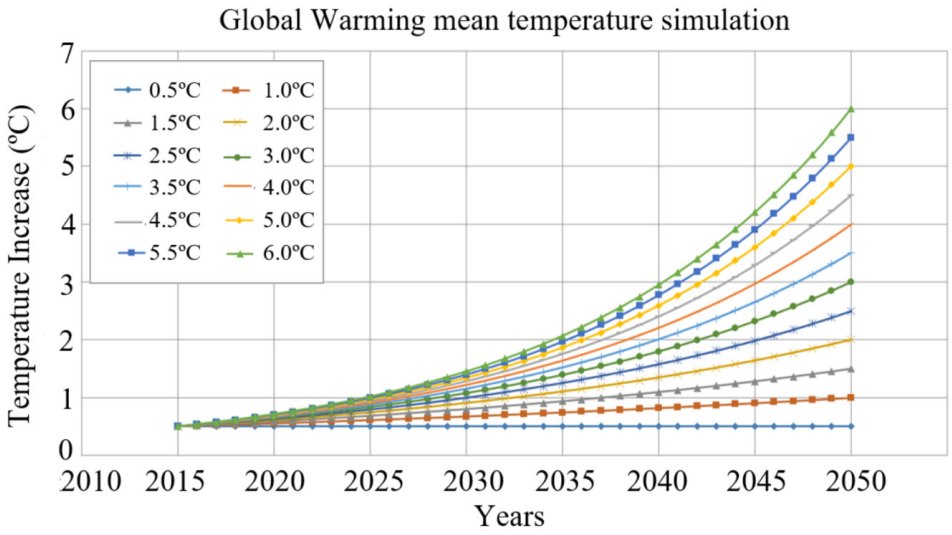

Figure 11. Simulation of the average temperature increase in the different scenarios.

The curves for the thermal increase have been built according to Eqs. (3) and (4):

$$\Delta T_x = t_0 . a^x \tag{3}$$

$$a = \sqrt[35]{\frac{t_f}{t_0}} \tag{4}$$

where ΔT_x represents the thermal increase (y-axis), t_0 is the initial temperature (0.5 ºC for 2015), t_f is the maximum admissible temperature for 2050 (in the 2DS), 35 is the number of intervals from 2015 to 2050 and x is the number of intervals for which we liked to know the warming (for 2030, x=15).

The equation obtained after merging Eqs. (1) to (4) directly relates the performance loss to the expected evolution in temperature over time (Eq. 5). The different curves of the evolution of performance of the PV plant in each scenario have been represented in a joint manner in Figure 12.

$$\text{Performace} = 0.0122\left(t_0.\left(\sqrt[35]{\frac{t_f}{t_0}}\right)^{year_i - year_0}\right)^4 - 0.1353\left(t_0.\left(\sqrt[35]{\frac{t_f}{t_0}}\right)^{year_i - year_0}\right)^3 + 0.1128\left(t_0.\left(\sqrt[35]{\frac{t_f}{t_0}}\right)^{year_i - year_0}\right)^2 + 0.0979\left(t_0.\left(\sqrt[35]{\frac{t_f}{t_0}}\right)^{year_i - year_0}\right) + 99.9568 \tag{5}$$

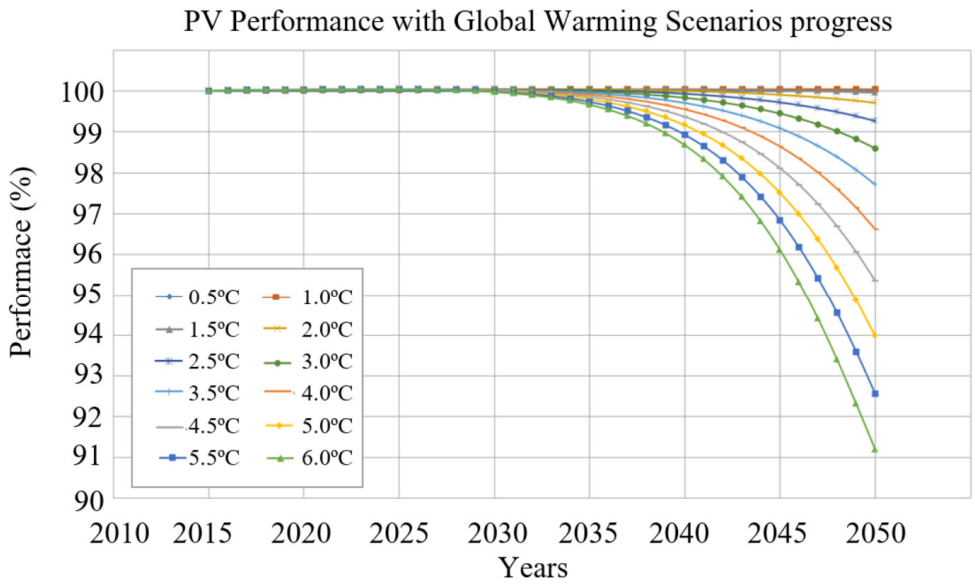

Figure 12. Performance curve of the PV installation over time for different global warming scenarios

3.3. Energy and economic losses of the PV installation.

The expected economic loss of the PV plant as a result of global warming in the 2015-2050 interval have been calculated from Eq. (5), considering a gradual warming. It was assumed that the installation is active during such period, with similar panels to the original ones and without degradation of the equipment. Our 5 MW PV plant has an average generation of 2822 full load hours (14.12 GWh/year). The expected accumulated generation until 2050 (without losses) will be 508 GWh. In a scenario of average global warming of 2 ºC, the expected accumulated generation will be 507.97 GWh. The calculated (accumulated) economic losses in the year 2050 represent a 0.01 %, or $ 3,395 (2018 USD), considering a sales price of 68.7 $/MWh [4]. Regarding the emissions, the loss of performance means that other conventional sources will have to compensate for this shortfall. This would lead to an increase of emissions of 16.3 tCO_2 eq., considering the average emissions of the Spanish energy mix (0.33 tCO_2 by MWh [53]). In a global warming scenario of 6 ºC, the expected accumulated production is 500.75 GWh, with an accumulated loss of 1.43 %. This represents $ 485,507 (2018 USD) and 2332 tCO_2 eq. of additional emissions. The losses are reduced due to the exponential evolution of warming.

4. Discussion

A model of energy production of a PV plant was built, taking into account the global irradiation but also the temperature of the site, the wind and other additional fictitious variables generated from the specific date and hour. Based on ANN and TDNN, the methodology showed a good capacity to reproduce the maximum energy that can be produced according to all the environmental conditions, especially using all the input variables and the fictitious variables, together with the memory effect of the TDNN.

A detailed exploration of the data was performed, where correlation was appreciated between the fictitious variables and the records in which the greatest loss of performance occurred.

Once the production model was optimized, the impact of climate change on PV generation in the plant was analysed. It is shown that the ambient temperature affects the performance of the panels, as well as their thermal dynamics during the day. One of the findings was a greater reduction of the performance of the PV panels during the first hours of the day (in the ascending part of the power curve), which might be due to the fact that the thermal increases have a greater impact on those hours

with traditionally lower temperatures. Then, the thermal increases due to climate change were simulated in order to assess the impact on production. Several scenarios of global temperature increase were simulated and the loss of performance of the plant over time was calculated.

Our results show that an increase of the temperatures will lead to a reduction of the performance of PV plants and, thus, a lower level of electricity generation for the same installed capacity. In turn, an increase in capacity will be needed and, thus, more investment in new PV capacity will be required to make up for such shortfall in order to comply with the COP21 Paris objectives.

It has been shown that, for the scenario of a global warming of 2 ºC, the thermal increase will start to influence the performance of PV installations since 2040, with a small impact in 2050. However, in a scenario of 6 ºC, the impact will be high, and the reduction in performance will be close to 10 %.

These results only show the loss of performance due to the thermal increase (according the hypothesis "*ceteris paribus*"), but other impacts such as changes in local irradiance, wind flows, and other factors would need to be considered. The study did not take into account the loss of performance of the panels due to their own degradation. The joint effect of all of these factors should be considered in future studies.

References

1. Ming, T.; de_Richter, R.; Liu, W.; Caillol, S. Fighting global warming by climate engineering: Is the Earth radiation management and the solar radiation management any option for fighting climate change? *Renewable and Sustainable Energy Reviews*, Volume 31, March 2014, Pages 792-834, ISSN 1364-0321, https://doi.org/10.1016/j.rser.2013.12.032.
2. Sansaniwal, S.K.; Sharma, V.; Mathur, J. Energy and exergy analyses of various typical solar energy applications: A comprehensive review. *Renewable and Sustainable Energy Reviews*, Volume 82, Part 1, 2018, Pages 1576-1601, ISSN 1364-0321, https://doi.org/10.1016/j.rser.2017.07.003.
3. Sampaio, P.G.V.; González, M.O.A. Photovoltaic solar energy: Conceptual framework. *Renewable and Sustainable Energy Reviews*, Volume 74, 2017, Pages 590-601, ISSN 1364-0321, https://doi.org/10.1016/j.rser.2017.02.081.
4. Breyer, C.; Koskinen, O. Philipp Blechinger, Profitable climate change mitigation: The case of greenhouse gas emission reduction benefits enabled by solar photovoltaic systems. *Renewable and Sustainable Energy Reviews*, Volume 49, 2015, Pages 610-628, ISSN 1364-0321, https://doi.org/10.1016/j.rser.2015.04.061.
5. World Energy Outlook 2015. *International Energy Agency*. November 2015. ISBN: 978-92-64-24366-8, ISSN: 2072-5302. https://www.iea.org/reports/world-energy-outlook-2015
6. New Energy Outlook 2016. Long-term projections of the global energy sector. Solar. *Bloomberg New Energy Finance.* June 2016.
7. de la Parra, I.; Muñoz, M.; Lorenzo, E.; García, M.; Marcos, J.; Martínez-Moreno, F. PV performance modelling: A review in the light of quality assurance for large PV plants. *Renewable and Sustainable Energy Reviews*, Volume 78, 2017, Pages 780-797, ISSN 1364-0321, https://doi.org/10.1016/j.rser.2017.04.080.
8. Fant, C.; Schlosser, C.A.; Strzepek, K. The impact of climate change on wind and solar resources in southern Africa. *Applied Energy*, Volume 161, 2016, Pages 556-564, ISSN 0306-2619, https://doi.org/10.1016/j.apenergy.2015.03.042.
9. Han, Y.; Wang, N.; Ma, M.; Zhou, H.; Dai, S.; Zhu, H. A PV power interval forecasting based on seasonal model and nonparametric estimation algorithm. *Solar Energy*, Volume 184, 2019, Pages 515-526, ISSN 0038-092X, https://doi.org/10.1016/j.solener.2019.04.025.
10. Solaun, K.; Cerdá, E. Climate change impacts on renewable energy generation. A review of quantitative projections. *Renewable and Sustainable Energy Reviews*, Volume 116, 2019, 109415, ISSN 1364-0321, https://doi.org/10.1016/j.rser.2019.109415.
11. Pryor, S.C.; Barthelmie, R.J. Climate change impacts on wind energy: A review. *Renewable and Sustainable Energy Reviews*, Volume 14, Issue 1, 2010, Pages 430-437, ISSN 1364-0321, https://doi.org/10.1016/j.rser.2009.07.028.
12. Davy, R.; Gnatiuk, N.; Pettersson, L.; Bobylev, L. Climate change impacts on wind energy potential in the European domain with a focus on the

Black Sea. *Renewable and Sustainable Energy Reviews*, 2017 , ISSN 1364-0321, https://doi.org/10.1016/j.rser.2017.05.253.

13. Lydia, M.; Kumar, S.S.; Selvakumar, A.I.; Kumar, G.E.P. A comprehensive review on wind turbine power curve modeling techniques. *Renewable and Sustainable Energy Reviews*, Volume 30, February 2014, Pages 452-460, ISSN 1364-0321, http://dx.doi.org/10.1016/j.rser.2013.10.030.
14. Taslimi-Renani, E.; Modiri-Delshad, M.; Elias, M.F.M.; Rahim, N.A. Development of an enhanced parametric model for wind turbine power curve. *Applied Energy*, Volume 177, 1 September 2016, Pages 544-552, ISSN 0306-2619, http://dx.doi.org/10.1016/j.apenergy.2016.05.124.
15. Pelletier, F.; Masson, C.; Tahan, A. Wind turbine power curve modelling using artificial neural network. *Renewable Energy*, Volume 89, April 2016, Pages 207-214, ISSN 0960-1481, http://dx.doi.org/10.1016/j.renene.2015.11.065.
16. Lapira, E.; Brisset, D.; Ardakani, H.D.; Siegel, D.; Lee, J. Wind turbine performance assessment using multi-regime modeling approach. *Renewable Energy*, Volume 45, September 2012, Pages 86-95, ISSN 0960-1481, http://dx.doi.org/10.1016/j.renene.2012.02.018.
17. Chen, Z.; Chen, Y.; Wu, L.; Cheng, S.; Lin, P.; You, L. Accurate modeling of photovoltaic modules using a 1-D deep residual network based on I-V characteristics. *Energy Conversion and Management*, Volume 186, 2019, Pages 168-187, ISSN 0196-8904, https://doi.org/10.1016/j.enconman.2019.02.032.
18. Lindsay, N.; Libois, Q.; Badosa, J.; Migan-Dubois, A.; Bourdin, V. Errors in PV power modelling due to the lack of spectral and angular details of solar irradiance inputs. *Solar Energy*, Volume 197, 2020, Pages 266-278, ISSN 0038-092X, https://doi.org/10.1016/j.solener.2019.12.042.
19. Seapan, M.; Hishikawa, Y.; Yoshita, M.; Okajima, K. Temperature and irradiance dependences of the current and voltage at maximum power of crystalline silicon PV devices. *Solar Energy*, Volume 204, 2020, Pages 459-465, ISSN 0038-092X, https://doi.org/10.1016/j.solener.2020.05.019.
20. Kermadi, M.; Chin, V.J.; Mekhilef, S.; Salam, Z. A fast and accurate generalized analytical approach for PV arrays modeling under partial shading conditions. *Solar Energy*, Volume 208, 2020, Pages 753-765, ISSN 0038-092X, https://doi.org/10.1016/j.solener.2020.07.077.
21. Chao, P.; Li, W.; Liang, X.; Shuai, Y.; Sun, F.; Ge, Y. A comprehensive review on dynamic equivalent modeling of large photovoltaic power plants. *Solar Energy*, 2020, ISSN 0038-092X, https://doi.org/10.1016/j.solener.2020.06.051.
22. Wang, F.K.; Mamo, T. Gradient boosted regression model for the degradation analysis of prismatic cells. *Computers & Industrial Engineering*, Volume 144, 2020, 106494, ISSN 0360-8352, https://doi.org/10.1016/j.cie.2020.106494.
23. Kumari, P.; Toshniwal, D. Extreme gradient boosting and deep neural network based ensemble learning approach to forecast hourly solar irradiance. *Journal of Cleaner Production*, Volume 279, 2021, 123285,

ISSN 0959-6526, https://doi.org/10.1016/j.jclepro.2020.123285.

24. Akram, M.W.; Li, G.; Jin, Y.; Chen, X.; Zhu, C.; Ahmad, A. Automatic detection of photovoltaic module defects in infrared images with isolated and develop-model transfer deep learning. *Solar Energy*, Volume 198, 2020, Pages 175-186, ISSN 0038-092X, https://doi.org/10.1016/j.solener.2020.01.055.

25. Yap, W.K.; Karri, V. An off-grid hybrid PV/diesel model as a planning and design tool, incorporating dynamic and ANN modelling techniques. *Renewable Energy*, Volume 78, 2015, Pages 42-50, ISSN 0960-1481, https://doi.org/10.1016/j.renene.2014.12.065.

26. Yona, A.; Senjyu, T.; Saber, A.Y.; Funabashi, T.; Sekine, H.; Kim, C. "Application of Neural Network to One-Day-Ahead 24 hours Generating Power Forecasting for Photovoltaic System", *2007 International Conference on Intelligent Systems Applications to Power Systems*, Toki Messe, Niigata, 2007, pp. 1-6, doi: 10.1109/ISAP.2007.4441657, https://ieeexplore.ieee.org/document/4441657.

27. Mellit, A.; Pavan, A.M. Performance prediction of 20kwp grid-connected pho- tovoltaic plant at trieste (italy) using artificial neural network. *Energy Conversion and Management,* 51 (12) (2010) 2431–2441, https://doi.org/10.1016/j.enconman.2010.05.007.

28. Jung, Y.; Jung, J.; Kim, B.; Han, S.U. Long short-term memory recurrent neural network for modeling temporal patterns in long-term power forecasting for solar PV facilities: Case study of South Korea. *Journal of Cleaner Production*, Volume 250, 2020, 119476, ISSN 0959-6526, https://doi.org/10.1016/j.jclepro.2019.119476.

29. Almonacid, F; Pérez-Higueras, P.J.; Fernández, E.F.; Hontoria, L. A methodology based on dynamic artificial neural network for short-term forecasting of the power output of a PV generator. *Energy Conversion and Management*, Volume 85, 2014, Pages 389-398, ISSN 0196-8904, https://doi.org/10.1016/j.enconman.2014.05.090.

30. Raza, M.Q.; Nadarajah, M.; Ekanayake, C. On recent advances in PV output power forecast. *Solar Energy*, Volume 136, 2016, Pages 125-144, ISSN 0038-092X, https://doi.org/10.1016/j.solener.2016.06.073.

31. Ahmed, R.; Sreeram, V.; Mishra, Y.; Arif, M.D. A review and evaluation of the state-of-the-art in PV solar power forecasting: Techniques and optimization. *Renewable and Sustainable Energy Reviews*, Volume 124, 2020, 109792, ISSN 1364-0321, https://doi.org/10.1016/j.rser.2020.109792.

32. Hamou, S.; Zine, S.; Abdellah, R. Efficiency of PV Module under Real Working Conditions. *Energy Procedia*, Volume 50, 2014, Pages 553-558, ISSN 1876-6102, https://doi.org/10.1016/j.egypro.2014.06.067.

33. El Mentaly, L.; Amghar, A.; Sahsah, H. The prediction of the maximum power of PV modules associated with a static converter under different environmental conditions. *Materials Today: Proceedings*, Volume 24, Part 1, 2020, Pages 125-129, ISSN 2214-7853, https://doi.org/10.1016/j.matpr.2019.07.704.

34. Mellit, A.; Sağlam, S.; Kalogirou, S.A. Artificial neural network-based model for estimating the produced power of a photovoltaic module. *Renewable Energy*, Volume 60, 2013, Pages 71-78,

ISSN 0960-1481, https://doi.org/10.1016/j.renene.2013.04.011.

35. Das, U.K.; Tey, K.S.; Seyedmahmoudian, M.; Idna Idris, M.Y.; Mekhilef, S.; Horan, B.; Stojcevski, A. SVR-Based Model to Forecast PV Power Generation under Different Weather Conditions. *Energies* 2017, 10, 876. https://doi.org/10.3390/en10070876.
36. Wu, Y.K.; Chen, C.R.; Rahman, H.A. A Novel Hybrid Model for Short-Term Forecasting in PV Power Generation. International Journal of Photoenergy. *Solar Energy and Clean Energy: Trends and Developments* 2014.Volume 2014, Article ID 569249. https://doi.org/10.1155/2014/569249.
37. Patel, J.; Shah, S.; Thakkar, P.; Kotecha, K. Predicting stock market index using fusion of machine learning techniques. *Expert Systems with Applications*, Volume 42, Issue 4, 2015, Pages 2162-2172, ISSN 0957-4174, https://doi.org/10.1016/j.eswa.2014.10.031.
38. Dhabl, A. Renewable Power Generation Costs in 2018. *International Renewable Energy Agency*, IRENA 2019. ISBN 978-92-9260-126-3. https://www.irena.org/-/media/Files/IRENA/Agency/Publication/2019/May/IRENA_Renewable-Power-Generations-Costs-in-2018.pdf. (Accessed on 2 Oct 2019)
39. Rodríguez-López, M.A.; Cerdá, E.; del Rio, P. Modeling wind-turbine power curves: effect of environmental temperature on wind energy generation. *Energies* 2020, 13(18), 4941; https://doi.org/10.3390/en13184941.
40. Rodríguez-López, M.A.; López-González, L.M.; López-Ochoa, L.M.; Las-Heras-Casas, J. Methodology for Detecting Malfunctions and Evaluating the Maintenance Effectiveness in Wind Turbine Generator Bearings Using Generic versus Specific Models from SCADA Data. *Energies* 2018, 11, 746. https://doi.org/10.3390/en11040746.
41. Ata, R. Artificial neural networks applications in wind energy systems: a review. *Renewable and Sustainable Energy Reviews*, Volume 49, 2015; p. 534-562. http://dx.doi.org/10.1016/j.rser.2015.04.166.
42. Nayeripour, M.; Mansouri, M.M. An advanced analytical calculation and modeling of the electrical and mechanical harmonics behavior of Doubly Fed Induction Generator in wind turbine. *Renewable Energy*, Volume 81, 2015; p.275-285. http://dx.doi.org/10.1016/j.renene.2015.03.018.
43. Ramirez-Rosado, I.J.; Fernandez-Jimenez, L.A.; Monteiro, C.; Sousa, J.; Bessa, R. Comparison of two new short-term wind-power forecasting systems. *Renewable Energy*, Volume 34, Issue 7, 2009; p.1848-1854. http://dx.doi.org/10.1016/j.renene.2008.11.014.
44. Fernandez-Jimenez, L.A.; Muñoz-Jimenez, A.; Falces, A.; Mendoza-Villena, M.; Garcia-Garrido, E,; Lara-Santillan, P.M.; Zorzano-Alba, E.; Zorzano-Santamaria, P.J. Short-term power forecasting system for photovoltaic plants. *Renewable Energy*, Volume 44, 2012; p.311-317. http://dx.doi.org/10.1016/j.renene.2012.01.108.
45. Akarslan, E.; Hocaoglu, F.O. A novel adaptive approach for hourly solar radiation forecasting. *Renewable Energy*, Volume 87, Part 1, 2016; p.628-633. http://dx.doi.org/10.1016/j.renene.2015.10.063.
46. Anamika; Peesapati, R.; Kumar, N. Estimation of GSR to ascertain solar electricity cost in context of deregulated

electricity markets. *Renewable Energy*, Volume 87, Part 1, 2016; p.353-363. http://dx.doi.org/10.1016/j.renene.2015.10.038.

47. Santhosh, T.V.; Gopika, V.; Ghosh, A.K.; Fernandes, B.G. An approach for reliability prediction of instrumentation & control cables by artificial neural networks and Weibull theory for probabilistic safety assessment of NPPs. *Reliability Engineering & System Safety*, Volume 170, 2018, Pages 31-44, ISSN 0951-8320, https://doi.org/10.1016/j.ress.2017.10.010.

48. Phys Org, 2016. https://phys.org/news/2016-11-solar-island-effect-large-scale-power.html. (Accessed on 23 Jun 2018).

49. Edalat, M.M.; Stephen, H. Effects of two utility-scale solar energy plants on land-cover patterns using SMA of Thematic Mapper data. *Renewable and Sustainable Energy Reviews*, Volume 67, 2017, Pages 1139-1152, ISSN 1364-0321, https://doi.org/10.1016/j.rser.2016.09.079.

50. Schlechtingen, M.; Ferreira-Santos, I.; Achiche, S. Wind turbine condition monitoring based on SCADA data using normal behavior models. Part 1: System description. *Applied Soft Computing*, Volume 13, Issue 1, 2013; p. 259-270. http://dx.doi.org/10.1016/j.asoc.2012.08.033.

51. Kusiak, A.; Verma, A. Analyzing bearing faults in wind turbines: A data-mining approach. *Renewable Energy*, Volume 48, 2012; p. 110-116. http://dx.doi.org/10.1016/j.renene.2012.04.020.

52. National Aeronautics and Space Administration (NASA), http://climate.nasa.gov/system/internal_resources/details/original/647_Global_Temperature_Data_File.txt (Accessed on 12 Dec 2017).

53. CNMC (Comisión Nacional de los mercados y la competencia). https://gdo.cnmc.es/CNE/resumenGdo.do?anio=2015. (Accessed on 1 May 2019).

Optimizing the energy generation cost with renewable resources using generic algorithms and evaluating the impact of Electrical Vehicles.

Abstract: Climate change represents a serious global challenge which requires the adoption of decarbonisation strategies everywhere. It is a widely shared view that the uptake of low-carbon technologies, including renewable energy technologies, is a critical alternative to reduce greenhouse gas emissions, whose accumulation lead to global warming. The scenarios proposed in this paper foresee a transition to an electrification of the economy which replaces fossil fuel consumption on both the generation and demand sides, with the incorporation of electric vehicles or heat pumps, among others. On the other hand, renewable generation presents great variability, being very difficult to match generation with demand, and its integration remains a big challenge. This integration is facilitated by a series of technical and regulatory solutions, such as the use of batteries, demand management systems, etc. This article provides a methodology based on genetic algorithms and Monte Carlo simulations to determine the level of technical resources which would minimize the cost of power generation in a 100% renewable generation environment in semi-isolated or completely isolated micro-grid systems. The consumption and supply of an urban center in southern Spain with several renewable electricity plants (photovoltaic and wind) in nearby sites as well as the integration of a fleet of purely electric vehicles was simulated, and the costs of the energy consumed were evaluated.

Keywords: Climate change, microgrids, renewable energy integration, energy prices

1. Introduction

Taking into account population growth and the aspiration for greater levels of economic development, humanity needs more and more energy. Unfortunately, the use of traditional fossil fuels is one of the main causes of global warming [1]. As it is well-known, the accumulation of greenhouse gas (GHG) emissions is directly related to the combustion of fossil fuels in all sectors of the economy, notably electricity generation, transport and industry [2, 3]. Climate change mitigation requires reductions of GHG emissions, but the world economy is "addicted" to energy [4]. In short,climate change mitigation will require the adoption of decarbonisation strategies everywhere and the electrification of energy demand.

A low carbon economy will also be an economy with lower primary energy consumption. This requires a profound change in the ways in which energy is transformed, distributed and consumed. In addition, the change in the energy model becomes a main vector of the new logics of production and consumption which will require changes in both the transformation processes of primary energy (and electrical energy) and the consumption processes, radically affecting sectors such as building, industry and transport [5, 6, 7, 8].

One of the main transformations in the energy sector will come from the transition from large centralized generation plants to distributed generation with renewable energy sources. Spain's solar and wind potential favors distributed generation, which will facilitate the creation of a multitude of local business models [9]. Distributed generation ranges from a single home to a neighborhood community and even a cooperative in a small urban group that generates electricity for self-consumption or sale. Distributed generation with small plants [10] and self-consumption can also lead to the creation and management of micro distribution networks, including the creation of local energy markets. The price of energy will depend, not only on supply and the demand at all times, but also on the location. Those locations that are particularly windy, sunny or with good water resources would have an advantage.

The technology required for distributed generation is a reality, but substantial improvements in the network will be needed [11, 12, 13] together with the establishment of a clear regulatory and normative framework. The authors of a recent paper [14], analyzed the regulatory challenges in the face of high penetrations of distributed energy resources (generation, batteries, demand management, etc.), and point out that the current Spanish regulation is not adequate and should be reviewed in depth to allow an equal competition between central and distributed resources.

Wind and solar (photovoltaic and thermal) are the renewable energy technologies (RETs) considered to be the main alternatives for this reduction in emissions and energy dependence [4, 15] [16, 17, 18]. Solar energy is an abundant and perpetual cheap source [1, 19, 20]. Several simulation models show that RETs play a crucial role in reducing global warming and keeping it below 1.5º-2ºC [3, 21]. On the other hand, solar photovoltaic (PV) electricity has experienced a large cost reduction, from 75.6 $/W installed in 1976 to 0.63 $/W in 2015 (2018 USD) [22].

From the demand side, the electric vehicle (EV) is expected to represent a turning point in the transition as well as a great economic engine. It is estimated that, in the United States, the use of EVs will lead to the reduction of 6.5 million barrels of oil per day, that is, more than 50% of the total oil imported in the United States [23]. Spain has an important automobile industry, which accounted for 11% of GDP in 2020 [24]. The innovation and adaptation of its production plants in order to provide competitive products will represent a great opportunity for the country. Other countries such as Germany or France already give incentives to decarbonize transport and encourage the purchase of electric vehicles [25, 26]. Germany is considering to forbid the registration of conventional vehicles in 2030 and promote the installation of fast charging points for electric vehicles (the fear of running out of charge in vehicles is one of its main social barriers [23], called "range ansiety". The German government, which evaluates the marginal damage of CO_2 at 70 €/tCO_2 [27], agreed in mid-2016 with local car manufacturers to implement several incentives in order to encourage the development of EVs, with the additional objective to repower its car industry. These incentives include: 1) direct purchase subsidies (criticized by certain authors [27]), although shared with manufacturers; 2) support for the installation of 15,000 new fast charging points before 2020[5]; 3) replacement of 4,800 vehicles of the public fleet with EVs and; 4) exemption from road tax for new 100% electric vehicles (for a period of 10 years).

This article tries to respond to the growing interest in modeling the optimal structure of isolated networks with a high integration of renewables on the one hand, and the impact of EVs on these networks on the other hand. It presents a methodology to perform an efficient dimensioning of resources, with the aim to reduce the cost of energy generation by combining renewable generation sources with the greatest penetration, as well as energy storage and some demand management tools, taking into account the requirement that energy security should be guaranteed and that supply cuts should be avoided. In addition, the impact on the cost of energy generation by the progressive integration of EVs has been evaluated, thus combining the two topics of interest.

Several publications provide interesting insights on these research fields. Joaquin Delgado et al. [29] presented an analysis of the impact on the grid considering several penetration rates in Portugal (100 thousand, 500 thousand and 1 million of Battery Electric Vehicles (BEV)), concluding that there won't be any problem to integrate them in the current grid structure, using the surplus energy from pumping storage and exports. The consumption considered for the BEV cars is low, considering a daily route for 33km per car (maximum battery autonomy in the 2018 BEV), which is 36% lower compared to this study They assumed a consumption of 0.2105 kWh/km per car, whereas 0.185kWh/km is the consumption used in this paper. Nevertheless, their research does not consider 100% renewable generation scenarios and distributed generation.

[5] The Combined Charging System technology [28], traditionally adopted by European EVs since 2012, will be used. The aim is to establish the bases of the standards in Europe.

On the contrary, Mengyu Li et al. [30] modeled the impact of electric-vehicle-grid integration in a 100% renewable electricity grid in Australia, using a GIS-based electricity supply-demand model simulating an hourly competitive-bidding process over a year. In the study, they show how uncontrolled charging will increase the LCOE by 14.6% with an EV penetration of 100% (8.9% with a 50% penetration). Nevertheless, the LCOE could be reduced by 3.4% with a 100% EV penetration using controlled charging strategies. The additional installed capacity would be around 64%.

Kevin Joseph et al. [31] analyzed the impact of the penetration of EV on the grid in Reykjavík over the period 2019-2050, concluding that the Electrical Vehicle (EV) could be a great risk for grid reliability due to the fact that peak consumption could be increased between 67% and 114%. Naresh Kumar and Suresh Kumar [32] presented several tools to minimize this impact through a smart control of the EV load. These authors pointed to the need to perform an optimized design of the renewable installed capacity. Whereas, in our study, the EV is assumed to involve an additional electricity consumption, [32] considered EV as an equipment with the option to inject energy to the grid (V2G- Vehicle to Grid).

Baojun Sun [33] developed an optimization multi-objective model to determine wind and PV installed capacity, taking into account the batteries needed to integrate the EV fast charge systems (FEVCS-WPE) based on a hybrid algorithm combining the multi-objective particle swarm optimization (MOPSO) algorithm and the Technique for Order Preference by Similarity to Ideal Solution (TOPSIS) method. Their objective was the minimization of generation costs and emissions.

Konstantinos Boulouchos [34] used Monte-Carlo simulations on power flows to analyze the impact of different EV penetration scenarios in the grid. Their results suggest that grid configuration as well as locally higher EV shares are relevant for line loading assessments, whereas car modeling and people's charging behavior play minor roles.

Pouria Emrani and Hamed Hashemi [35] also used Monte Carlo simulations to assess seasonal energy demand changes. Their results illustrated that Plug-in Hybrid Electric Vehicles and heat storage systems could act as appropriate solutions to decrease the operation costs of a residential energy hub.

J. Graça Gomes et al. [36] presented a methodology to size, in a cost-effective way, the installed capacity and storage systems needed in isolated grids with renewable energy. For their optimal grid configuration, the LCOE is 0.21 €/kWh (0.25 $/kWh). The impact of the EV penetration is not considered. Fatin et al. [37] obtained similar results, with the LCOE ranging between 0.204 $/kWh and 0.532 $/kWh, depending on the operating strategy.

Mark Kipngetich et al. [38] argue that the installed capacity in an isolated network needs to be planned and that its operations should be known in detail. They provide a model to optimize the cost of power generation and analyze the techno-economic performance in an isolated micro grid with high penetration of renewables which combine wind, PV, diesel generators, batteries and thermal storage systems.

However, none of the aforementioned contributions to the literature jointly assess how the renewable generation of the network should be sized in order to minimize the cost of energy generation [39], as well as the impact of the penetration of EVs on the costs of energy generation. This article tries to cover this gap in the literature. Compared to previous contributions, it advances knowledge on several fronts. At a methodological level, it provides a novel methodology based on the combination of Monte Carlo simulations and Genetic Algorithms (GA) in order to optimize the configuration of the grid components to minimize the generation costs. At an empirical level, the paper analyses the impact of EV penetration on electricity generation costs.

Accordingly, the paper is structured as follows. The next section describes the analytical model. The optimization algorithm is discussed in Section 3 and the results of the simulation are provided in section 4. Section 5 shows the results regarding the dimensioning of the grid with the renewable resources and the impact of EVs on the energy costs. Section 6 closes with the most relevant conclusions.

2. Materials and Methods

This section describes the analytical model used to simulate the cost of energy, taking into account several scenarios with respect to the number of households, EV penetration and energy storage.

We have modeled consumption in a group of households, which is used to simulate the consumption in groups of 1000, 5000, 20000 and 50000 households. For each of these scenarios, we have analyzed the impact of the penetration of EV, from a penetration of 0% to 100% at 10% intervals. Regarding energy storage, we have considered a scenario without batteries, another one with a maximum number of batteries (one per household) and, finally, a scenario without limitations on storage.

2.1. Description of the consumption profiles of the model

2.1.1. Description of electricity consumption profiles in households

This section shows a statistical characterization of the energy consumption of households in a coastal town in Spain, which was carried out based on their historical consumption for a period of one year. Given that all the energy consumption in the homes in this region is mostly electricity, it was to be expected that this consumption would increase in the summer months due to the use of air conditioning devices and, in winter, as a result of using electric heating systems. The selected population group does not have a natural gas installation, and most of them are single-family homes.

A total of 985,312 daily consumption records were available, i.e., a total of 23,647,488 hourly consumption records. These data correspond to the set of 2,700 homes in the municipality during 2015.

Figure 1 shows the typical box and whisker plot, the average weekly electricity consumption of the dwellings during a year. It can be seen that there is a significant number of users who consume more electricity in the winter (weeks 52 to 20 in), with a lower consumption in spring and autumn. In the winter months, the dispersion in the data with respect to the average consumption increases towards one side of the average, possibly due to an increase in the consumption of the habitual residents of the municipality and the absence of occasional residents who own a second home. In summer (weeks 27 to 36), average and median consumption increases, reducing dispersion compared to winter.

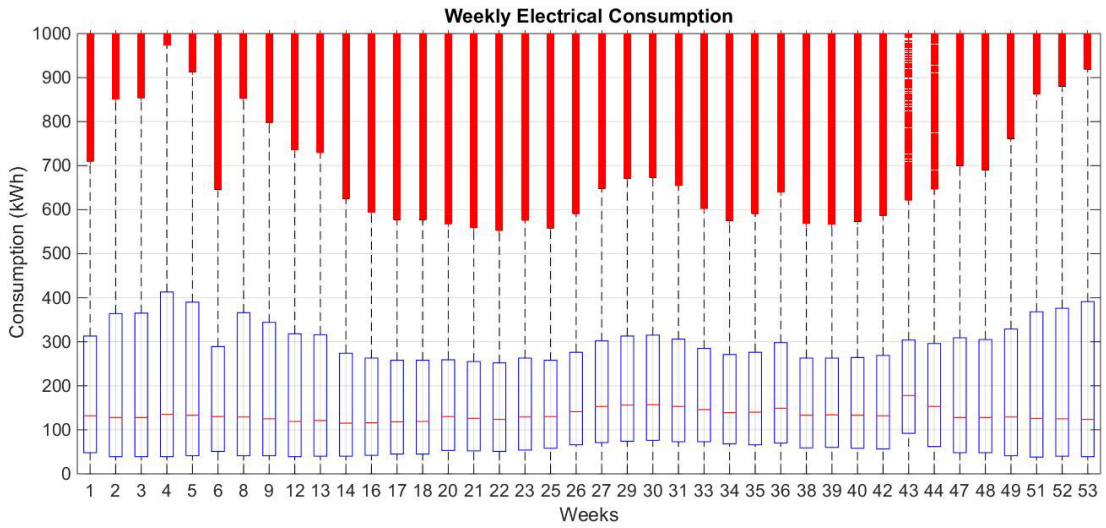

Figure .- 1 Average weekly consumption over the course of a year, based on data for 2,700 homes.

Data on the average consumption over the week for each of the seasons of the year (Figures 2a-2d) show that, in winter (Figure 2a), the global daily consumption is similar every day of the week whereas, in the rest of the seasons, the days with the greatest dispersion in the global daily consumption are those in the weekend (Saturday and Sunday in Figures 2b-2d).

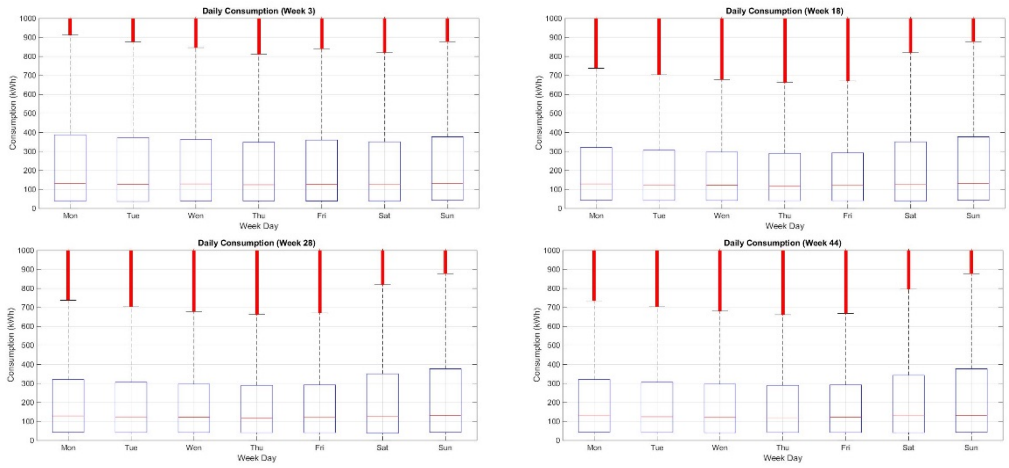

Figure .- 2 Daily global average consumption in several weeks over the year, based on information on 2,700 households.

Regarding intraday consumption, Figure 3 shows the average hourly consumption within a day. The profiles of several months (January, April and July) and days of the week are compared. It is observed that the peak of consumption of days in January (mainly Monday) is practically twice the peak in other months.

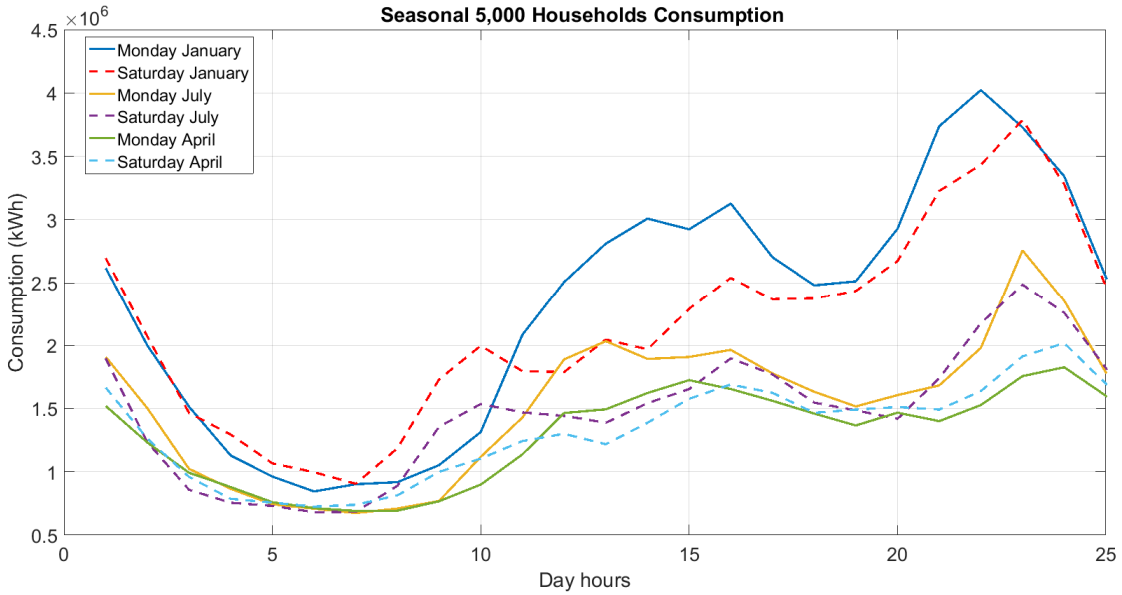

Figure .- 3 Average intraday consumption for various days of the week and times of the year

From the consumption dates, a total of 8,736 probabilistic consumption models were made (adjustment to a Weibull function), based on the week of the year (52 weeks), the weekday (7 days) and the time of day (24 hours). This partition was made in order to grasp the difference that exists in consumption in the seasons of the year, during the week (working days vs. weekends) and in the hours of daily activity. Based on this characterization, a simulation of the hourly consumption of a certain number of households was carried out for each hour, with the total consumption of the town being the sum of the independent random consumptions generated by the model [40, 41]. We decided to use the Weibull function instead of the normal distribution function, due to the fact that the normal function is symmetrical, whereas the consumption of the population in a given hour is not symmetrical. Thus, the Weibull function provides better fitting results.

Figure 4 shows the results of several simulations for a population group of 5000 households. It can be observed that the Monte Carlo simulation model correctly reproduces the different consumption patterns which are typical of weekends (11/14/2009 and 11/15/2009).

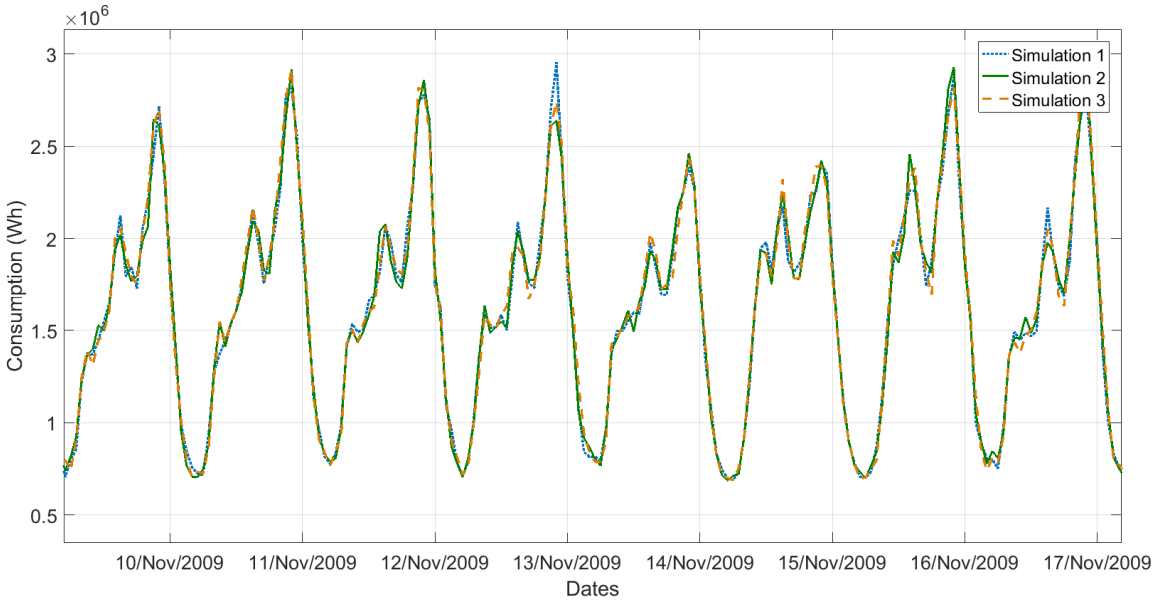

Figure 4-. Example of several different simulations of the electricity consumption of a population group of 5,000 households ($N_{households}$).

The number of dwellings in the population group ($N_{households}$) changes across different scenarios (5,000, 10,000, 15,000 and 20,000) in order to assess the impact of the population size on the cost of the energy generated.

2.1.2. Description of electricity consumption profiles in homes

In the previously analyzed electricity consumption scenarios, the consumption of EVs has a negligible or non-existent impact since their current penetration is very low. For this reason, the EV has been considered as an additional consumption that must be taken into account in future consumption models. Both the batteries of the EVs and those of the homes can be used as regulation elements and help to integrate renewables into the grid, since they can store excess electricity from renewable sources at times of low consumption. This study analyzes whether this equipment also helps to reduce the cost of power generation.

To estimate the energy consumption of EVs throughout the day, it was assumed that there are 1.6 vehicles per home (according to the National Statistics Institute, INE) and each vehicle travels an average of 50km [42] per day. The energy consumed to travel this distance is 9.25kWh, taking into account that the average consumption of a BMW i3 electric vehicle is 18.5 kWh per 100 km, with a maximum capacity of 27.2 kWh) [43]. To keep the vehicle battery full, it will need to be recharged every day with used energy. Based on these premises, the average daily consumption in a population of 5,000 homes would be 3,700 MWh, although the demand curve varies throughout the day.

$$Consume_{EV\_diario} = N_{EV} \cdot 50 \cdot 9.25kWh \quad (1)$$

$$N_{EV} = EV_{penetration\_level} \cdot 1.6 \cdot N_{households} \quad (2)$$

where $EV_{penetration\_level}$ is the penetration percentage of the EV in the population. A penetration level of 1 will mean that all vehicles in the population center are electric.

The EV load curves of the National Renewable Energy Laboratory (NREL) [44] were used to determine the intraday consumption profile, adapting the accumulated daily consumption to the one corresponding to the population group being analyzed. According to this study, the electricity consumption of EVs during weekends is 2% lower than on weekdays. The percentage distribution of EV consumption made by NREL along the different hours of the day ($Consume_{EV\_intra\_daily\_ratio}$) is shown in Figure 5. The consumption in one of the different analyzed scenarios was provided in Figure 4.

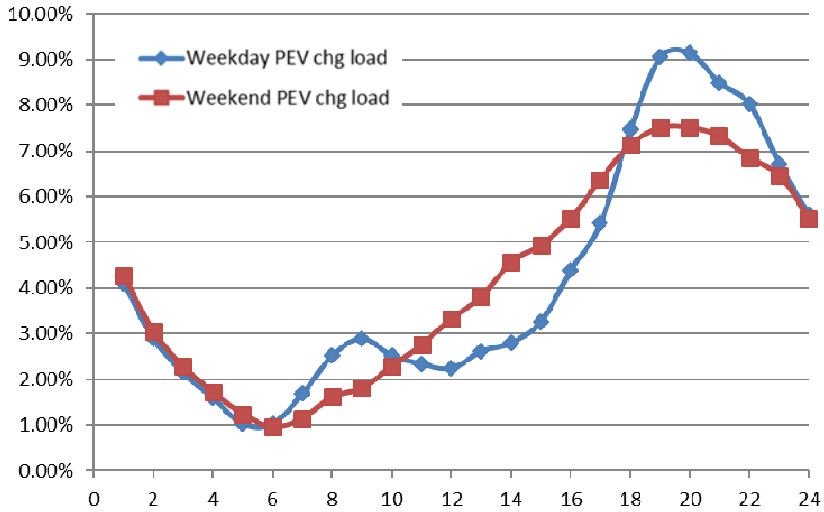

Figure .- 5 Daily load curves ($Consumption_{EV\_intra\_daily\_ratio}$) of EV on weekdays and weekends.

2.2. Renewable Generation

In order to simulate the supply of electric energy to the population group, the generation profiles of real renewable plants were used for a period of 2 years (duration of the simulation). Wind and photovoltaic were the RETs considered.

2.2.1. Wind generation profile

, The production history of a wind farm was used for the simulation of wind generation. The wind farm is built by 25 horizontal axis wind turbines of 1.5MW ($P_{windturbine\_max}$) of unit power each [45, 46].

For this study, the average production for each wind turbine ($P_{windturbine\_mean}(t) = P_{windturbine\_max} . P_{windturbine\_mean\_ratio}(t)$) was characterized for each time stamp (t), in such a way that the optimization algorithm can simulate the average wind production as a function of the number of simulated wind turbines in each iteration ($P_{Wind}(t) = N_{Wind\_turbines} \times P_{windturbine\_mean}(t)$). Figure 6 represents the generation profile of $P_{windturbine\_mean\_ratio}(t)$ used in the study (with a ratio of load between 0 and 1), calculated as:

$$P_{windturbine\_mean\_ratio}(t) = \frac{\sum_{n=1}^{n=25} P_{windturbine_{n_{ratio}}}(t)}{25} \quad (3)$$

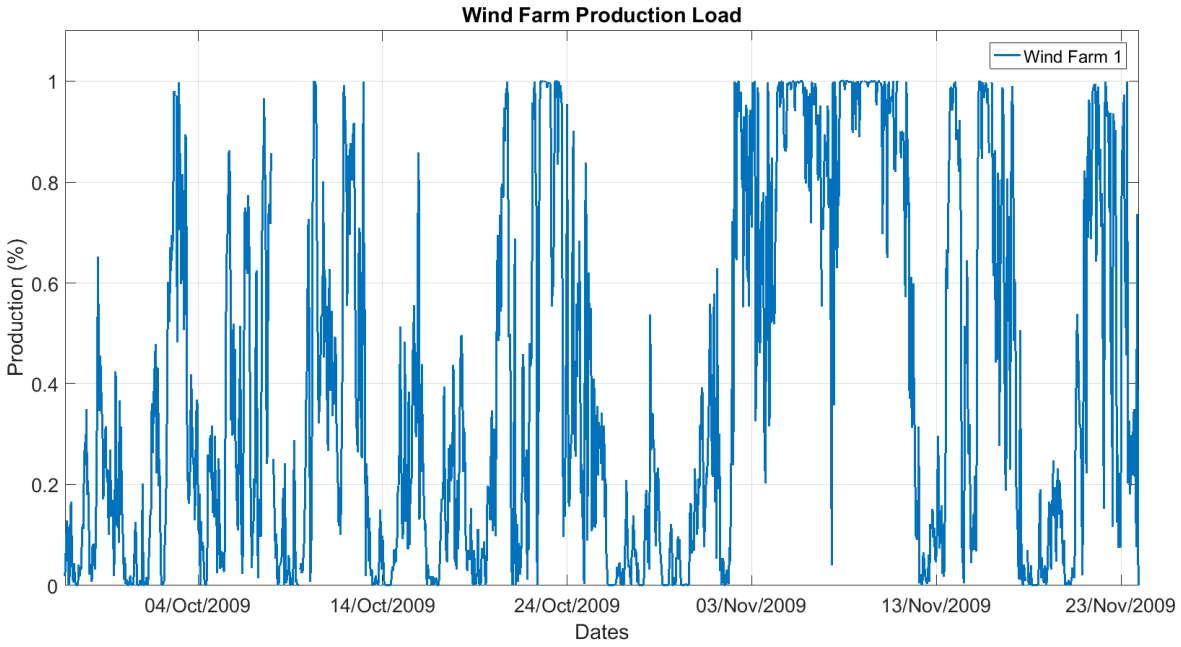

Figure.- 6 Temporary production ratio of an average wind turbine ($P_{windturbine\_mean\_ratio}$) as a ratio of load (1 equals 1.5 MW)

The algorithm determines the number of wind turbines ($N_{Wind\_turbines}$), with the average generation profile ($P_{windturbine\_mean\_ratio}$) and maximum power of the wind turbines ($P_{windturbine\_max}$), which are necessary in the energy mix of the microgrid to guarantee energy supply and meet the main goal of reducing electricity generation costs.

Since the original wind generation data were recorded at ten minute intervals, it was necessary to calculate the average power generated in an hourly interval.

2.2.2. Photovoltaic generation profile

In photovoltaic solar plants, solar radiation is transformed into electricity due to the photovoltaic effect [47], which was first observed by Becquerel in 1837. The study was carried out using production data from a photovoltaic plant with panels on solar tracking poles systems, which tend to have lower losses due to temperature than fixed installations on roofs. The PV generation profile would change when combining the existing generating plants with a wide adoption of fixed panels on roofs, a technology that is expected to represent a high percentage of installed photovoltaic power according to the IEA scenarios [3, 18].

In the case of PV panels, as with the characterization of the average wind turbine, models were developed using a large quantity of production data from 50 individual plants during one year. A unique model for a typical panel ($P_{PVmean}(t) = P_{PVmean\_ratio}(t) \cdot P_{PV\_max}$) of 100 kW of peak power (P_{PV_max}) was built, combining all the production registers. Thus, the photovoltaic generation profile at the site is defined according to the following expression, $PPV(t) = N_{PV\_panels} \cdot P_{PVmean}(t)$.

Figure 7 shows the power curve of the mean panel ($P_{PVmean\_ratio}(t)$) as a percentage of the peak power of the panel for the site during several consecutive days. As expected, PV generation can be very low at times, which affects the need to have different sources of electricity from renewable origin in order to avoid supply cuts in the isolated network.

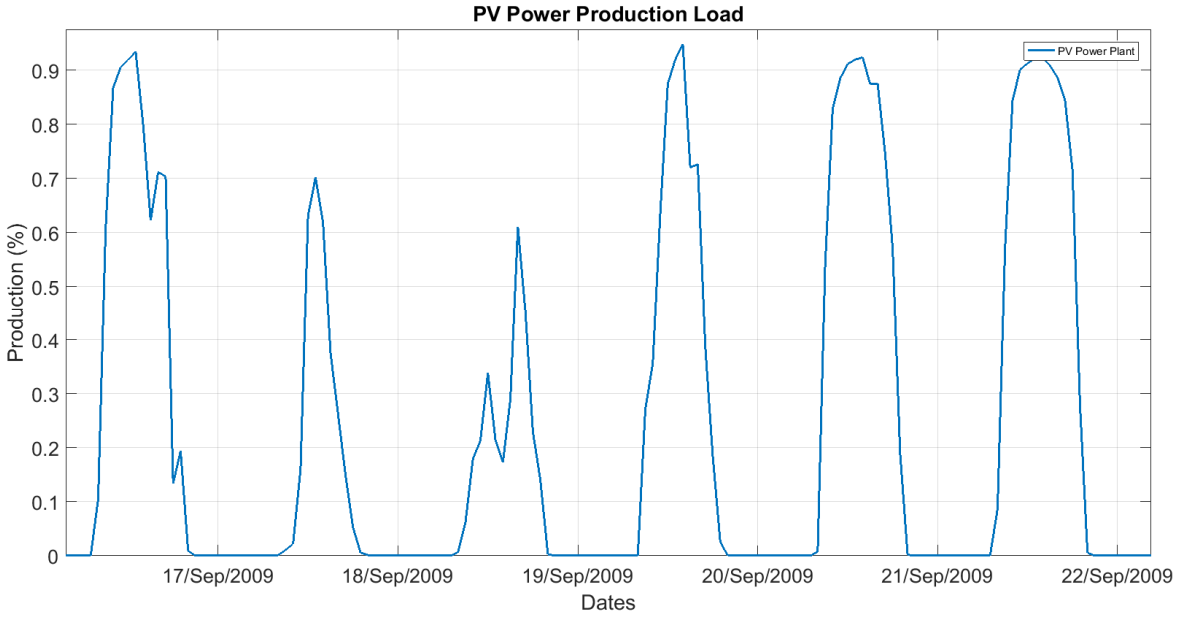

Figure.- 7 Average panel PV generation curve ($P_{PVmean\_ratio}(t)$) as a ratio of load (1 equals 100kW).

The designed algorithm sizes the number of 100kW panels which are necessary to supply the population group, considering the shown average generation profile ($P_{PVmean}(t)$).

2.3. Management tools for the integration of renewables in the system

Given that renewable energy generation and demand do not usually coincide in volume and time, the need for the use of technologies or mechanisms to integrate renewables into the grid is evident, avoiding the use of conventional back-up plants and large interconnection networks between consumption centers and generation plants. There are three classic ways to match demand and generation: 1. storing the surplus energy generated and using it afterwards; 2. reducing demand at a given moment through demand management mechanisms, and; 3. bringing electricity of renewable origin from other locations through distribution networks. In the present study, demand management capacity was not considered, leaving it for future studies.

2.3.1. Storage: Batteries in households and vehicles.

There are different storage technologies, including pumping stations, chemical systems (hydrogen generation, for example) or electric batteries [48]. Electric batteries are then postulated as the main way to store surplus energy during renewable production peaks [49, 50].

In the present study, EVs have been considered only as electricity consumption devices and not as electricity-storing ones. Household batteries are the only ones that would offer additional storage capacity, with subsequent injection of electricity into the grid.

Fixed batteries in households will be used mainly to store the surplus of isolated self-consumption facilities for later use, whereas in facilities connected to the grid, net meeting or a duly regulated compensation system could be chosen. EV manufacturers, such as BMW [51], are looking for formulas to reuse EV batteries at the end of their useful life, since it is the most expensive component of this type of vehicle. For example, BMW has proposed to use the battery of their i3 model as domestic equipment after a recall from the vehicle. This battery maintains 70% of its capacity after several years of use. This battery model has been used in the present study, with the ratio (from 0 to 1) of households with a battery ($Per_{household\_bats}$) being one of the variables that the algorithm must calculate.

$$N_{household\_bats} = N_{households} \cdot Per_{household\_bats} \quad (4)$$

As mentioned above, each home will have 1.6 EVs [52]. According to BNEF [51], EV batteries, which will later be used as "Second Life" (domestic battery), will have a capacity of 22-33kWh. For this study, 22kWh batteries (Bats_energy_suply) were used by households. The cost of MWh thanks to this "Second Life" strategy and economies of scale will achieve costs of 49 $/MWh (2016 USD), compared to 100-200 $/MWh ($ 172) for other similar products. For being conservatives, in the present study we have considered 100$/MWh. We have also done a "Ceteris Paribus" analysis, reducing this cost to 80$/MWh to evaluate the impact of this cost in the LCOE of the system. For future studies, different scenarios will be done.

2.3.2. Interconnection with the external network and netmetering.

When the electricity consumption of the population group cannot be supplied with internal resources, energy from conventional distribution networks will need to be imported. In the present study it has not been considered that the inter-supply connections between isolated population groups could have a management system through "net metering", in such a way that the excess energy of the population group could be injected into the network ($P_{netmetering}$ (t)> 0) and subsequently recovered as imported energy ($P_{netmetering}$ (t) <0) from the grid. In the present study, it has been assumed that the energy imported from the grid will have a cost of 134 $/MWh, the current price in the Iberian wholesale market in 2021 [53]. We have not considered the option of net metering, since otherwise the general population would become an electricity generator of the system. In this case, the system would be injected with low cost renewable energy and it could be considered as a battery of infinite capacity.

3. Power generation cost optimization algorithm.

Genetic algorithms (GA) are adaptive methods that can be used to solve search and optimization problems [54]. They are based on the genetic process of living organisms. By imitating this process, genetic algorithms [33] are able to gradually create solutions for real-world problems. The evolution of these solutions towards optimal values of the problem depends, to a large extent, on their adequate coding.

GA use a direct analogy with natural behavior. They work with a population of individuals, each of whom represents a feasible solution to a given problem. Figure 8 shows the process followed by the GA [54].

Each individual is assigned a value or score, related to the goodness of the aforementioned solution (that is, the lower the cost of the energy generated and consumed in the system). In nature, this would be equivalent to the degree of effectiveness of an organism in the competition for certain resources. The greater the adaptation of an individual to the problem, the greater the probability that it will be selected to reproduce, crossing its genetic material with another individual which has been selected in the same way. This crossing will produce new individuals (descendants of the previous ones), which share some of the characteristics of their parents.

The lower the adaptation of an individual, the lower the probability that it will be selected for reproduction and, therefore, that its genetic material is propagated over successive generations.

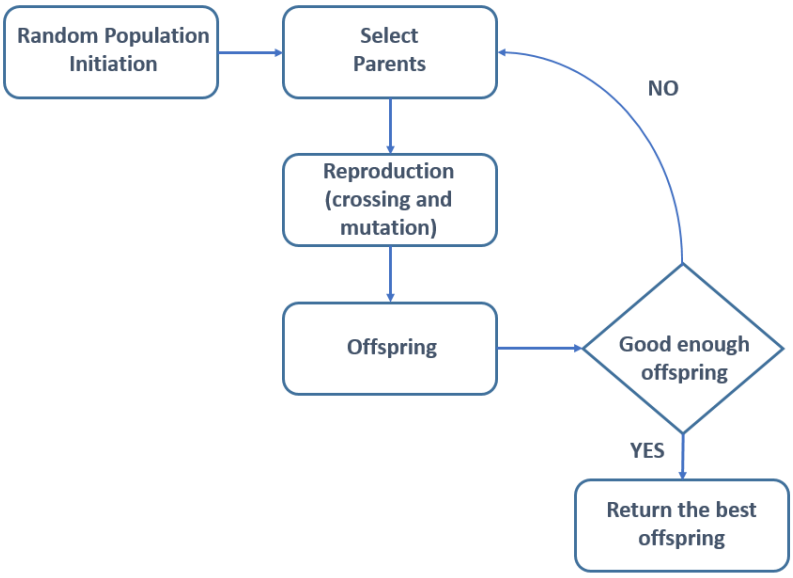

Figure.- 8 Flowchart of GA evolution.

In this way, a new population of possible solutions is produced, which replaces the previous one and verifies that it contains a greater proportion of good characteristics compared to the previous population. Thus, the good characteristics spread through the population over successive generations, favoring the crossing of the best adapted individuals, the most promising areas of the search space being explored. If the GA has been well designed, the population will converge towards an optimal solution to the problem.

In the present study, the GA should look for the combination of the following input variables that minimizes the cost of the energy consumed:

- Number of wind turbines ($N_{windturbines}$).
- Number of PV panels ($N_{PVPanels}$).
- Percentage of households with batteries ($Per_{household\_bats}$).

The algorithm will have several restrictions:

- The energy consumption of the population group ($Consumpion_{Total}$) depends on the number of households ($N_{households}$) and the ratio of EV penetration ($EV_{penetration\_level}$).

Different values of these parameters have been used in order to create different scenarios and evaluate their impact on the cost of power generation.

$$Consumption_{Total} = \sum_{t=1}^{t=8760} Consumption_{Households}(t) + \sum_{t=1}^{t=8760} Consumption_{EV}(t) \quad (5)$$

$$Consumption_{Households}(t) = \sum_{n=1}^{n=N_{households}} Consumption_{Simulated\_for\_household_n\_and\_hour_t}(n) \quad (6)$$

$$Consumption_{EV}(t) = N_{EV} \cdot Consume_{EV\_diario} \cdot \sum_{t=1}^{t=8760} Consumption_{EV\_intra\_daily\_ratio}(t) \quad (7)$$

where $Consumption_{EV\_intra\_daily\_ratio}$ corresponds to the energy consumption at t according to the daily ratio.

- The maximum number of wind turbines will be the one that can generate enough accumulated energy to supply the necessary demand from the population center throughout the year ($Consumption_{Total}$). In other words, if the population center needs 100MWh per year and that energy can be supplied with 9.5 average wind turbines (P_{wind_mean}), then the maximum number of wind turbines will be 10.

$$N_{Max\_Windturbines} = \frac{\sum_{t=1}^{t=8760} Consumption\,(t)}{\sum_{t=1}^{t=8760} P_{Wind\_mean}\,(t)} \quad (8)$$

$$P_{Wind_{mean}}(t) = P_{Windturbine\_mean\_ratio}\,(t) \cdot P_{Windturbine\_max} \quad (9)$$

The maximum number of wind turbines and PV panels could be limited manually, for example, if space restrictions are considered. However, this is not within the scope of this study.

- The maximum number of PV panels will be the one that complements wind generation until the total annual energy consumption ($Consumption_{Total}$) is reached.

$$N_{Max\_PVPanels} = \frac{\sum_{t=1}^{t=8760}[Consumption\,(t) - (N_{Max_{Windturbines}} \cdot P_{Wind_{mean}}\,(t))]}{\sum_{t=1}^{t=8760} P_{PV\_mean}\,(t)} \quad (10)$$

- The excess electricity generated that cannot be stored in batteries, or matched with consumption at t, will be considered as lost energy ($Energy_{Lost}$), since it cannot be injected into the grid. This energy generated but not used will contribute to increase the cost of the rest of the energy being consumed in the internal network. Increasing the level of availability of batteries will make this term disappear, and it will also allow balancing the demand to other hours with a low consumption.
- The consumed energy at each moment t must be supplied from the different sources, starting with the renewable energy mix generated in that time interval, then extracted from the batteries and finally imported from the grid.

Additional considerations:

- Wind generation costs are \$50/MWh ($Cost_{Wind}$) [55].
- PV MWh generation costs are \$56/MWh ($Cost_{PV}$) [55].
- The cost of each MWh consumed from batteries has been established at 100\$ ($Cost_{Bats}$) [51].

- The cost of each MWh consumed from the external grid has been established at 134$ ($Cost_{Grid}$) [53].
- The cost of renewable energy generation has been calculated in each simulation based on the number of wind turbines ($N_{windturbines}$) and the number of PV panels ($N_{PVPanels}$) according to the following algorithm:

$$Ecost_{Renewable} = \frac{\sum_{t=1}^{t=8760}(Production_{Wind}(t) \cdot Cost_{Wind} + Porduction_{PV}(t) \cdot Cost_{PV})}{\sum_{t=1}^{t=8760}(Production_{Wind}(t) + Porduction_{PV}(t))} \quad (11)$$

The renewable energy which is not consumed immediately will be stored. When this energy is subsequently consumed from the batteries, it does so at a cost of $ECost_{Bats}$.

The algorithm defines, for each iteration, the physical configuration of the network and simulates the temporal profile for the entire year. For each instant t, the origin of the energy that feeds the population group is determined. In this way, the formula to be optimized by the algorithm is defined as:

$$ECost_{kWh} = \frac{\sum_{t=1}^{t=8760}(Energy_{Renewable}(t) + Energy_{Bats}(t) + ECost_{Netmetering}(t) + Energy_{Lost}(t))}{\sum_{t=1}^{t=8760}(Consumption_{Households}(t) + Consumption_{EV}(t))} \quad (12)$$

4. Model simulation results.

This section shows the results of the simulations which have been carried out in order to illustrate and interpret the behavior of the system. Figure 9 shows a fragment of the simulation of renewable generation carried out for a population group of 5000 households. In the figure, wind generation ($Production_{Wind}$ (t)) is shown in blue and PV generation ($Production_{PV}$ (t)) is shown in red. The gray dotted line represent the total renewable energy being generated ($Production_{Total}$ (t)).

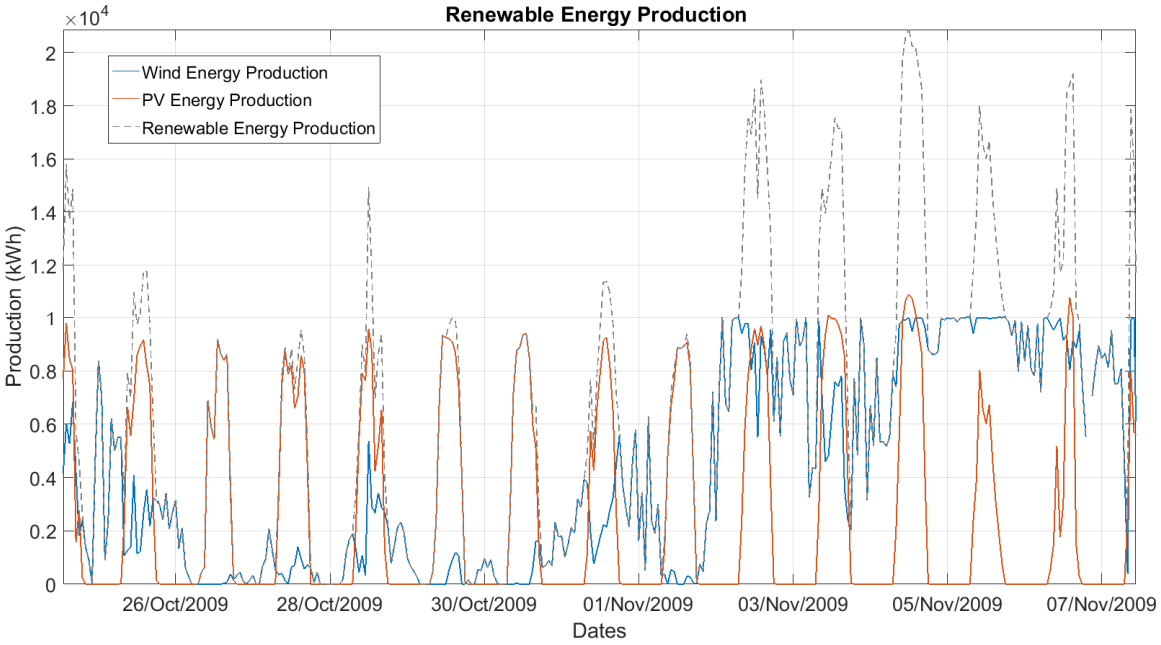

Figure 9.- Profile of wind, photovoltaic and total renewable production for a group of 5,000 households.

It can be observed that production is practically nil in some hours between October 26th and October 31st and it will be necessary to use battery systems and/or electricity fed from the external network.

Figure 10 shows the simulation for the consumption of homes and EVs, considering in this case a 100% penetration of EVs (1.6 vehicles per house). It is observed how the consumption of EVs, at least in the municipality under study, considerably increases the electricity consumption of the population group.

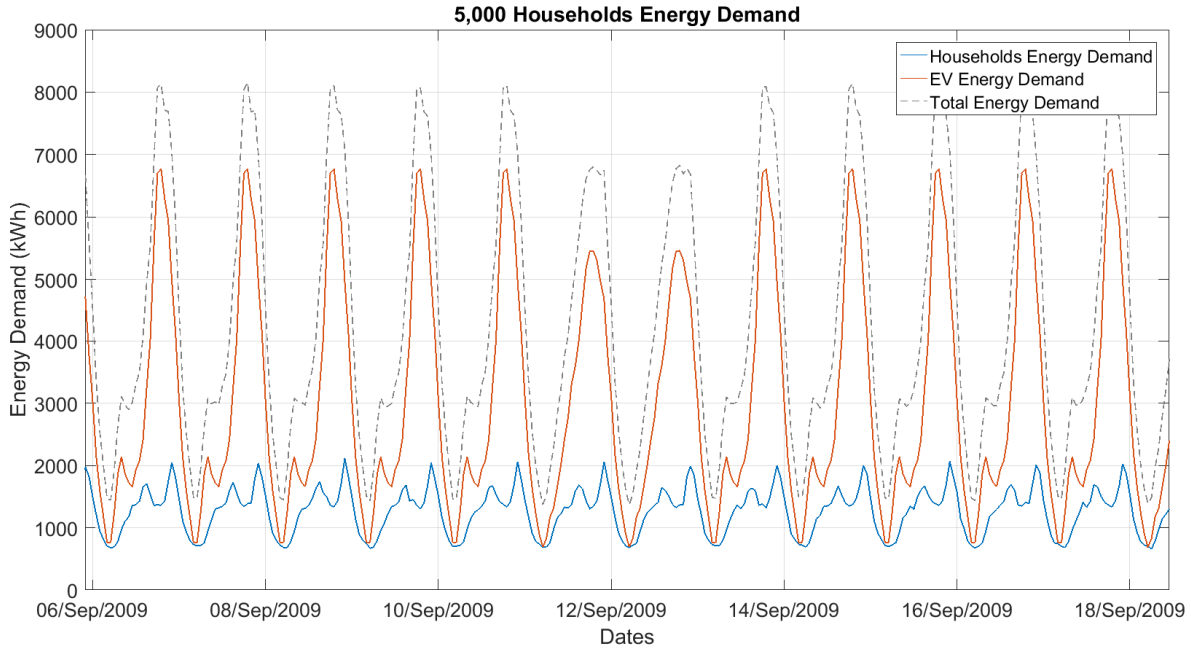

Figure 10.- Energy consumption of households and EVs (100% penetration).

Figure 11 provides, both, the renewable generation profiles (in blue) and the energy consumption profile (in red) and allows us to compare them and, thus, to identify the energy balance, which is represented in gray. Therefore, if more energy is generated than it is necessary at that time, the resulting profile will be positive and, when less renewable energy is available than it is necessary, the balance will be negative. It will be in these moments when the batteries will supply electricity and, in case this is not enough, electricity will have to be imported from the network.

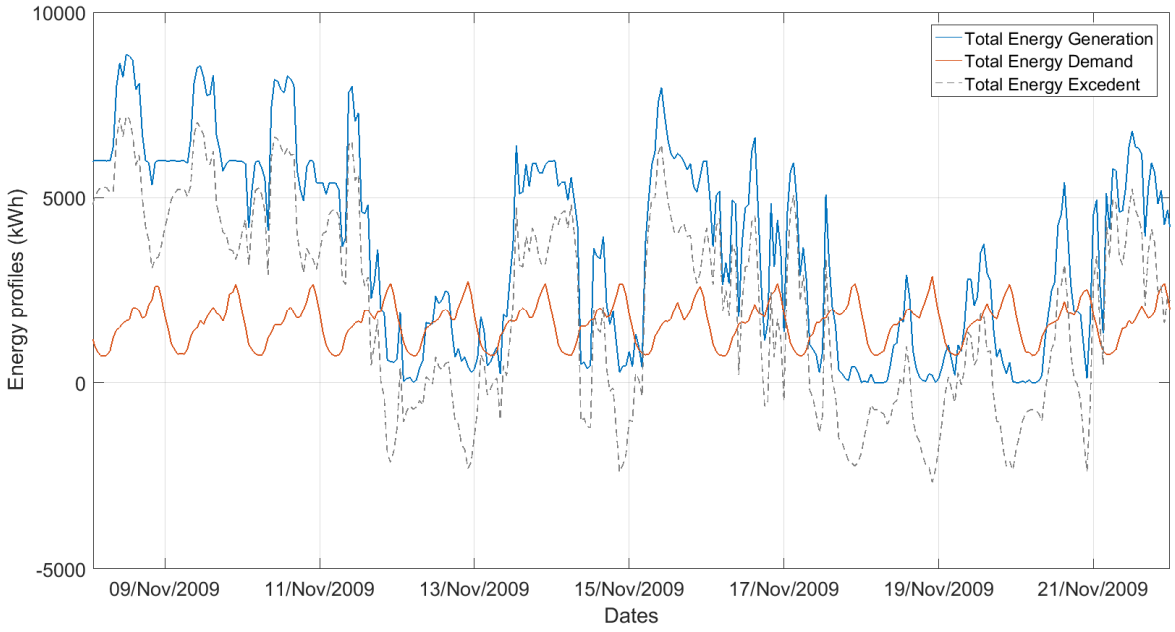

Figure 11 .- Simulation of generation and consumption profiles.

Next, the charge level of the batteries is checked and, if the surplus renewable energy is positive and there is storage capacity available in the batteries, then the energy is stored until the maximum level of the batteries is reached. In addition, the hourly charging capacity of the batteries is taken into account (7.4kWh / battery)[6], in such a way that if the energy surplus is too large to fully charge the battery, this excess must be injected into the grid or the energy will be lost if the limits established in the algorithm are exceeded. At each moment t, the maximum charge energy flow of the batteries will be $E_{Bats\_flow\_max} = 7.4 \times N_{households} \times Per_{household\_bats}$. $Per_{household\_bats}$ is the ratio of households with batteries, and it can be higher than 1 depending on the simulation scenario.

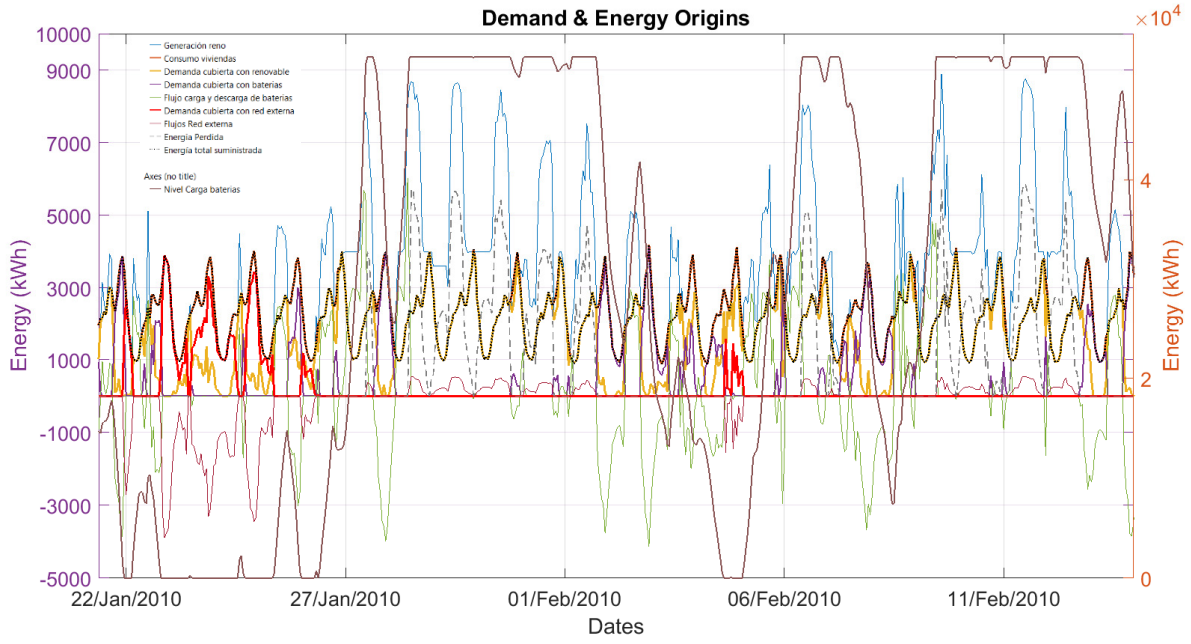

Figure 12.- Illustration of the most representative profiles. In right axis the battery charge level.

[6] Fast charging chargers allow up to 105kWh but are not recommended for everyday use.

Figure 12 shows the most representative profiles and the part of the demand which is covered with each source. On the other hand, it is observed that the batteries of the homes quickly reach their maximum storage level (right axis) and if there are several consecutive days of high wind and solar resources, a large part of the energy is lost or injected into the grid (in scenarios with low levels of storage). It is necessary to raise the level of energy storage within the urban group, since it is not enough to install a battery per home, taking into account the characteristics considered.

It can be observed that there are days in which practically all the demand is covered with energy from the external network.

5. Results.

This section compares the results obtained when executing the optimization algorithm for three scenarios: (1) a scenario without any limitation of battery storage capacity; (2) a scenario in which the maximum storage capacity is limited to 1 battery per household and; (3) a scenario without storage batteries. The main objective is to evaluate the cost of generating electricity in each of them and identify how the penetration of EVs affects the electricity price and the configuration of the system.

Scenario 1 represents the configuration which is necessary to achieve an isolated system without connection to the external supply network.

5.1. Comparative evolution of the cost of power generation.

The LCOE shows a negligible variation with respect to the size of the population group in towns with 5000 households or more (Table 1). However, the cost rises slightly in all scenarios as the level of EV penetration increases (Figure 13). In less populated towns (1000 households), the LCOE is higher when the penetration of the EV is lower than 60-70%, and similar values to the ones of other larger towns are obtained, as shown in Figure 13.

Table 1.- LCOE in $ / MWh for the different scenarios

(1)	**EV Penetration**										
Households	**0**	**0.1**	**0.2**	**0.3**	**0.4**	**0.5**	**0.6**	**0.7**	**0.8**	**0.9**	**1**
1000	81.17	82.05	84.75	85.32	85.82	72.41	69.74	68.7	68.48	68.53	68.7
5000	67.68	67.86	68.6	67.97	68.15	68.53	68.34	68.47	68.75	68.6	68.7
20000	67.8	67.74	67.86	68.03	68.14	68.26	68.38	68.44	68.54	68.62	68.69
50000	67.72	67.76	67.87	68.01	68.14	68.26	68.37	68.46	68.55	68.63	68.69
(2)	**EV Penetration**										
Households	**0**	**0.1**	**0.2**	**0.3**	**0.4**	**0.5**	**0.6**	**0.7**	**0.8**	**0.9**	**1**
1000	100.66	100.57	100.27	100.3	100.07	86.19	82.23	81.07	80.67	80.69	80.92
5000	79.28	78.52	78.9	79.66	79.98	80.12	80.38	80.51	80.92	80.82	80.91
20000	78.25	78.41	78.76	79.08	79.45	79.88	80.34	80.54	80.67	80.81	80.94
50000	78.2	78.35	78.68	79.05	79.43	79.86	80.33	80.55	80.69	80.82	80.94
(3)	**EV Penetration**										
Households	**0**	**0.1**	**0.2**	**0.3**	**0.4**	**0.5**	**0.6**	**0.7**	**0.8**	**0.9**	**1**
1000	100.66	100.57	100.27	100.3	100.34	86.19	82.23	81.07	80.67	80.69	80.92
5000	79.35	79.47	80.63	79.78	79.98	80.65	80.38	80.51	80.92	80.82	80.91
20000	79.42	79.39	79.54	79.79	80.03	80.21	80.39	80.54	80.67	80.81	80.94
50000	79.33	79.4	79.57	79.8	80.02	80.21	80.39	80.55	80.69	80.82	80.94

When the number of homes is low, the connection of a new wind turbine to the network greatly affects the reduction of the cost of generation, mainly due to the high cost of battery storage. However, when the size of the population increases, these price fluctuations are cushioned, because a greater absolute number of batteries are available in the system. In these small cities, the LCOE will increase until wind energy can be used to feed the system.

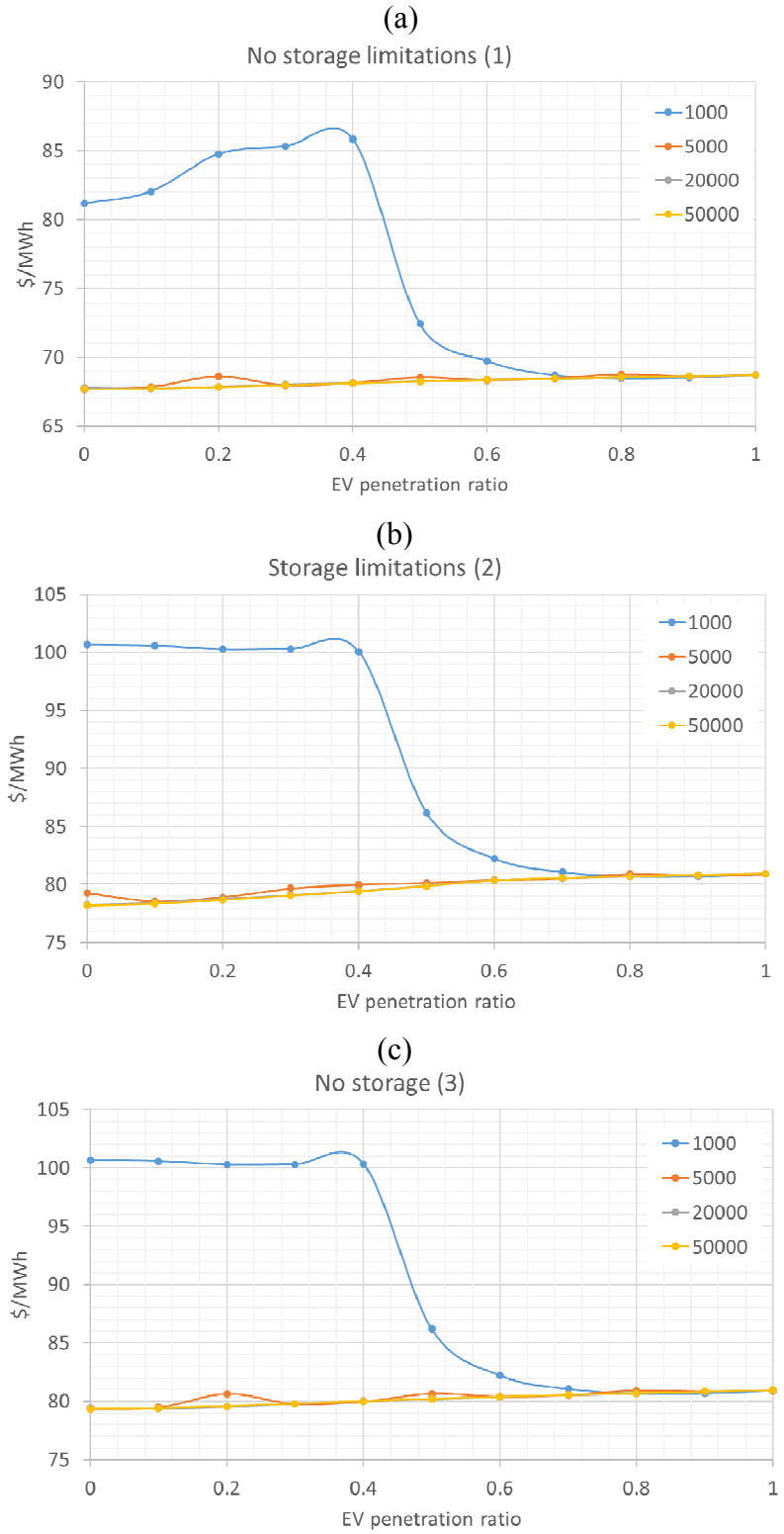

Figure 13.- LCOEs in Scenario 1 (a), scenario 2 (b) and scenario 3(c) (the colors refer to the number of households).

In the previous graphs, it is shown how the EV input can help reduce the cost of power generation in small towns where the consumption is low and unbalanced. However, this cost of power generation slightly increases with the EV in towns with 5000 or more households. In scenarios (2) and (3), the LCOE is close to 100$/MW€ because most of the energy comes from batteries (Figure 18). This is because energy is generated with PV panels during the day and the consumption is at the beginning and at the end of the day when the solar resource is not available and, thus, the energy has to be stored during the day. These scenarios are quite similar regarding the LCOE.

It can be concluded that in a scenario (1) with sufficient backup battery systems, costs of 68-69 $/MWh would result, whereas in scenarios (2) and (3) the costs would be around $ 79-81 / MWh, i.e. 17% higher than in scenario (1).

Comparing scenarios (2) and (3), the use of a small share of batteries can help to reduce the LCOE between 0 and 1.1% when the EV penetration is lower than 70%.

5.2. System sizing.

Figures 14a and 14b show the number of wind turbines and PV panels which are necessary in order to provide electricity to the different population centers. In the case of the population group of 1000 homes, it is clearly observed (when the EV penetration ratio rises by 0.5) that the introduction of a new wind turbine in the system leads to the oscillations in the energy generation costs which have been discussed above (in figure 13). This configuration of renewable resources is the same in the three analysed scenarios (1-3) (Table 2), since it meets the requirement that the energy generated at the site be the same as the one consumed there, the ultimate goal being to avoid interactions with the external network (isolated system). This was the main objective of the study (i.e. to size the system to minimize the cost of generation), leading to the results shown in table 1.

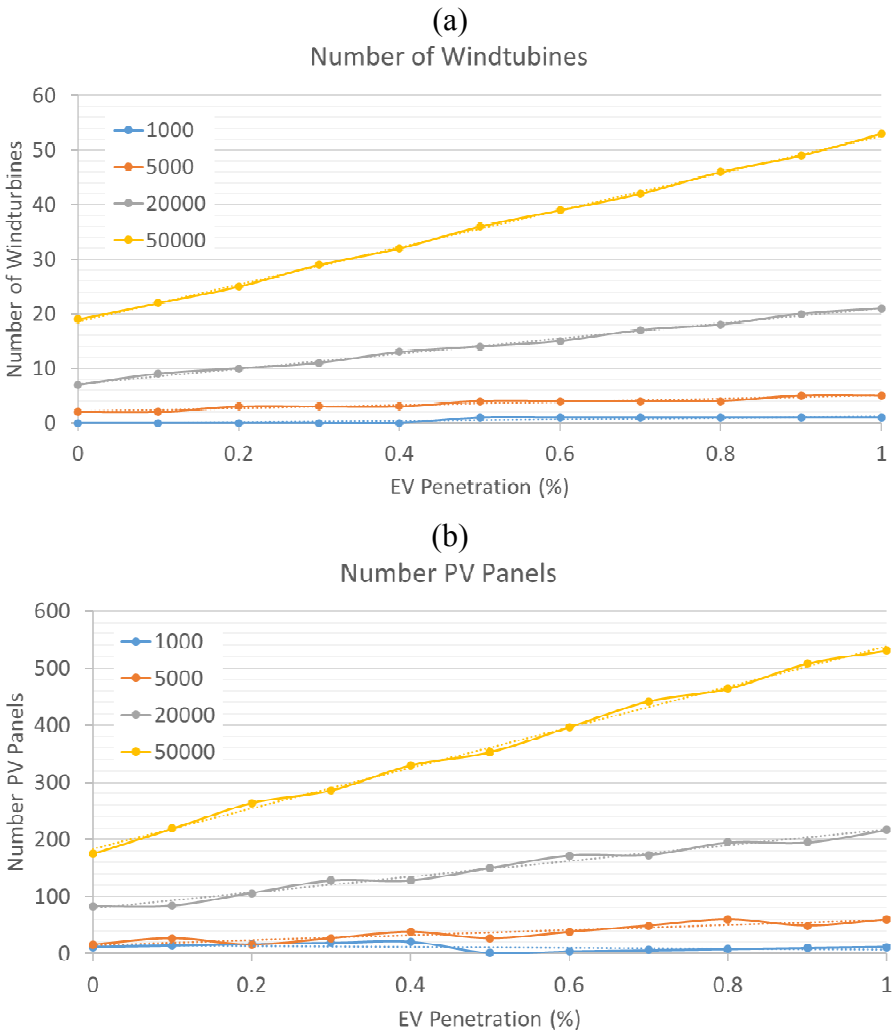

Figure 14.- Number of wind turbines (a) and PV panels (b) needed to produce the energy required in the population nucleus (the color represents the number of households).

Table 2.- System sizing in different scenarios.

	Number of wind turbines										
	EV Penetration										
Households	**0**	**0.1**	**0.2**	**0.3**	**0.4**	**0.5**	**0.6**	**0.7**	**0.8**	**0.9**	**1**
1000	0	0	0	0	0	1	1	1	1	1	1
5000	2	2	3	3	3	4	4	4	4	5	5
20000	7	9	10	11	13	14	15	17	18	20	21
50000	19	22	25	29	32	36	39	42	46	49	53
	Number of PV panels										
	EV Penetration										
Households	**0**	**0.1**	**0.2**	**0.3**	**0.4**	**0.5**	**0.6**	**0.7**	**0.8**	**0.9**	**1**
1000	12	14	17	19	21	1	4	6	8	10	12
5000	16	27	16	27	38	27	38	49	60	49	60
20000	83	84	106	128	128	150	172	173	195	195	217
50000	175	219	264	286	330	353	397	442	464	508	531

The need for storage batteries (Figure 15) increases when the penetration of EVs surpasses the ratio of 0.6-0.7 regardless of the population size. The population group of 1000 households gets an important reduction of storage capacity (kWh/household) when the EV penetration ratio is higher than 0.7. In scenarios (2) and (3), the storage capacity is limited to the number of homes (with a unit capacity of 22kWh and 70% efficiency) (scenario 2) and 0 batteries (scenario 3). Scenario (2) casts doubts on the possibility that the small number of batteries will help to reduce the LCOE, which is closely linked to the production profile and the combination of wind and solar resources.

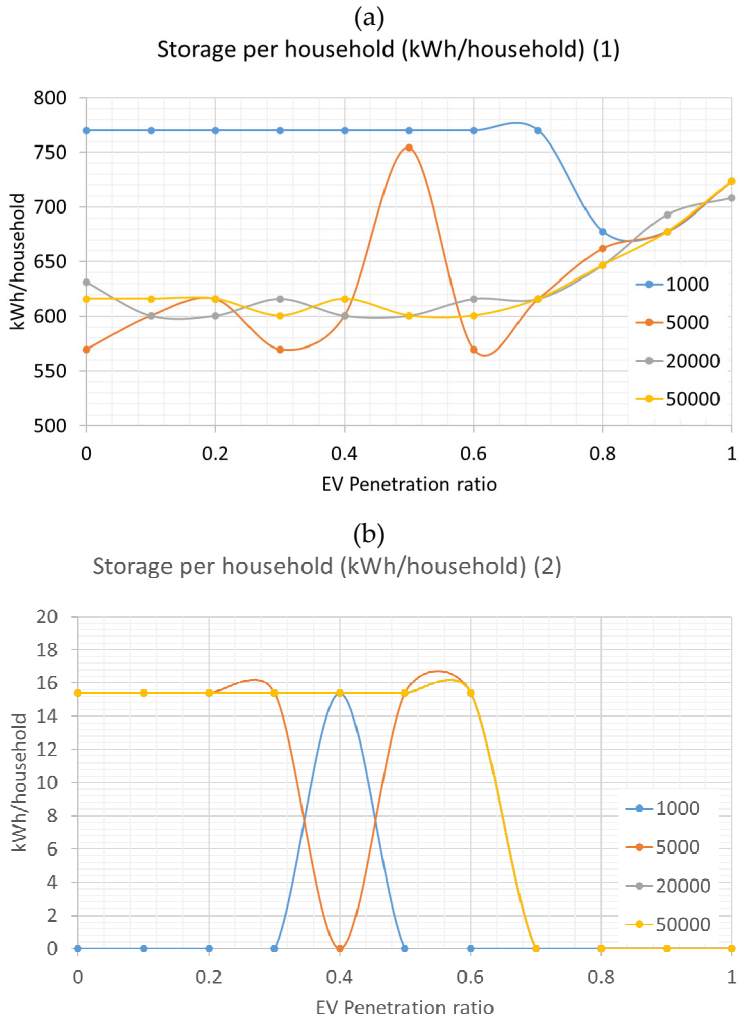

Figure 15 .- Storage capacity per household required in scenario 1 to minimize the cost of power generation (number of households in color).

Figure 16 shows that the need for storage per dwelling increases considerably as the number of dwellings in the population group increases, going from 50000 batteries in small cities with 1000 households to 2,000,000 batteries in cities with 50,000 households. The ratio kWh/household is similar in cities with 5000 or more households, 600kWh per dwelling are necessary with EV penetration ratios below 0.7, and 700 kWh/household are needed with an EV penetration ratio of 1. In a population group of 1000 dwellings a larger storage capacity (around 780kWh per dwelling).

These results suggest that the need for storage is related to the number of dwellings (Figure 16), especially when the size of the population group is large. This is also related to the seasonal period (i.e., less resources in the summer). Given the seasonality of the wind resource, the battery system is clearly penalized if the requirement of being completely energy self-sufficient is to be met. Figure 17 shows the

battery charge and discharge flow in scenario 1, indicating that electricity can be stored in the winter for later consumption in the summer. It confirms the need to store large amounts of energy to cover seasonal differences.

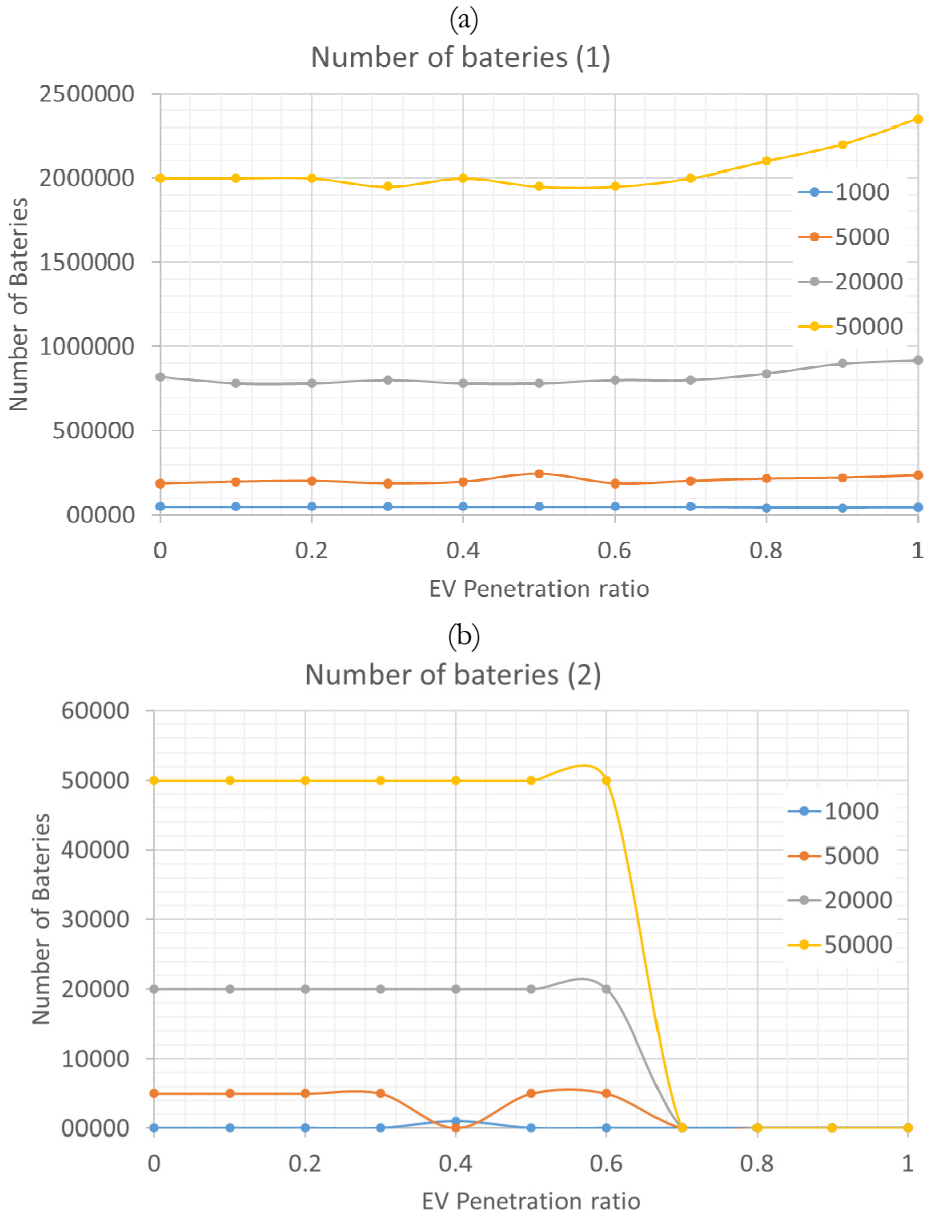

Figure 16.- Number of batteries for each population group and depending on the introduction of EV (number of households in color).

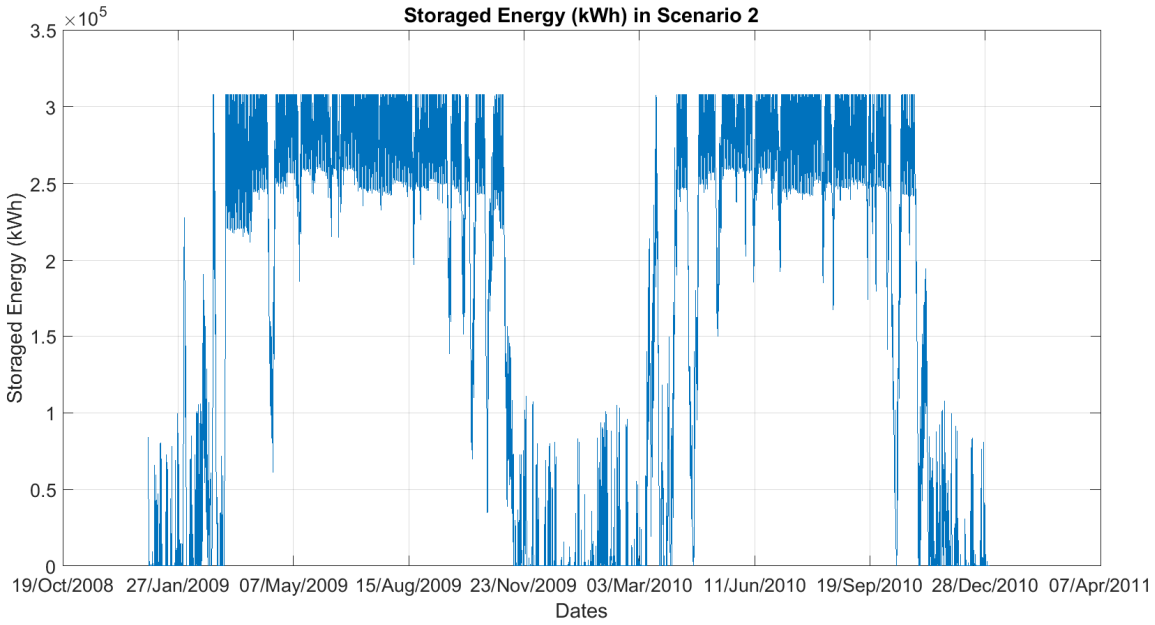

Figure 17.- Battery charge and discharge flow in scenario 2.

5.3. Assessment of the origins of energy.

An analysis of the percentage flows of energy shows that, in scenario (1) and with population groups of 5000 or more households, around 65% of the energy consumed has a renewable energy origin (Figure 18), producing a decrease in said percentage as EV penetration increases, being replaced by energy from batteries, which increases the cost of energy. In this scenario, it is possible not to acquire energy from the grid. The level of storage of the batteries allows storing the entire generation surplus in order to be consumed when it is needed. The required storage capacity tends to be 35% of the total energy consumed in the population group.

In population groups of 1000 households, when the EV penetration ratio is lower than 0.5, most of the energy comes from batteries. This means that the energy is generated, stored in the batteries and consumed latter. That is due to the fact that only PV panels are available to produce electricity and there is only generation during the day. In Scenario (3), the energy from batteries is replaced with energy from the external grid and the lost energy is similar to this imported energy. It is a bit higher due to the fact that the installed capacity is dimensioned to produce slightly more than the energy consumed in the city.

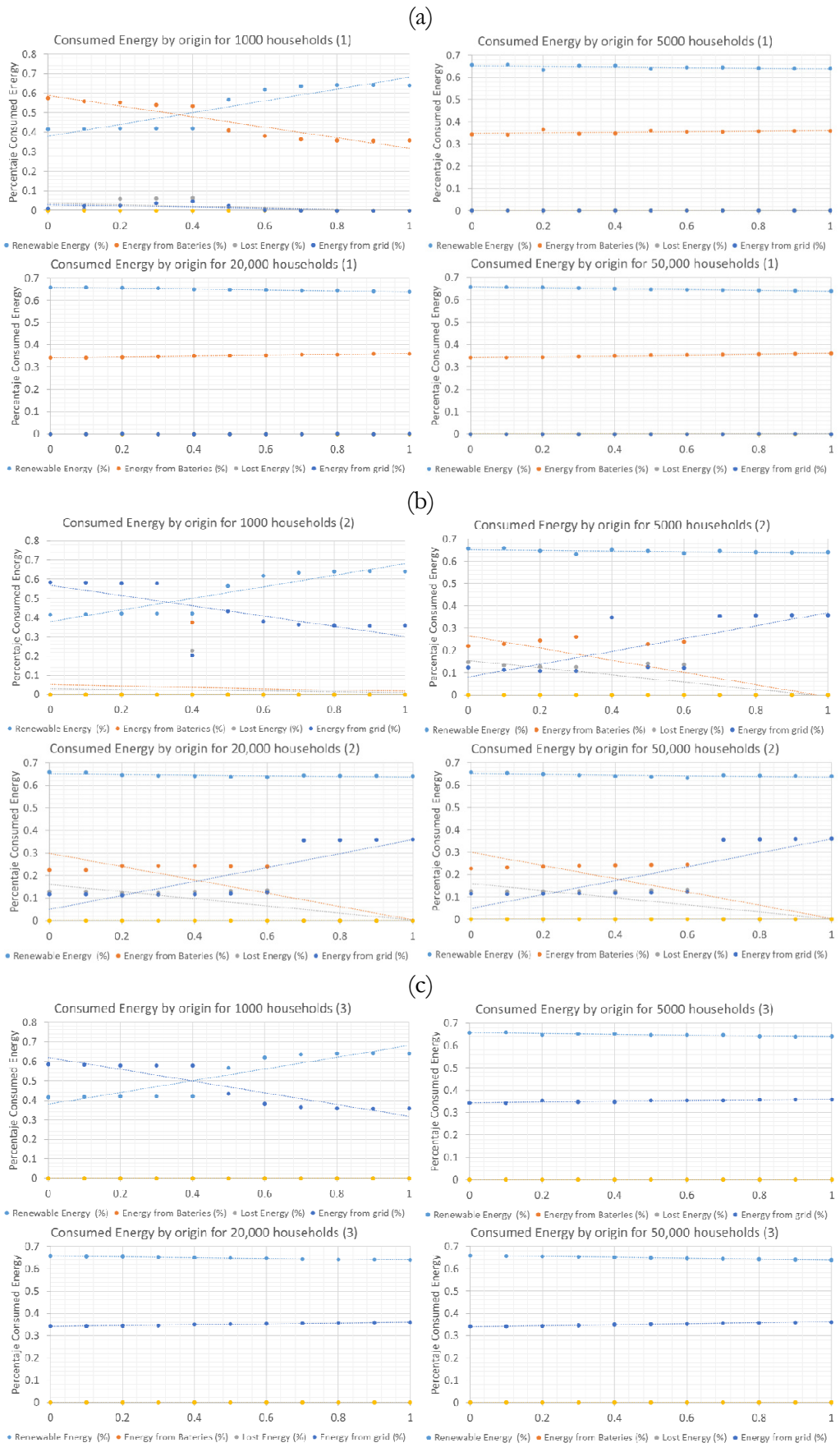

Figure 18.- Percentage distribution by sources of energy consumed by scenario (from 1 to 3 from top to bottom) and EV penetration level for different population groups.

Figure 18 shows that in a scenario with limited storage capacity (2) and without the possibility of injecting electricity into the network, there is a loss of around 14% of renewable energy and it is necessary to import 12% of electricity from the network. However, a lower storage capacity (1 battery per home), with an EV penetration ratio below 0.7, is able to supply a significant amount of energy (25%), mainly that of intraday consumption. However, in scenario (3) without storage capacity, all the energy that cannot be directly matched to renewable generation comes from the external grid (35%).

Figure 19 shows the energy consumed per each scenario and the EV penetration ratio. This energy is divided by source, taking in consideration the energy from renewable resources, batteries and the grid as well as the energy lost (produced but not used). In scenario 1, there won't be any lost energy due to the fact that all the surplus energy is stored in the batteries. Nevertheless, in the other scenarios, the energy lost is close to the energy consumed from the grid although slightly higher, as explained before. We can also observe that, with EV penetration, there is a higher difference between the consumed renewable energy and the energy from the grid (scenario 3), the consumed renewable energy and the energy from the grid in combination with batteries (scenario 2) and the consumed renewable energy and the energy from the batteries (scenario 1).

(a)

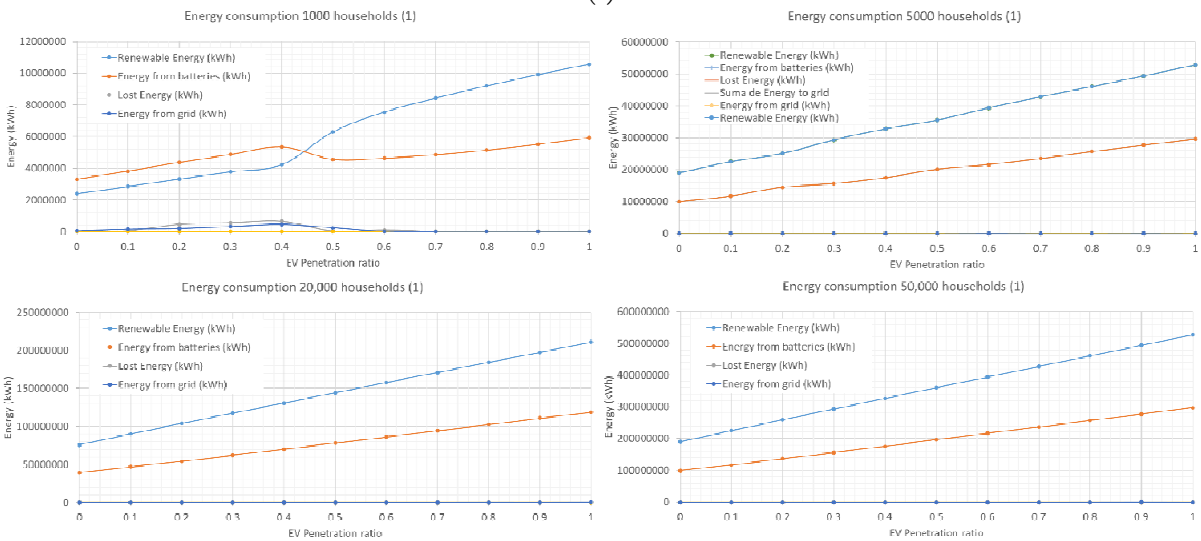

(b)

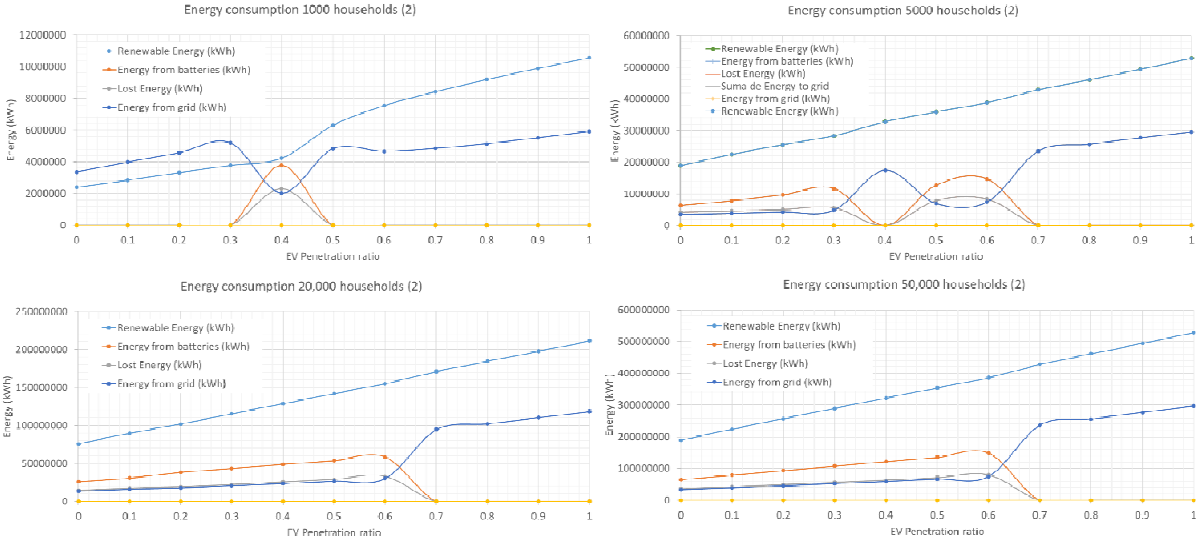

(c)

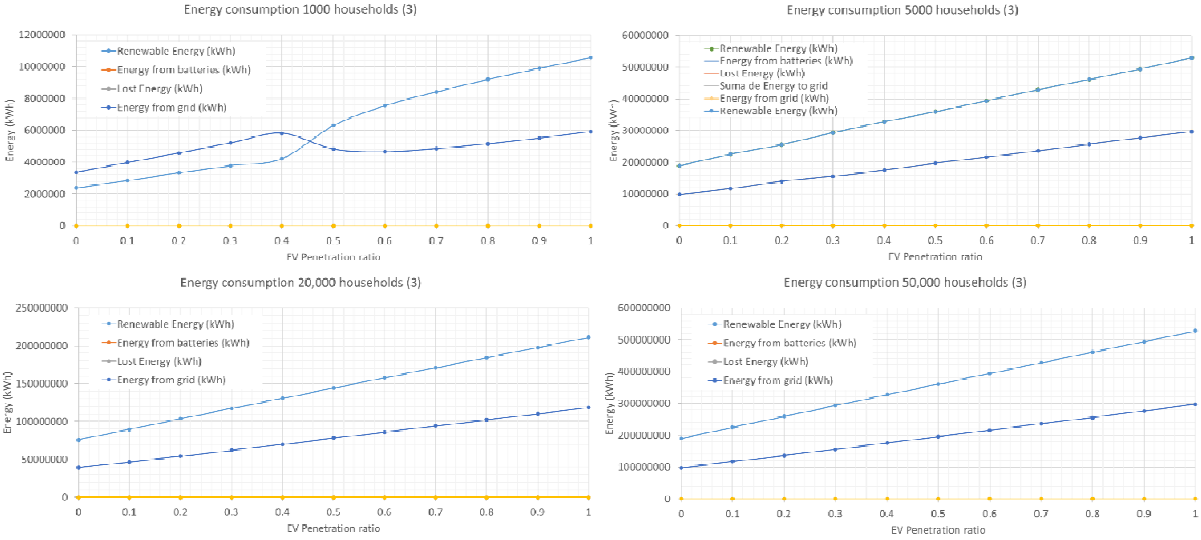

Figure 19.- Total energy from different sources (for a simulation period of 2 years), per scenario (from 1 to 3 from top to bottom) and EV penetration level for different population groups.

5.4. Assessment of the impact of LCOE reductions.

5.4.1. LCOE reductions in batteries.

The LCOE in each scenario was analysed by varying the LCOE of the energy from batteries from 100 to 80$/MWh. In Figure 20 and Table 3, it is observed that for cities with 5000 or more, and scenario (1), the LCOE pass from 68 $/MWh to 61 $/MWh (with a EV penetration ratio of 0) and from 69 $/MWh to 61.5 $/MWh (with a EV penetration ratio of 1). That represent a reduction in the general LCOE of 10%.

In cities with 1000 households, and scenario (1), the LCOE is increased from 86 $/MWh to 75 $/MWh in case the EV penetration ratio is 0.4, and from 81 $/MWh to 69 $/MWh in case the EV penetration ratio is 0. That represent a reduction in the general LCOE of 13%.

In Scenario (2), it is observed that for cities with 5000 or more the LCOE pass from 79 $/MWh to 74 $/MWh (with an EV penetration ratio of 0) and from 81 $/MWh to 77 $/MWh (with an EV penetration ratio of 1). That represent a reduction in the general LCOE of 5-6%.

In cities with 1000 households, and scenario (1), the LCOE is increased from 100 $/MWh to 92.5 $/MWh in case the EV penetration ratio is 0.4, and from 100 $/MWh to 95 $/MWh in case the EV penetration ratio is 0. That represent a reduction in the general LCOE of 5-7.5%.

In Scenario (3) there are no changes due to the fact that batteries are not used.

(a)

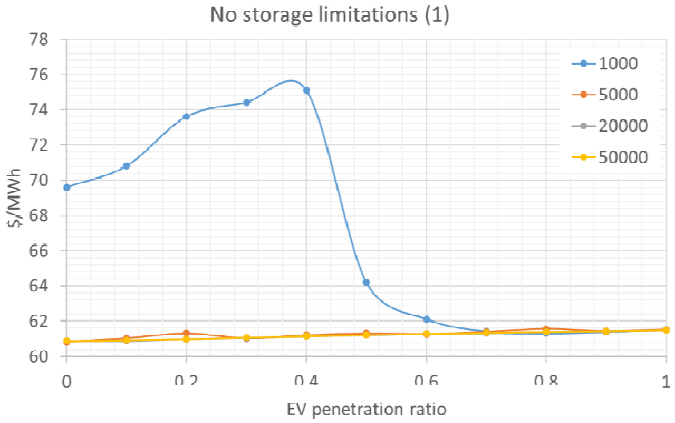

(b)

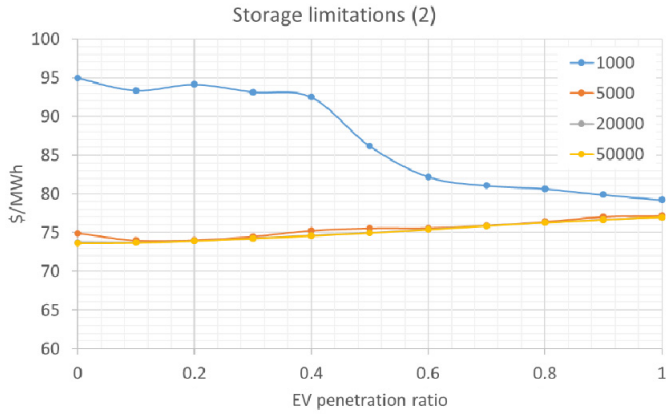

(c)

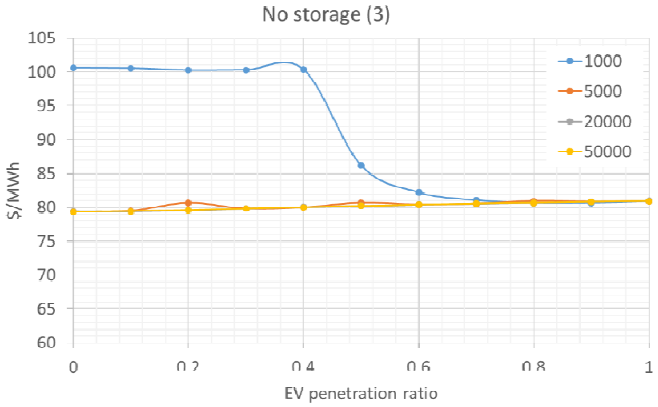

Figure 20.- LCOE resulting in Scenario 1 (a), scenario 2 (b) and scenario 3(c) with 80% costs reductions of the energy from batteries (number of households in color).

Table 3.- LCOE in $ / MWh for the different scenarios with 80% cost reductions in the LCOE from batteries

(1)	EV Penetration										
Households	**0**	**0.1**	**0.2**	**0.3**	**0.4**	**0.5**	**0.6**	**0.7**	**0.8**	**0.9**	**1**
1000	69.6	70.81	73.61	74.42	75.11	64.21	62.12	61.4	61.3	61.37	61.51
5000	60.83	61.03	61.3	61.03	61.2	61.3	61.26	61.38	61.55	61.42	61.52
20000	60.89	60.89	60.99	61.06	61.14	61.22	61.27	61.33	61.38	61.43	61.48
50000	60.87	60.92	60.98	61.07	61.14	61.22	61.28	61.34	61.39	61.43	61.48
(2)	**EV Penetration**										
Households	**0**	**0.1**	**0.2**	**0.3**	**0.4**	**0.5**	**0.6**	**0.7**	**0.8**	**0.9**	**1**
1000	94.94	93.34	94.13	93.15	92.5	86.2	82.22	81.06	80.66	79.88	79.24
5000	74.92	73.98	74.03	74.47	75.25	75.56	75.58	75.9	76.4	77.03	77.15
20000	73.73	73.68	73.9	74.22	74.59	74.95	75.39	75.85	76.27	76.64	76.97
50000	73.62	73.67	73.92	74.24	74.56	74.93	75.38	75.84	76.26	76.63	76.97
(3)	**EV Penetration**										
Households	**0**	**0.1**	**0.2**	**0.3**	**0.4**	**0.5**	**0.6**	**0.7**	**0.8**	**0.9**	**1**
1000	100.61	100.53	100.24	100.28	100.32	86.2	82.22	81.06	80.66	80.67	80.9
5000	79.37	79.49	80.65	79.81	79.99	80.67	80.4	80.52	80.93	80.83	80.92
20000	79.43	79.4	79.55	79.8	80.04	80.21	80.39	80.54	80.67	80.81	80.94
50000	79.34	79.41	79.57	79.8	80.02	80.21	80.39	80.55	80.69	80.82	80.93

5.4.2. LCOE reductions in PV panels.

The LCOE in each scenario was analysed, changing the LCOE of the energy from PV panels from 56 to 44.8 $/MWh. In Figure 21 and Table 4, it is observed that for cities with 5000 or more households, and scenario (1), the LCOE goes down from 68 $/MWh to 65 $/MWh (with an EV penetration ratio of 0) and from 69 $/MWh to 66 $/MWh (with an EV penetration ratio of 1), i.e. a reduction of 4.5% in the general LCOE

In cities with 1000 households, and scenario (1), the LCOE is reduced from 86 $/MWh to 81 $/MWh in case the EV penetration ratio is 0.4, and from 81 $/MWh to 77 $/MWh in case the EV penetration ratio is 0. That represents a 5-6% reduction in the general LCOE.

In scenario (2), it is observed that for cities with 5000 or more households, the LCOE goes down from 79 $/MWh to 77 $/MWh (with an EV penetration ratio of 0) and from 81 $/MWh to 78 $/MWh (with an EV penetration ratio of 1). This represents a 2.5% reduction in the general LCOE.

In cities with 1000 households and scenario (1), the LCOE decreases from 100 $/MWh to 93.5 $/MWh in case the EV penetration ratio is 0.4, and from 100 $/MWh to 95 $/MWh in case the EV penetration ratio is 0, a reduction of 5-6.5% in the general LCOE.

In Scenario (3), and for cities with 5000 or more, the LCOE is reduced from 79 $/MWh to 77 $/MWh (with an EV penetration ratio of 0) and from 81 $/MWh to 78 $/MWh (with an EV penetration ratio of 1). This represents a reduction of 2.5-4% in the general LCOE.

In cities with 1000 households, and scenario (1), the LCOE decreases from 100 $/MWh to 96 $/MWh in case the EV penetration ratio increases from 0 to 0.4 (a 4% reduction in the general LCOE).

The LCOE reduction from PV panels helps to reduce the general cost of the system, although in a small portion. The impacts are greater in small cities, where the ratio of energy from PV panels is higher.

(a)

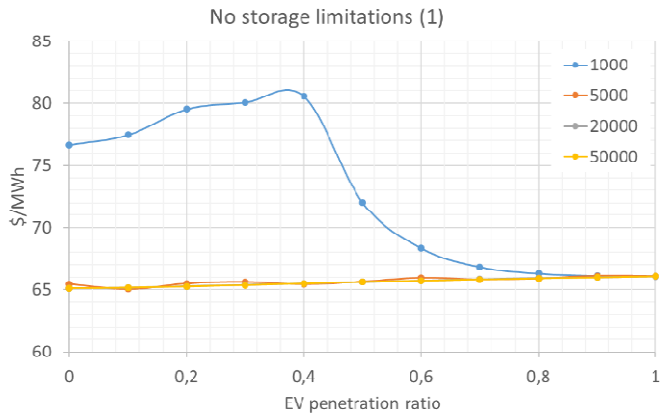

(b)

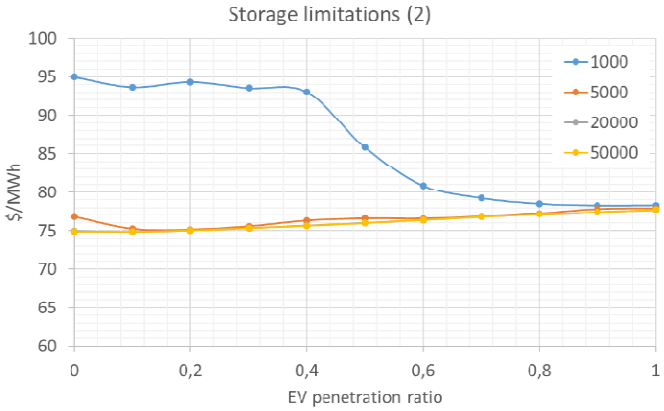

(c)

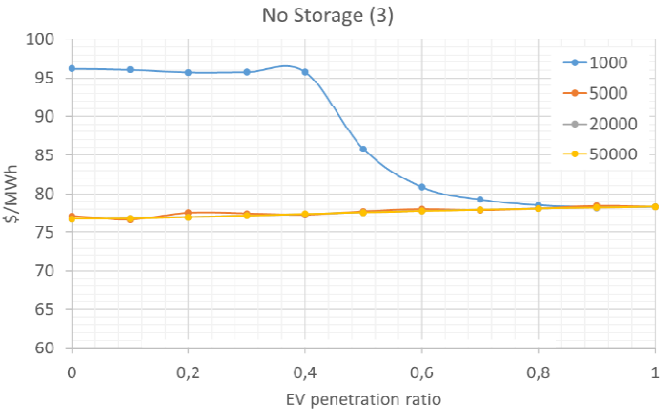

Figure 21.- LCOE resulting Scenario 1 (a), scenario 2 (b) and scenario 3 (c) with 80% costs reductions of the energy from PV panels (number of households in color).

Table 4.- LCOE in $ / MWh for the different scenarios with 80% cost reductions in the LCOE from PV panels

(1)	EV Penetration										
Households	**0**	**0.1**	**0.2**	**0.3**	**0.4**	**0.5**	**0.6**	**0.7**	**0.8**	**0.9**	**1**
1000	76.65	77.45	79.53	80.07	80.55	72.01	68.33	66.82	66.29	66.1	66.08
5000	65.44	65.04	65.48	65.61	65.42	65.63	65.94	65.8	65.88	66.09	66.07
20000	65.12	65.14	65.26	65.37	65.48	65.59	65.71	65.82	65.92	65.97	66.04
50000	65.11	65.14	65.24	65.35	65.48	65.61	65.71	65.81	65.9	65.98	66.06
(2)	**EV Penetration**										
Households	**0**	**0.1**	**0.2**	**0.3**	**0.4**	**0.5**	**0.6**	**0.7**	**0.8**	**0.9**	**1**
1000	94.95	93.66	94.32	93.54	93.03	85.82	80.86	79.22	78.5	78.27	78.3
5000	76.78	75.24	75.14	75.55	76.29	76.56	76.54	76.81	77.28	77.84	77.92
20000	74.99	74.86	75.06	75.35	75.67	76.01	76.38	76.79	77.15	77.47	77.76
50000	74.89	74.88	75.05	75.34	75.64	75.98	76.38	76.78	77.14	77.47	77.76
(3)	**EV Penetration**										
Households	**0**	**0.1**	**0.2**	**0.3**	**0.4**	**0.5**	**0.6**	**0.7**	**0.8**	**0.9**	**1**
1000	96.2	96.08	95.74	95.77	95.81	85.82	80.86	79.22	78.5	78.27	78.3
5000	77.12	76.65	77.51	77.43	77.25	77.69	77.99	77.85	78.06	78.41	78.29
20000	76.74	76.81	76.98	77.14	77.34	77.55	77.75	77.92	78.05	78.16	78.29
50000	76.74	76.78	76.95	77.14	77.36	77.56	77.73	77.9	78.05	78.18	78.3

6. Discussion.

This paper has provided a methodology based on genetic algorithms and Monte Carlo simulations to determine the level of technical resources which would minimize the cost of power generation in a 100% renewable generation environment in semi-isolated or completely isolated micro-grid systems. The consumption and supply of an urban center in southern Spain with several renewable electricity plants (photovoltaic and wind) in nearby sites as well as the integration of a fleet of purely electric vehicles were simulated, and the costs of the energy consumed were evaluated.

The genetic algorithm has provided excellent performance results, seeking the optimal solution and complying with the established restrictions. The high speed of convergence of the algorithm would allow carrying out several types of experiments. For example, the change in the price of energy in any situation could be assessed by varying other parameters such as the energy costs of the grid or batteries. This provides a fruitful avenue for future research.

The LCOE in the population groups analyzed in their isolated configuration from the grid, and with the support of a sufficient electric battery system, will be around 68 $ /MWh, depending on the cost of the rest of the resources. In this scenario, 65% of the energy consumed will come from renewable generation directly, whereas the remaining 35% will come from renewable energy stored in batteries. Although solar energy will tend to be cheaper than wind, batteries make it is more economical to combine wind generation with PV.

Wind generation plants produce a large amount of energy per installed unit, but a high number of homes are necessary to achieve a minimum number of wind turbines that would make up a wind farm. However, the seasonality of wind energy means that high levels of storage are necessary in the medium term (intra-annual), or there would be a need to bring energy from other locations to supply certain consumptions, such as vehicles, using for example green hydrogen.

Population groups with a lower number of homes will have higher energy generation costs than medium-sized groups that allow wind power generation. Further research should be devoted to the analysis of the use of mini wind and fixed PV.

During the early stages of EV penetration, up to a penetration of 40%, the LCOE in small household groups will increase. In larger groups, the penetration of EV will increase the cost of power generation, due to the need to use more batteries in order to meet intraday consumption. This is especially obvious when the penetration of EVs is above 60-70%. This also affects the relative storage need (kWh/dwelling), although this ratio decreases in small size population groups after EV penetration reaches 70%.

Having storage capacity, even if it is limited to one battery per home, allows storage and consumption of up to 25% of the consumption of the population group, and can help to reduce the LCOE by 1.1% due to the fact that it helps to cover intraday variations and avoid the use of energy from the external grid.

Reductions of 20% in the LCOE of the batteries can lead to reductions of the general LCOE in the range of 5% to 13%, depending on the scenario, whereas a 20% reduction in the LCOE of PV generation could reduce the general LCOE between 2.5% to 6.5%.

References

1. Priscila Gonçalves Vasconcelos Sampaio, Mario Orestes Aguirre González, Photovoltaic solar energy: Conceptual framework, In Renewable and Sustainable Energy Reviews, Volume 74, 2017, Pages 590-601, ISSN 1364-0321, https://doi.org/10.1016/j.rser.2017.02.081.
2. M. Asif, T. Muneer, Energy supply, its demand and security issues for developed and emerging economies, Renewable and Sustainable Energy Reviews, Volume 11, Issue 7, September 2007, Pages 1388-1413, ISSN 1364-0321, http://dx.doi.org/10.1016/j.rser.2005.12.004.
3. International Energy Agency. World Energy Outlook 2015.November 2015. ISBN: 978-92-64-24366-8, ISSN: 2072-5302.
4. Tingzhen Ming, Renaud de_Richter, Wei Liu, Sylvain Caillol, Fighting global warming by climate engineering: Is the Earth radiation management and the solar radiation management any option for fighting climate change?, Renewable and Sustainable Energy Reviews, Volume 31, March 2014, Pages 792-834, ISSN 1364-0321, https://doi.org/10.1016/j.rser.2013.12.032.
5. Vassileva I, Campillo J. Increasing energy efficiency in low-income households through targeting awareness and behavioral change. Renewable Energy, Volume 67, 2014; p.59-63. http://dx.doi.org/10.1016/j.renene.2013.11.046.
6. Fateh Belaïd, Thomas Garcia, Understanding the spectrum of residential energy-saving behaviours: French evidence using disaggregated data, Energy Economics, Volume 57, June 2016, Pages 204-214, ISSN 0140-9883, http://dx.doi.org/10.1016/j.eneco.2016.05.006.
7. David I. Stern, Modeling international trends in energy efficiency, Energy Economics, Volume 34, Issue 6, November 2012, Pages 2200-2208, ISSN 0140-9883, http://dx.doi.org/10.1016/j.eneco.2012.03.009.
8. Miranda A. Schreurs, Breaking the impasse in the international climate negotiations: The potential of green technologies, Energy Policy, Volume 48, September 2012, Pages 5-12, ISSN 0301-4215, http://dx.doi.org/10.1016/j.enpol.2012.04.044.
9. Blanca Moreno, Ana Jesús López, The effect of renewable energy on employment. The case of Asturias (Spain), Renewable and Sustainable Energy Reviews, Volume 12, Issue 3, 2008, Pages 732-751, ISSN 1364-0321, https://doi.org/10.1016/j.rser.2006.10.011.
10. E. Fernández Domínguez, J. Xiberta Bernat, Restructuring and generation of electrical energy in the Iberian Peninsula, Energy Policy, Volume 35, Issue 10, 2007, Pages 5117-5129, ISSN 0301-4215, https://doi.org/10.1016/j.enpol.2007.04.028.
11. Dörte Fouquet, Policy instruments for renewable energy – From a European perspective, Renewable Energy, Volume 49, 2013, Pages 15-18, ISSN

0960-1481, https://doi.org/10.1016/j.renene.2012.01.075.

12. Paul Simshauser, Distribution network prices and solar PV: Resolving rate instability and wealth transfers through demand tariffs, Energy Economics, Volume 54, 2016, Pages 108-122, ISSN 0140-9883, https://doi.org/10.1016/j.eneco.2015.11.011.
13. Colleen Lueken, Pedro M.S. Carvalho, Jay Apt, Distribution grid reconfiguration reduces power losses and helps integrate renewables, Energy Policy, Volume 48, 2012, Pages 260-273, ISSN 0301-4215, https://doi.org/10.1016/j.enpol.2012.05.023.
14. https://www.oxfordenergy.org/publications/oxford-energy-forum-issue-104/
15. Christian Breyer, Otto Koskinen, Philipp Blechinger, Profitable climate change mitigation: The case of greenhouse gas emission reduction benefits enabled by solar photovoltaic systems, In Renewable and Sustainable Energy Reviews, Volume 49, 2015, Pages 610-628, ISSN 1364-0321, https://doi.org/10.1016/j.rser.2015.04.061.
16. New Energy Outlook 2016. Long-term projections of the global energy sector. Solar. June 2016.
17. Sunil Kumar Sansaniwal, Vashimant Sharma, Jyotirmay Mathur, Energy and exergy analyses of various typical solar energy applications: A comprehensive review, In Renewable and Sustainable Energy Reviews, Volume 82, Part 1, 2018, Pages 1576-1601, ISSN 1364-0321, https://doi.org/10.1016/j.rser.2017.07.003.
18. International Energy Agency. World Energy Investment 2016. September 2016. 61 2016 20 1E1. ISBN: 978-92-64-26283-6.
19. Christian Breyer, Otto Koskinen, Philipp Blechinger, Profitable climate change mitigation: The case of greenhouse gas emission reduction benefits enabled by solar photovoltaic systems, In Renewable and Sustainable Energy Reviews, Volume 49, 2015, Pages 610-628, ISSN 1364-0321, https://doi.org/10.1016/j.rser.2015.04.061.
20. Ryan Wiser, Dev Millstein, Trieu Mai, Jordan Macknick, Alberta Carpenter, Stuart Cohen, Wesley Cole, Bethany Frew, Garvin Heath, The environmental and public health benefits of achieving high penetrations of solar energy in the United States, In Energy, Volume 113, 2016, Pages 472-486, ISSN 0360-5442, https://doi.org/10.1016/j.energy.2016.07.068.
21. New Energy Outlook 2016. Long-term projections of the global energy sector. Solar. June 2016.
22. Renewable Power Generation Costs in 2018, International Renewable Energy Agency, IRENA (2019), Abu Dhabi. ISBN 978-92-9260-126-3 https://www.irena.org/publications/2019/May/Renewable-power-generation-costs-in-2018
23. Benjamin K. Sovacool, Richard F. Hirsh, Beyond batteries: An examination of the benefits and barriers to plug-in hybrid electric vehicles (PHEVs) and a vehicle-to-grid (V2G) transition, Energy Policy, Volume 37, Issue 3, 2009, Pages 1095-1103, ISSN 0301-4215,

https://doi.org/10.1016/j.enpol.2008.10.005.

24. https://www.eleconomista.es/ecomotor/motor/noticias/10667695/07/20/Los-fabricantes-de-vehiculos-elevaron-su-facturacion-un-9-en-2019-hasta-los-69500-millones-de-euros.html
25. Steven J. Skerlos, James J. Winebrake, Targeting plug-in hybrid electric vehicle policies to increase social benefits, Energy Policy, Volume 38, Issue 2, 2010, Pages 705-708, ISSN 0301-4215, https://doi.org/10.1016/j.enpol.2009.11.014.
26. Joram H.M. Langbroek, Joel P. Franklin, Yusak O. Susilo, The effect of policy incentives on electric vehicle adoption, Energy Policy, Volume 94, 2016, Pages 94-103, ISSN 0301-4215, https://doi.org/10.1016/j.enpol.2016.03.050.
27. Georg Hirte, Stefan Tscharaktschiew, The optimal subsidy on electric vehicles in German metropolitan areas: A spatial general equilibrium analysis, Energy Economics, Volume 40, 2013, Pages 515-528, ISSN 0140-9883, https://doi.org/10.1016/j.eneco.2013.08.001.
28. https://en.wikipedia.org/wiki/Combined_Charging_System
29. Joaquim Delgado, Ricardo Faria, Pedro Moura, Aníbal T. de Almeida, Impacts of plug-in electric vehicles in the portuguese electrical grid, Transportation Research Part D: Transport and Environment, Volume 62, 2018, Pages 372-385, ISSN 1361-9209, https://doi.org/10.1016/j.trd.2018.03.005.
30. Mengyu Li, Manfred Lenzen, Dai Wang, Keisuke Nansai, GIS-based modelling of electric-vehicle–grid integration in a 100% renewable electricity grid, Applied Energy, Volume 262, 2020, 114577, ISSN 0306-2619, https://doi.org/10.1016/j.apenergy.2020.114577.
31. Kevin Joseph Dillman, Reza Fazeli, Ehsan Shafiei, Jón Örvar G. Jónsson, Hákon Valur Haraldsson, Brynhildur Davíðsdóttir, Spatiotemporal analysis of the impact of electric vehicle integration on Reykjavik's electrical system at the city and distribution system level, Utilities Policy, Volume 68, 2021, 101145, ISSN 0957-1787, https://doi.org/10.1016/j.jup.2020.101145.
32. Naresh Kumar Golla, Suresh Kumar Sudabattula, Impact of Plug-in electric vehicles on grid integration with distributed energy resources: A comprehensive review on methodology of power interaction and scheduling, Materials Today: Proceedings, 2021, ISSN 2214-7853, https://doi.org/10.1016/j.matpr.2021.03.306.
33. A multi-objective optimization model for fast electric vehicle charging stations with wind, PV power and energy storage, Journal of Cleaner Production, Volume 288, 2021, 125564, ISSN 0959-6526, https://doi.org/10.1016/j.jclepro.2020.125564.
34. Jochen Stiasny, Thierry Zufferey, Giacomo Pareschi, Damiano Toffanin, Gabriela Hug, Konstantinos Boulouchos, Sensitivity analysis of

electric vehicle impact on low-voltage distribution grids, Electric Power Systems Research, Volume 191, 2021, 106696, ISSN 0378-7796, https://doi.org/10.1016/j.epsr.2020.106696.

35. Pouria Emrani-Rahaghi, Hamed Hashemi-Dezaki, Optimal Scenario-based Operation and Scheduling of Residential Energy Hubs Including Plug-in Hybrid Electric Vehicle and Heat Storage System Considering the Uncertainties of Electricity Price and Renewable Distributed Generations, Journal of Energy Storage, Volume 33, 2021, 102038, ISSN 2352-152X, https://doi.org/10.1016/j.est.2020.102038.
36. J. Graça Gomes, H.J. Xu, Q. Yang, C.Y. Zhao, An optimization study on a typical renewable microgrid energy system with energy storage, Energy, Volume 234, 2021, 121210, ISSN 0360-5442, https://doi.org/10.1016/j.energy.2021.121210.
37. Md. Fatin Ishraque, Sk. A. Shezan, M.M. Ali, M.M. Rashid, Optimization of load dispatch strategies for an islanded microgrid connected with renewable energy sources, Applied Energy, Volume 292, 2021, 116879, ISSN 0306-2619, https://doi.org/10.1016/j.apenergy.2021.116879.
38. Mark Kipngetich Kiptoo, Mohammed Elsayed Lotfy, Oludamilare Bode Adewuyi, Abdul Conteh, Abdul Motin Howlader, Tomonobu Senjyu, Integrated approach for optimal techno-economic planning for high renewable energy-based isolated microgrid considering cost of energy storage and demand response strategies, Energy Conversion and Management, Volume 215, 2020, 112917, ISSN 0196-8904, https://doi.org/10.1016/j.enconman.2020.112917.
39. World Energy Perspective. Cost of Energy Technologies. www.worldenergy.org . ISBN: 978 0 94612 130 4
40. Cai, G.; Wang, W.; Lu, J. A Novel Hybrid Short Term Load Forecasting Model Considering the Error of Numerical Weather Prediction. Energies 2016, 9, 994. https://doi.org/10.3390/en9120994
41. http://www.omie.es/aplicaciones/datoshist/datoshist.jsp
42. http://www.heraldo.es/noticias/economia/2014/07/06/los_espanoles_reducen_uso_del_coche_hacen_menos_000_ano_297970_309.html
43. https://movilidadelectrica.com/prueba-real-de-autonomia-en-autovia-del-bmw-i3-94ah/
44. California Plug-In Electric Vehicle Infrastructure Projections: 2017-2025. NREL. 2018. CEC-600-2018-001. https://www.nrel.gov/docs/fy18osti/70893.pdf
45. M. Lydia, S. Suresh Kumar, A. Immanuel Selvakumar, G. Edwin Prem Kumar, A comprehensive review on wind turbine power curve modeling techniques, Renewable and Sustainable Energy Reviews, Volume 30, February 2014, Pages 452-460, ISSN 1364-0321, http://dx.doi.org/10.1016/j.rser.2013.10.030.
46. Rodríguez-López, M.A.; Cerdá, E.; del Rio, P. Modeling wind-turbine power curves: effect of environmental temperature on wind energy generation. *Energies* 2020, 13(18), 4941; https://doi.org/10.3390/en13184941.

47. Sunil Kumar Sansaniwal, Vashimant Sharma, Jyotirmay Mathur, Energy and exergy analyses of various typical solar energy applications: A comprehensive review, In Renewable and Sustainable Energy Reviews, Volume 82, Part 1, 2018, Pages 1576-1601, ISSN 1364-0321, https://doi.org/10.1016/j.rser.2017.07.003.
48. F. Geth, T. Brijs, J. Kathan, J. Driesen, R. Belmans, An overview of large-scale stationary electricity storage plants in Europe: Current status and new developments, Renewable and Sustainable Energy Reviews, Volume 52, 2015, Pages 1212-1227, ISSN 1364-0321, https://doi.org/10.1016/j.rser.2015.07.145.
49. Jasna Tomić, Willett Kempton, Using fleets of electric-drive vehicles for grid support, Journal of Power Sources, Volume 168, Issue 2, 2007, Pages 459-468, ISSN 0378-7753, https://doi.org/10.1016/j.jpowsour.2007.03.010.
50. Henrik Lund, Willett Kempton, Integration of renewable energy into the transport and electricity sectors through V2G, Energy Policy, Volume 36, Issue 9, 2008, Pages 3578-3587, ISSN 0301-4215, https://doi.org/10.1016/j.enpol.2008.06.007.
51. Claire Curry, Yayoi Sekine and Colin McKerracher, Bloomberg (BNEF), "BMW changes forward with residential stationary storage product". Advanced Transport, 22 June 2016.
52. Instituto Nacional de Estadística (INE). www.ine.es
53. Operador del Mercado Ibérico de Energía (OMIE). https://www.omie.es/es/market-results/interannual/daily-market/daily-prices?scope=interannual&system=1
54. Tim Felling, Development of a genetic algorithm and its application to a bi-level problem of system cost optimal electricity price zone configurations, Energy Economics, Volume 101, 2021, 105422, ISSN 0140-9883, https://doi.org/10.1016/j.eneco.2021.105422 .
55. Projected costs of generating electricity. International Energy Agency (IEA). 2020 Edition. NEA No. 7531. https://www.iea.org/reports/projected-costs-of-generating-electricity-2020

Conclusions and further research

1. Overview

The objective of this thesis has been to contribute to the quantification of how climate change may impact the energy sector. Specifically, effects to the generation of renewable electricity and how demand behavior will change energy prices in scenarios with distributed renewable generation and the replacement of the current vehicle fleet to EV, has been analyzed.

Everything seems to indicate that the identified impacts will affect the sector's value chain including, among other things, the supply and demand of electricity [1, 2].

In the case of supply, renewable generation has received greater attention than conventional generation, as its availability is more closely linked to climate variables [3]. Wind and photovoltaic generation have been the most studied thus far as shown in Chapters 1 and 2.

With regards to energy generation prices, it would depend on the energy mix, the grid configuration and EV penetration between others. In the housing sector, as discussed in Chapter 3, a gradual change in EV penetration can bring both benefits (helping the integration of renewables within the grid) and costs (an increase in energy prizes of the system due to additional storage systems).

2. Impacts on wind and photovoltaic energy production

This thesis has dedicated two chapters to the quantitative study of the impacts of global warming on wind and photovoltaic generation in two selected plants (Chapters 1 and 2). In both cases, wehave developed methodologies that focus specifically on the impact of ambient temperature increases, as opposed to the large number of other variables that can also affect both types of generation in the long term. Both chapters take an individual approach to specific plants, as well as the incorporation of economic variables.

In previous literature, it was found recent efforts mainly oriented toward the improvement of the evaluation of the actual power performance. Authors proposed methodologies for wind resource estimation using predictive models based on ANN, non-lineal regression techniques, between others, to model the power curve. Regarding energy losses in the wind farm due to environmental changes, previous contributions have analysed the impact of climate change on electricity generation with RETs in general and wind energy in particular. Several publications provided a review proposing possible mechanisms through which global climate variability and change could influence wind energy resources. They concluded that evidences for small magnitude changes could only appear by the end of twenty-first century.

The modeling of PV panels has historically been carried out with white-box type models based on physical equations. On the other hand, black-box models use data-driven approaches, which need no predetermined equivalent circuits and only rely on the measured data to directly build the black-box model. There are several techniques based on machine learning and deep learning such as ANN, supported vector regression (SVR), random forest (RF), gradient-boosted (GB), convolutional neural networks (CNN) or recurrent neural networks (RNN), among others. ANN were used in this paper. Previous studies used one ANN model to predict solar irradiation based on more commonly available weather data, and another ANN to predict the power output from a PV array. The authors

use, in the same study, ANN for forecasting and modeling. Similar contributions with RNN were also used by authors in order to learn the periodic trends from data, with the final objective of estimating the performance of the PV panel over time. Recent studies provided a classification of the different methodologies to model the power curve of PV panels, mentioning, among others, persistent forecast, physical model, statistical techniques, new techniques as Fuzzy and hybrid systems (ANFIS, adaptive neuro-fuzzy inference system). In such study, the main factors which are considered in the models are reviewed, including the main environmental variables which affect the performance of PV plants and show the correlation of those variables with electricity production. We could see in the conclusions of other researchers that outperformance losses are closed to 10 % at working temperatures of 50 ºC.

Compared to those contributions, this thesis advances knowledge on several fronts. It provides methodologies to model the wind turbines power curve for the assessment of production losses, using a combination of ANNs and Fuzzy logic rules. This combined system takes into account the effect of the control system on the power curve model, whereas this effect is disregarded in the previous literature. If this effect is not included, then a poor adjustment in the transition parts of the power curve results. Second, although previous studies consider air density as a parameter in their model, the environmental temperature is used in this paper as a parameter with an indirect relation with air density. Our methodology reduces the number of input variables which are needed in order to take into account the effect of air density from five or six to just one. This is useful since the air density measurement during the resource evaluation process may be available for wind farms, but not during the whole life cycle of the asset. Third, a two-stage model (formed by two ANN in cascade) was used to simulate the production in the ramp of the power curve. In contrast, only one ANN or SVM model was used to characterize this part of the power curve in the previous literature. Fourth, an analysis of the impact of global warming on wind energy production is carried out, using a model of wind energy generation based on ANN. The energy and economic losses in the wind farm used for this study have been assessed. Whereas simulations are mostly carried at macroscopic level in the literature and special attention to environmental temperature is not given, different scenarios with several increases in environmental temperature due to global warming at wind farm level are simulated in this thesis.

Compared to previous contributions in the field of PV systems, this thesis refines previous ANN methodologies to better characterize the power curve for PV generation in a real location using neural networks with TDNN and combining techniques provided in other publications in order to directly estimate the expected power. Second, for such model, two fictitious entry variables have been created (date/season and hour), which improve the predictive capability of the models. Third, a parametric model to assess the performance loss of a PV plant as a function of environmental temperature (and not only for the temperature of the PV panels) has been developed. Finally, the production losses in the analysed plant are simulated under different scenarios corresponding to different increases in ambient temperature.

Otherwise, the methodologies vary. In both cases we have experimented with several methods and data sets until finding those that best fit the existing data and objectives. In the case of wind generation, we have worked with a model that simulates the production of the wind turbines based on environmental and technical variables, due to wind plants are controlled according power curves. These relate active power with wind speed throughout a given reference period and for an specific

air density, which has a direct correlation to external temperature and consequently this is linked to global warming.

Chapter 2 has demonstrated the significant impact that changes in mean ambient temperature can have on photovoltaic generation. Both in chapter 1 and 2, based on simulated global warming projections representing different official scenarios, an estimate of how individual plants may be affected can be obtained in terms of performance and profit losses.

In this sense, wind energy production plants are more resilient to the effects of global warming. However, as it shown in chapter 3 the seasonality of this technology need to be accompanied with the photovoltaic power plants that could have a significant impact. If these performance losses are not considered when the installed capacity is dimensioned to supply to an isolated consumption group, the system could present inefficiencies and electricity supply cuts.

If global warming is not stopped additional investment in PV power plants or other renewables with storage systems would be needed. If the lack of renewable energy is covered with conventional energy sources, the equivalent CO_2 emissions reduction would not be achieved.

In any case, the conclusions are compelling and suggest that the decrease in PV performance decreases have a significant impact on the operating margins and investment parameters of PV power. This poses a threat not onlyto the stability of the electricity supply, but also to the mitigation of climate change. This performance losses will increase the impact pointed by other studies of the research group [4].

The study has not taken in to account possible changes in other ambient variables like wind direction, intensity or density, global irradiation, and other macroscopic changed that could affect to the frequency of clouds, seasonal changes, etc. In subsequent works not included in this thesis, we will continue our research in this regard, looking for different climate change scenarios to be simulated. In this regard, in other geographical contexts, changes in extreme wind patterns will be highly relevantand may occasionally cause substantial damage to facilities [5].

3. Impact of the electric vehicle penetration in energy generation prices

Chapter 3 examined the impact of the penetration of electrical vehicles on demand and energy generation prices in scenarios of isolated and non-isolated grids with self-generation renewable power plants and battery systems. In this case, the focus is on one hand, on determining the influence of electrical vehicles on electricity generation prices and, on the other hand, determining the optimal configuration of renewable generation and storage assets to minimize the electricity generation costs.

Several publications provide interesting insights on these research fields. Authors presented an analysis of the impact on the grid considering several penetration rates, nevertheless, their research does not consider 100% renewable generation scenarios and distributed generation. The general conclusions were that the Electrical Vehicle (EV) could be a great risk for grid reliability due to the fact that peak consumption could be increased between 67% and 114%. There are publications were authors presented several tools to minimize this impact through a smart control of the EV load. These authors pointed to the need to perform an optimized design of the renewable installed capacity.

Other authors presented a methodology to size, in a cost-effective way, the installed capacity

and storage systems needed in isolated grids with renewable energy. For their optimal grid configuration, the LCOE is 0.21 €/kWh (0.25 $/kWh). The impact of the EV penetration is not considered. Other related publications, obtained similar results, with the LCOE ranging between 0.204 $/kWh and 0.532 $/kWh, depending on the operating strategy. Nevertheless, in our scenario the LCOE would be around 0.68$/kWh.

However, none of the aforementioned contributions to the literature jointly assess how the renewable generation of the network should be sized in order to minimize the cost of energy generation, as well as the impact of the penetration of EVs on the costs of energy generation. This thesis tries to cover this gap in the literature. Compared to previous contributions, it advances knowledge on several fronts. At a methodological level, it provides a novel methodology based on the combination of Monte Carlo simulations and Genetic Algorithms (GA) in order to optimize the configuration of the grid components to minimize the generation costs. At an empirical level, the paper analyses the impact of EV penetration on electricity generation costs.

After analyzing the evolution on demand in different penetration scenarios, it can be concluded, that electrical vehicles will help to integrate renewables to the grid on a first stage, residential demand is the most influenced by meteorology.

Other finding, shows that would be more efficient and economical the combination of wind and PV productions systems instead of only PV systems despite its lower generation costs. Nevertheless, wind generation has a great seasonal variance, that would require a big storage capacity to balance the winter production to supply the summer demand. That evince the necessity of other long term storage technologies and not only electrical batteries.

Smaller population groups will have higher energy generation cost than medium-sized groups that allow wind power generation.

During the early stages of EV penetration, up to a penetration of 40%, the LCOE in small household groups will increase. In larger groups, the penetration of EV will increase the cost of power generation, due to the need to use more batteries in order to meet intraday consumption. This is especially obvious when the penetration of EVs is above 60-70%. This also affects the relative storage need (kWh/dwelling), although this ratio decreases in small size population groups after EV penetration reaches 70%.

Having storage capacity, even if it is limited to one battery per home, allows storage and consumption of up to 25% of the consumption of the population group, and can help to reduce the LCOE by 1.1% due to the fact that it helps to cover intraday variations and avoid the use of energy from the external grid.

Reductions of 20% in the LCOE of the batteries can lead to reductions of the general LCOE in the range of 5% to 13%, depending on the scenario, whereas a 20% reduction in the LCOE of PV generation could reduce the general LCOE between 2.5% to 6.5%.

In any case, we must be cautious due the large number of variables that could influence demand in the long term. We have continued working on a more complete framework that integrates other representative social, technical and economic aspects as regulation or prize policy, demand management or other renewable storage technologies.

4. Limitations and future research

As noted in the introduction, determining the impact of climate change in the long term is a difficult challenge and is subject to a large number of variables in a context of uncertainty. On the other hand, the necessity to evolve to new generation and consumption scenarios will introduce uncertainties difficult to evaluate now. Therefore,in the different chapters we have worked to simplify the scope of the reality studied.

Other limitations of the study have to do with the lack of information or resolution. The projections used in Chapter 3 offer a limited resolution, although the results have been contrasted with alternative methods. The series of electricity demand data in Chapter 3, for its part, is limited when compared to the scope and precision of climate data. For instance, consumption should be also associated with environmental conditions and it has not been considered in this Study. In addition, this consumption correspond to a small town in the southern coast of Spain, and the energy consumption may be different in other places where the environmental conditions are extreme in summer or winter.

According with what it is shown in Chapters 1 and 2, the energy production will be affected by the external temperature, so the installed capacity in scenarios form Chapter 3 have to be increased. On the other hand, the consumption would vary with the global warming effect.

Chapter 1 have been completed and published, and Chapter 2 has been presented in a congress and now is being considered for publication, nevertheless we acknowledge its limitations and would like to continue working on unexplored ideas as challenges and potential future lines of research. The literature in this field is still emerging and also follows this path. Some technical limitations in Chapter 3, such as the consideration of changes in wind direction or expanding the resolution of the bins, have been taken into account in subsequent investigations. We continue to work to improve our ability to explain generation and demand match.

There are other lines of research that seem relevant. One of them is to quantify how the incorporation of adaptation measures can affect the impacts. The ability to adapt may differ depending on capital needs and the amortization periods of the plants and their infrastructure.

On the other hand, in the case of hydroelectricity, the potential for conflicts of use between the energy sectors and other users of the resource could lead to another line of research, both geographically localized and multisectoral.

In future research, we will analyze the global impact in PV performance production considering the global warming expected in different regions according other authors. We will also evaluate the impact in the albedo effect of the planet due to land use changes with the PV panels. Regarding the last part of this thesis, we will analyze LCOE changes depending on wind energy costs, and the use of massive storage systems like batteries at industrial scale or long term storage energies (hydrogen or similar). We will also analyze how LCOE changes in case EV are used to inject energy in the electrical grid. We will also analyze LCOE changes in bigger population cities.

Finally, it is important to shed some light on the impacts on less studied technologies, such as solar or bioenergy, which will play a relevant role in the future of generation and may also be affected [6, 7].

References

1. Schaeffer R, Szklo AS, Pereira de Lucena AF, Moreira Cesar Borba BS, Pupo Nogueira LP, Fleming FP, et al. Energy sector vulnerability to climate change: A review. Energy 2012;38:1–12. https://doi:10.1016/j.energy.2011.11.056.
2. Ebinger J, Vergara W. Climate Impacts on Energy Systems: key issues for energy sector adaptation. Washington, DC, USA: The World Bank; 2011.
3. Contreras-Lisperguer R, de Cuba K. The Potential Impact of Climate Change on the Energy Sector in the Caribbean Region. OAS Pap 2008.
4. Solaun, K.; Cerdá, E. Climate change impacts on renewable energy generation. A review of quantitative projections. Renewable and Sustainable Energy Reviews, Volume 116, 2019, 109415, ISSN 1364-0321, https://doi.org/10.1016/j.rser.2019.109415.
5. Pryor SC, Barthelmie RJ. Assessing the vulnerability of wind energy to climate change and extreme events. Clim Change 2013;121:79–91. https://doi:10.1007/s10584-013-0889-y.
6. International Energy Agency. 2018 World Energy Outlook: Executive Summary. International Energy Agency; 2018.
7. Cronin J, Anandarajah G, Dessens O. Climate change impacts on the energy system: a review of trends and gaps. Clim Change 2018;151:79–93.

Resumen

Esta Tesis se tituló Impactos del Cambio Climático en la Generación de Energía Renovable y Escenarios de Generación de Energía.

El cambio climático se atribuye, entre otras variables, a las emisiones de gases de efecto invernadero producidas por el sector energético (incluyendo el transporte). Al mismo tiempo, el cambio climático se espera que pueda afectar a este sector cambiando la disponibilidad de sus recursos, alterando sus condiciones habilitantes y transformando los patrones de la demanda.

Esta Tesis aborda los impactos del cambio climático en la generación renovable y cambios en el comportamiento de la demanda de electricidad, proporcionando una introducción a las transformaciones más relevantes proyectadas por la literatura y desarrollando metodologías y análisis cuantitativos que determinan el impacto específico en tres casos de estudio.

El primer y el segundo capítulo se centran en determinar los cambios esperados en la generación eólica y fotovoltaica en plantas específicas, con especial atención en el calentamiento global. Ambos proporcionan proyecciones físicas y económicas de los cambios esperados, junto con conclusiones para el desarrollo de políticas energéticas.

El último capítulo profundiza en cómo el cambio climático y los escenarios propuestos para frenarlo, pueden afectar a la demanda de electricidad de una región, debido a los cambios esperados en las infraestructuras de generación y en cambios por el lado de la demanda como sería una elevada penetración de los vehículos eléctricos.

Los objetivos principales en los capítulos 1 y 2 fueron la estimación de cómo las plantas de energía individuales pueden verse afectadas en términos de rendimiento y pérdidas de ganancias, con base en proyecciones simuladas de calentamiento global que representan diferentes escenarios oficiales.

La metodología utilizada se basó en el uso de lógica difusa y redes neuronales artificiales para caracterizar la producción de las plantas de energía eólica y PV, teniendo en cuenta el efecto de la temperatura ambiente. Estos modelos complejos utilizaron como insumos variables como velocidad del viento, densidad del aire e irradiación entre otras, obteniendo excelentes resultados reproduciendo el comportamiento de las centrales bajo escenarios reales y simulados. Estos modelos de pérdidas de rendimiento, son una poderosa herramienta para que las empresas financieras determinen el retorno de las inversiones y la aprobación o no de los créditos.

Las conclusiones obtenidas fueron que las plantas de producción de energía eólica son más resistentes a los efectos del calentamiento global. Sin embargo, la estacionalidad de esta tecnología requiere que la generación energética se complemente con plantas fotovoltaicas, las cuales podrían tener un impacto significativo en su rendimiento, cercano al 10%. Si no se consideran estas pérdidas de rendimiento a la hora de dimensionar la capacidad instalada para abastecer a un grupo de consumo aislado, el sistema podría presentar ineficiencias y cortes de suministro eléctrico.

Si no se detiene el calentamiento global, se necesitarían inversiones adicionales en plantas de

energía fotovoltaica u otras energías renovables con sistemas de almacenamiento. Si la falta de energía renovable se cubre con fuentes de energía convencionales, no se lograría la reducción de emisiones de CO_2 equivalente.

En cualquier caso, las disminuciones del rendimiento fotovoltaico tienen un impacto significativo en los márgenes operativos y los parámetros de inversión de la energía fotovoltaica. Esto representa una amenaza no solo para la estabilidad del suministro eléctrico, sino también para la mitigación del cambio climático.

En la Tesis también se examinó el impacto de la penetración de vehículos eléctricos en la demanda y los precios de generación de energía en escenarios de redes aisladas y no aisladas con plantas de energía renovable como auto consumo y sistemas de baterías. En este caso, el estudió se enfocó por un lado en determinar la influencia de los vehículos eléctricos en los precios de generación eléctrica y, por otro lado, desarrollar un algoritmo que determinase la configuración óptima de los activos de generación y almacenamiento renovables para minimizar los costos de generación eléctrica.

Tras analizar la evolución de la demanda en diferentes escenarios de penetración, se puede concluir que los vehículos eléctricos ayudarán a integrar las renovables a la red en una primera etapa, siendo la demanda residencial la más influida por la meteorología. Sin embargo, una profunda penetración hará aumentar el LCOE. Presentamos una metodología basada en simulaciones de Monte Carlo y algoritmos genéticos para optimizar la configuración de los recursos de generación y almacenamiento con el objetivo de minimizar el LCOE del sistema, siendo una herramienta útil para los *Policy Makers*, gracias a la cantidad de escenarios que se pueden probar necesidad de recursos de computacionales.

Otro hallazgo realizado, de cara a minimizar el LCOE es más eficiente y económico la combinación de sistemas de producción eólicos y fotovoltaicos en lugar de solo sistemas fotovoltaicos a pesar de sus menores costes de generación. Sin embargo, la generación eólica tiene una gran variación estacional, lo que requeriría una gran capacidad de almacenamiento para equilibrar la producción invernal y abastecer la demanda de verano. Eso evidencia la necesidad de otras tecnologías de almacenamiento a largo plazo y no solo baterías eléctricas.

Los grupos de población más pequeños tendrán un costo de generación de energía más alto que otros grupos de tamaño mediano, ya que estos últimos pueden llegar a utilizar la generación de energía eólica. Los resultados mostraron que una pequeña capacidad de almacenamiento ayudará a gestionar un porcentaje importante de la energía consumida debido a que los balances energéticos diarios son los que requieren mayor control.

El cambio climático requiere la adopción de cambios en la forma en que generamos y consumimos energía. Debemos estar preocupados por el impacto real de esos cambios y el efecto del calentamiento global que tendrá sobre ellos y finalmente el impacto en nuestras economías. Necesitamos tener herramientas para evaluar todos los posibles impactos y tomar decisiones más precisas como *Policy Makers* para evaluar el impacto real en este complejo escenario.

Abstract

This Thesis was titled Climate Change Impacts on Renewable Energy Generation and Energy Generation Scenarios.

Climate change is attributed, among other factors, to greenhouse gas emissions produced by the energy sector (including the transport). At the same time, climate change is expected to affect this sector by changing the availability of resources, altering its enabling conditions and transforming demand patterns.

This thesis addresses climate change impacts on renewable generation and electricity demand by providing an overview of the most relevant transformations projected in literature and by developing methodologies and quantitative analysis to ascertain the specific infuence in three case-studies.

The first and second chapters are focus on estimating climate change impacts in wind and photovoltaic generation in specific plants. Both provide physical and economic projections of expected changes, along with conclusions for the development of energy policies.

The last chapter delves into how climate change and the scenarios proposed to curb it, can affect the demand for electricity in a region, due to the expected changes in the generation infrastructure and changes on the demand side such as a high penetration of electric vehicles.

The main goals in chapter 1 and 2 were the estimation of how individual power plants may be affected can be affected in terms of performance and profit losses, based on simulated global warming projections representing different official scenarios.

The methodology was based on the use of Fuzzy logic and artificial neural networks to characterize the production of the wind and PW power plants, tanking in consideration the effect of ambient temperature. These complex models used as inputs variables like wind speed, air density and irradiation between others, obtaining excellent results reproducing the behavior of the power plants under real and simulated scenarios. This performance losses models, are a powerful tool for financial enterprises to determine the return of the investments and the approval or not of credits.

The obtained conclusions were that wind energy production plants are more resilient to the effects of global warming. However, the seasonality of this technology needs to be accompanied with the photovoltaic power plants that could have a significant impact close to 10%. If these performance losses are not considered when the installed capacity is dimensioned to supply to an isolated consumption group, the system could present inefficiencies and electricity supply cuts.

If global warming is not stopped additional investment in PV power plants or other renewables with storage systems would be needed. If the lack of renewable energy is covered with conventional energy sources, the equivalent CO_2 emissions reduction would not be achieved.

In any case, PV performance decreases have a significant impact on the operating margins and

investment parameters of PV power. This poses a threat not only to the stability of the electricity supply, but also to the mitigation of climate change.

The Thesis also examined the impact of the penetration of electrical vehicles on demand and energy generation prices in scenarios of isolated and non-isolated grids with self-generation renewable power plants and battery systems. In this case, the focus is on one hand, on determining the influence of electrical vehicles on electricity generation prices and, on the other hand, designing an algorithm for determining the optimal configuration of renewable generation and storage assets to minimize the electricity generation costs.

After analyzing the evolution on demand in different penetration scenarios, it can be concluded, that electrical vehicles will help to integrate renewables to the grid on a first stage, residential demand is the most influenced by meteorology. A deep electrical vehicle penetration, will rise the LCOE of the system. We presented a methodology bases on Monte Carlo simulations and genetic algorithms to optimize the configuration of the generation and storage resources to minimize the LCOE of the system, being a tool useful for police makers tanks the number of scenarios that can be tested without spending a lot of computational resources.

Other finding shows that would be more efficient and economical the combination of wind and PV productions systems instead of only PV systems despite its lower generation costs. Nevertheless, wind generation has a great seasonal variance, that would require a big storage capacity to balance the winter production to supply the summer demand. That evince the necessity of other long term storage technologies and not only electrical batteries.

Smaller population groups will have higher energy generation cost than medium-sized groups that allow wind power generation. Results showed that a small storage capacity will help to manage an important percentage of the consumed energy due to the fact that daily energy balances are the ones than require more control.

Climate Change require the adoption of changes in the way we generate and consume energy. We need to be concern about the real impact of that changes and the effect of global warming will have over them and finally the impact on our economies. We need to have tools to evaluate all the possible impacts and to make more precise decisions as policy makers to evaluate the real impact in this complex scenario.